



**Universidade do Estado do Rio de Janeiro**  
**Centro de Tecnologia e Ciências**  
**Faculdade de Geologia**

Talitta Nunes Manoel

**Uma perspectiva integrada do magmatismo básico da faixa ribeira central:  
um estudo de caso em rochas da bacia Andrelândia e do complexo Juiz de  
Fora**

Rio de Janeiro  
2022

Talitta Nunes Manoel

**Uma perspectiva integrada do magmatismo básico da faixa ribeira central: um estudo  
de caso em rochas da bacia Andrelândia e do complexo Juiz de Fora**

Tese apresentada, como requisito parcial para  
obtenção do título de Doutor, ao Programa de Pós-  
Graduação em Geociências, da Universidade do  
Estado do Rio de Janeiro. Área de concentração:  
Evolução tectônica de Faixas Móveis.

Orientadora: Prof.<sup>a</sup> Dra. Monica da Costa Pereira Lavalle Heilbron  
Coorientadores: Prof.<sup>a</sup> Dra. Kathryn Ann Cutts e Prof. Dr. Ivo Dussin.

Rio de Janeiro

2022

CATALOGAÇÃO NA FONTE  
UERJ/REDE SIRIUS/CTCC

M285

Manoel, Talitta Nunes.

Uma perspectiva integrada do magmatismo básico da faixa ribeira central: um estudo de caso em rochas da bacia Andrelândia e do complexo Juiz de Fora / Talitta Nunes Manoel.– 2022.

71 f. : il.

Orientadora: Mônica da Costa Pereira L. Heilbron.

Coorientadores: Kathryn Cutts e Ivo Antonio Dussin

Tese (Doutorado) – Universidade do Estado do Rio de Janeiro,  
Faculdade de Geologia.

1. Geologia - Teses. 2. Magmatismo – Teses. 3. Geoquímica - Teses. 4. Rochas ígneas – Teses. I. Heilbron, Mônica da Costa Pereira L. II. Cutts, Kathryn. III. Dussin, Ivo Antonio. IV. Universidade do Estado do Rio de Janeiro. Faculdade de Geologia. V. Título.

CDU: 552.3

Bibliotecária Responsável: Priscila Freitas Araujo/ CRB-7: 7322

Autorizo, apenas para fins acadêmicos e científicos, a reprodução total ou parcial desta tese, desde que citada a fonte.

---

Assinatura

---

Data

Talitta Nunes Manoel

**Uma perspectiva integrada do magmatismo básico da faixa ribeira central: um estudo de caso em rochas da bacia Andrelândia e do complexo Juiz de Fora**

Tese apresentada, como requisito parcial para obtenção do título de Doutor, ao Programa de Pós-Graduação em Geociências, da Universidade do Estado do Rio de Janeiro. Área de concentração: Evolução tectônica de Faixas Móveis.

Aprovada em 14 de dezembro de 2022.

Orientadora: Prof.<sup>a</sup> Dr<sup>a</sup>. Mônica da Costa Pereira L. Heilbron  
Faculdade de Geologia – UERJ

Coorientadores: Prof.<sup>a</sup> Dr<sup>a</sup>. Kathryn Cutts  
GTK  
Prof. Dr. Ivo Antonio Dussin  
Faculdade de Geologia - UERJ

Banca Examinadora: \_\_\_\_\_  
Prof. Dr. Miguel A. T. Araujo Souza  
Universidade Federal do Rio Grande do Norte - UFRN

---

Prof.<sup>a</sup> Dr<sup>a</sup>. Regiane A. Fumes  
Universidade do Estado do Rio de Janeiro

---

Prof. Dr. Felipe C. F. Pereira  
Universidade do Estado do Rio de Janeiro

---

Prof. Dr. Elton Luiz Dantas  
Universidade de Brasilia

Rio de Janeiro

2022

## **AGRADECIMENTOS**

Agradeço em primeiro lugar aos meus pais, Maria Aparecida e Reginaldo, meus irmãos Marcus e Daniel e a Maria Luzirene. por todo apoio e incentivo ao longo dos anos.

Ao meu companheiro Felipe, por toda parceria e ombro amigo nos momentos difíceis.

À minha orientadora Monica Heilbron e aos meus corientadores Kathryn Cutts e Ivo Dussin pelo conhecimento e aprendizado durante esses 4 anos de doutorado.

Aos meus amigos por estarem sempre dispostos a me ouvir, aconselhar e me acompanhar durante grande parte da minha vida.

Muito Obrigada!

## RESUMO

MANOEL, Talitta Nunes. **Uma perspectiva integrada do magmatismo básico da faixa ribeira central:** um estudo de caso em rochas da bacia Andrelândia e do complexo Juiz de Fora. 2022. 71 f. Tese (Doutorado em Geociências) – Faculdade de Geologia, Universidade do Estado do Rio de Janeiro, Rio de Janeiro, 2022.

O magmatismo básico da Faixa Ribeira Central, investigado a partir das rochas da Bacia Andrelândia e do embasamento paleoproterozóico do Complexo Juiz de Fora, reflete importantes etapas da evolução tectônica durante a aglutinação do paleocontinente São Francisco no Neoproterozóico. Nesse contexto, foram realizadas análises petrográficas, litogeoquímicas e isotópicas (Sm-Nd, Rb-Sr, Lu-Hf e U-Pb em zircão) para avaliar as assinaturas geoquímicas e o momento de cristalização desses corpos máficos, bem como as condições metamórficas de alto grau a que foram submetidos. Os resultados evidenciam variações em elementos-traço (como Ti, Zr e REE) e em valores isotópicos de Sm-Nd ( $\epsilon_{Nd}$  entre +2 e -14), sugerindo a atuação de fontes mantélicas heterogêneas e possíveis episódios de contaminação crustal ao longo do rifteamento e posterior desenvolvimento de uma margem passiva hiperextendida. As idades U-Pb (entre 760 e 653 Ma) obtidas em zircões magmáticos e herdados, aliadas aos modelos de residência crustal TDM (1,9 a 1,1 Ga), apontam para a interação de magmas juvenis com porções retrabalhadas do embasamento paleoproterozóico. A integração desses dados isotópicos com as feições estruturais e paragenéticas indica múltiplos estágios de metamorfismo – de fácies anfibolito a granulito – associados à convergência Brasiliana (ca. 620–580 Ma). Do ponto de vista geodinâmico, as variações geoquímicas e isotópicas nos litotipos máficos fornecem novas evidências sobre a formação de bacias tipo rifte e sua evolução para margens passivas, bem como sobre o papel de retrabalhamento crustal e exumação de embasamento durante a colagem do Gondwana Ocidental. Esses resultados contribuem para uma melhor compreensão dos processos tectono-magmáticos que moldaram a Faixa Ribeira Central e ampliam as perspectivas acerca do regime geodinâmico neoproterozóico no sudeste do Brasil.

Palavras-chave: magmatismo básico; faixa Ribeira Central; neoproterozóico.

## ABSTRACT

MANOEL, Talitta Nunes. **An integrated perspective of the basic magmatism of the central ribeira belt:** a case study in rocks from the Andrelândia Basin and the Juiz de Fora Complex. 2022. 71 f. Tese (Doutorado em Geociências) – Faculdade de Geologia, Universidade do Estado do Rio de Janeiro, Rio de Janeiro, 2022.

The basic magmatism of the Central Ribeira Belt, investigated through the rocks of the Andrelândia Basin and the Paleoproterozoic basement of the Juiz de Fora Complex, reflects key stages of tectonic evolution during the amalgamation of the São Francisco paleocontinent in the Neoproterozoic. In this context, petrographic, lithogeochemical, and isotopic analyses (Sm-Nd, Rb-Sr, Lu-Hf, and U-Pb in zircon) were carried out to assess the geochemical signatures and crystallization timing of these mafic bodies, as well as the high-grade metamorphic conditions to which they were subjected. The results reveal variations in trace elements (such as Ti, Zr, and REE) and in Sm-Nd isotopic values ( $\epsilon_{\text{Nd}}$  between +2 and -14), suggesting the involvement of heterogeneous mantle sources and possible episodes of crustal contamination during rifting and the subsequent development of a hyper-extended passive margin. The U-Pb ages (ranging between 760 and 653 Ma) obtained from both magmatic and inherited zircons, combined with TDM crustal residence models (1.9 to 1.1 Ga), indicate an interaction between juvenile magmas and reworked portions of the Paleoproterozoic basement. The integration of these isotopic data with structural and paragenetic features suggests multiple stages of metamorphism—from amphibolite to granulite facies—associated with Brasilian convergence (ca. 620–580 Ma). From a geodynamic perspective, the geochemical and isotopic variations in the mafic lithotypes provide new evidence on the formation of rift-type basins and their evolution into passive margins, as well as on the role of crustal reworking and basement exhumation during the amalgamation of Western Gondwana. These results contribute to a better understanding of the tectono-magmatic processes that shaped the Central Ribeira Belt and broaden perspectives regarding the Neoproterozoic geodynamic regime in southeastern Brazil.

Keywords: basic magmatism; Central Ribeira belt; neoproterozoic.

## **LISTA DE FIGURAS**

Figura 1 –	Mapa de esboço tectônico simplificado modificado de Trouw et al. (2013) e Kuster et al (2020).....	16
Figura 2 –	Mapa tectônico da Faixa Ribeira central modificado de Heilbron <i>et al</i> (2017a) .....	20

## SUMÁRIO

<b>INTRODUÇÃO.....</b>	11
<b>1 GEOLOGIA REGIONAL.....</b>	15
1.1 A organização tectônica orogênica da Faixa Ribeira.....	15
1.2 As unidades da Bacia Andrelândia na Faixa do Ribeira: síntese e subdivisão simplificada adotada.....	16
1.3 Complexo Juiz de Fora.....	20
<b>2 METODOLOGIA.....</b>	23
<b>3 RESULTADOS.....</b>	24
3.1 An example of a Neoproterozoic hyperextended margin: An integrated perspective of the basic magmatism recorded in the Andrelândia Basin, central Ribeira Orogen, SE-Brazil.....	24
3.2 The polyphase evolution of the mafic rocks of the Juiz de Fora Complex: The record of two supercontinent cycles.....	44
<b>4 DISCUSSÃO.....</b>	62
<b>CONSIDERAÇÕES FINAIS.....</b>	64
<b>REFERÊNCIAS.....</b>	66

## INTRODUÇÃO

Rochas básicas toleíticas intercaladas com unidades metassedimentares são muito comuns em vários ambientes tectônicos, desde riftes continentais a margens passivas e planaltos oceânicos em regimes extensionais, inclusive rochas toleíticas em ambientes convergentes, como arcos magmáticos, bem como em ambientes tectônicos pós-colisão (Pearce & Cann, 1973; Pearce *et al.*, 1975; Pearce, 1983, 1987; Wilson, 1989; Saccani *et al.*, 2015).

Em muitas unidades metamórficas de alto grau expostas nos cinturões orogênicos profundamente erodidos do Gondwana Ocidental (Ganade de Araújo *et al.*, 2014; Coelho *et al.*, 2017; Tedeschi *et al.*, 2017; Kuster *et al.*, 2020; Figura 1), a configuração tectônica original da bacia precursora permanece comumente incerta porque a recristalização de alta temperatura e deformação oblitera muitas características primárias das rochas metassedimentares. Nos terrenos pré-cambrianos, o metamorfismo de alto grau é amplamente associado com episódios de grande formação e retrabalhamento da crosta continental, resultando em polimetamórficos características (Harley, 1989). Reconstruções pressão-temperatura-tempo (P-T-t) em rochas que têm fácies de anfibolito a granulito podem ser interessantes; no entanto, tais rochas estão se apresentando como uma ferramenta importante para determinar os ciclos geodinâmicos de cinturões orogênicos (e.g., Tedeschi *et al.*, 2017; Kunz *et al.*, 2020; Gutiérrez-Aguilar, 2021).

O estudo de proveniência U-Pb das unidades supracrustais normalmente não fornece idades de sedimentação precisas, já que muitas vezes a idade do zircão detritico mais jovem pode ser muito mais velha para suportar idades deposicionais, especialmente em configurações de fenda para margens passivas desenvolvidas em paleocontinentes cratônicos mais antigos (Santos, 2011; Belém *et al.*, 2011; Coelho *et al.*, 2017; Frugis *et al.*, 2018; Kuster *et al.*, 2020). Nestes casos, o estudo de rochas básicas intercaladas, tanto no que diz respeito às assinaturas geoquímicas-isotópicas quanto à geocronologia, podem ser ferramentas importantes para delimitar idades deposicionais e ambientes tectônicos.

Outro aspecto interessante para as bacias de rifte passado para margens passivas é a investigação do possível desenvolvimento dos dois membros finais, margens passivas ricas em magma (hiper-estendidas) e pobres em magma, como tem sido reconhecido nas margens passivas atuais (Sutra & Manatschal, 2011; Zalán *et al.*, 2011; Doré; Lundin *et al.*,

2015; Peron- Pindivic; Manatschal, 2019).

O Orógeno Ribeira (RO) integra o Sistema Orogênico Araçuaí-Ribeira (AROS), que representa uma das redes de cinturões orogênicos do Neoproterozóico e Paleozóico Inferior resultantes da fusão do Gondwana Ocidental. O AROS compõe um sistema orogênico profundamente erodido de 300 km de largura e 600 km de comprimento que corre aproximadamente paralelo à costa sudeste do Brasil (Trouw *et al.*, 2000, 2013; Campos Neto *et al.*, 2000, 2004; Heilbron *et al.* 2004, 2008, 2017a, Pedrosa-Soares *et al.* 2008; Alkmim *et al.*, 2017). A zona externa deste sistema orogênico compreende a margem passiva Neoproterozóica retrabalhada do paleocontinente São Francisco. Devido à deformação e metamorfismo relacionados à colagem Brasiliana, as unidades metassedimentares juntamente com rochas magmáticas sin-deposicionais afloram como gnaisses de alto grau, tectonicamente intercalados com lascas de embasamento altamente deformadas durante os episódios colisionais. É importante ressaltar que tanto o embasamento quanto às associações neoproterozóicas experimentaram metamorfismo de alto grau como resultado do empilhamento tectônico durante a Orogenia Brasiliana, associado a diferentes estágios da montagem de Gondwana Ocidental (e.g, Heilbron *et al.* 2000, 2017; Duarte *et al.*, 2000; Degler *et al.*, 2018; Cutts *et al.*, 2020; Almeida *et al.*, 2021; Mauri *et al.*, 2022). O Grupo Andrelândia ou Megassequência (Paciullo *et al.*, 2000; Heilbron *et al.*, 2017) tem sido considerado como representativo de uma bacia de margem passiva Neoproterozóica desenvolvida ao redor das margens sul e SSE do Cráton do São Francisco (SFC).

As unidades da bacia de Andrelândia estiveram envolvidas na convergência de dois cinturões diferentes, o Orógeno de Brasília mais antigo, com vergência leste a sul, e o Orógeno mais jovem, com vergência noroeste da Faixa Ribeira, ambos relacionados a construção do supercontinente Gondwana (e.g. Heilbron *et al.*, 2017). Muitos trabalhos anteriores usando dados U-Pb, Nd e Sr, e recentemente Lu-Hf (por exemplo, Frugis *et al.*, 2018; Lobato, 2018; Kuster *et al.*, 2020; Marimon *et al.*, 2020) contribuíram para discutir as fontes e idades deposicionais máximas para as unidades supracrustais do grupo Andrelândia entre os períodos Toniano e Criogeniano (900 a 670 Ma, e.g, Belém *et al.*, 2011; Frugis *et al.*, 2018).

Este trabalho traz novos dados petrográficos, geoquímicos, isotópicos e geocronológicos, bem como um mapeamento geológico das rochas metabásicas integradas

aos estudos U-Pb publicados do grupo Andrelândia, incluindo seu equivalente mais distal (Grupo Raposos), a fim de entender a tectônica configuração e processos envolvidos durante a evolução da bacia. Também será contemplado neste trabalho ortogranulitos máficos do Complexo Juiz de Fora, que corresponde a unidade de embasamento das supracrustais do Grupo Raposos. As rochas máficas investigadas foram selecionadas para estudo porque podem fornecer evidências sobre a evolução das configurações tectônicas ao longo do tempo durante a Orogenia Riaciana, mas eles também foram retrabalhados em alta temperatura durante a Orogênese Brasiliana. As rochas estudadas contêm granada + plagioclásio + clinopiroxênio + ortopiroxênio + anfibólio + quartzo + ilmenita como principal paragênese, indicam metamorfismo da fácie granulito (Bucher & Grapes, 2011). Neste trabalho apresentamos dados de química mineral, idades de zircônio U-Pb juntamente com a sistemática de Hf, isótopos de Sr e Nd e uma investigação petrocronológica usando mapeamento composicional quantitativo (Lanari *et al.*, 2013, 2014; Lanari; Duesterhoeft, 2019) em um esforço para desvendar a configuração tectônica e evolução das rochas máficas alojadas na Faixa Ribeira. Por fim, uma discussão sobre os dois principais estágios supercontinentais e a importância dos granulitos máficos na modelos tectônicos serão abordados.

Finalmente, os dados obtidos tanto para as metabásicas alojadas na bacia Andrelândia- Raposos quanto as que se encontram no embasamento do Complexo Juiz de Fora visam a contribuir para evolução geral da margem passiva Neoproterozóica da borda ESE do paleocontinente SF.

Inicialmente, o objetivo inicial foi calibrar a idade de deposição dos litotipos distais do Grupo Raposos e a configuração tectônica do magmatismo sin-sedimentar que é representado pela inserção de rochas metabásicas durante a evolução da bacia. Os estudos com foco no Grupo Raposos são escassos e fornecer uma sequência bem restrita é fundamental para melhorar esse segmento mal calibrado. Em um contexto mais global, o objetivo do primeiro artigo é entender a relação tectônica entre os corpos máficos e suas respectivas rochas hospedeiras durante o desenvolvimento da margem passiva de Andrelândia-Raposos na borda sul do Cráton do São Francisco.

Além da abordagem visando esse magmatismo Neoproterozóico, neste trabalho também buscou-se detalhar as condições metamórficas no tempo registradas nos ortogranulitos do Complexo Juiz de Fora, visto que essas rochas apresentam sua evolução

associada tanto a Orogenia Riaciana quanto a Orogenia Brasiliana. Maiores detalhes serão apresentados no resultado do segundo artigo. O estudo de ortogranulitos em especial os básicos fornecem informações sobre evolução dos ciclos orogênicos e em se tratando de um metamorfismo de alto grau espera-se que o aprimoramento da metodologia de aplicada a terrenos metamórficos de alto grau, proporcionando assim melhores condicionantes geocronológicas para reconstruções de bacias em todo o mundo.

## 1 GEOLOGIA REGIONAL

### 1.1 A organização tectônica orogênica da Faixa Ribeira

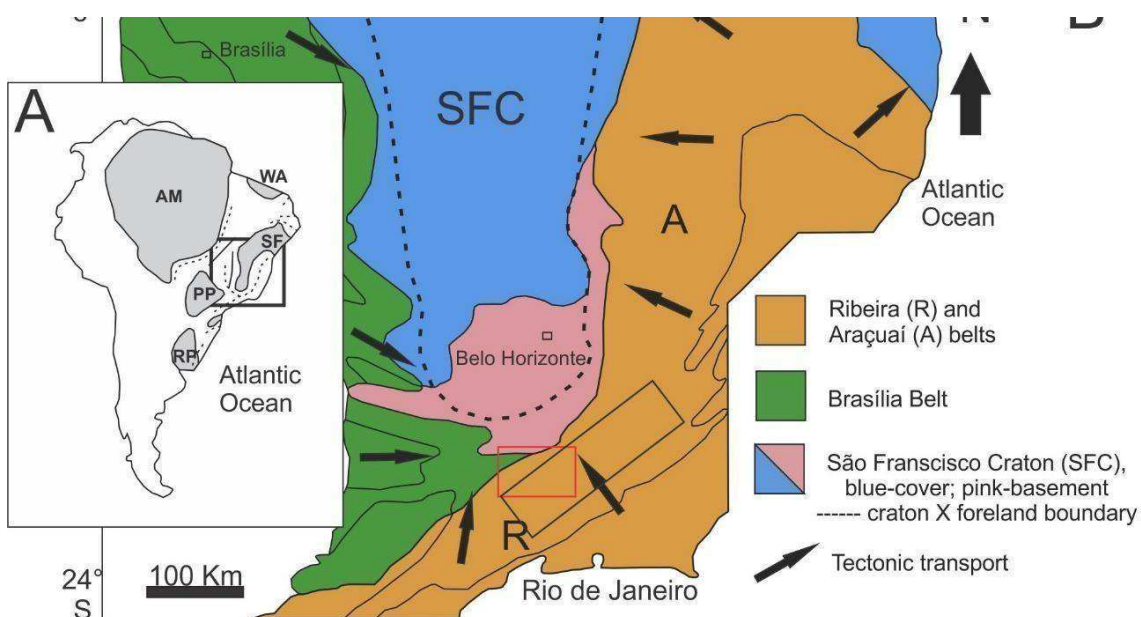
A amalgamação do Gondwana Ocidental levou à formação de vários sistemas orogênicos Neoproterozóicos-Cambrianos ao redor dos crátons Arqueano e Paleoproterozóico (Figura 1). O Sistema Orogênico Ribeira-Araçuaí (AROS) desenvolveu-se como resultado do fechamento do paleoceano Adamastor e colisões diacrônicas de diferentes terrenos tectonoestratigráficos, incluindo paleocontinentes e arcos magmáticos (e.g, Heilbron *et al.*, 2017; Pedrosa-Soares *et al.*, 2008, 2011; Alkmim *et al.*, 2017; Degler *et al.*, 2018), (Figura 1).

A organização tectônica do segmento central do Orógeno Ribeira compreende quatro terrenos tectono-estratigráficos de NW a SE, os terrenos Ocidental, Central, Oriental e Cabo Frio (Figura 2), progressivamente incorporados na porção sul do SFC (Heilbron *et al.* 2008; 2017a; 2020). O Terreno Ocidental (OcT) é estruturalmente subdividido em dois sistemas de lâminas de impulso de escala crustal (domínio alóctone) que configuram o Sistema de Empurrão Inferior (SEI) (Domínio Andrelândia) e o Sistema de Empurrão Superior (SES) (Domínio Juiz de Fora) (Heilbron *et al.*, 1998; 2000; 2010). O OcT engloba a margem passiva Neoproterozóica (Grupo Andrelândia - Paciullo *et al.*, 2000) e o embasamento cratônico retrabalhado (Heilbron *et al.*, 2010; Degler *et al.*, 2017; Cutts *et al.*, 2019; Bruno *et al.*, 2020; 2021).

No Sistema de Empurrão Inferior, o microcontinente Piedade e o Complexo Mantiqueira (Heilbron *et al.*, 1998; 2010; Duarte *et al.*, 2004; Bruno *et al.*, 2020; 2021,) representam as unidades do embasamento arqueano a paleoproterozóico que se dobraram juntamente com metassedimentos deformados do Grupo Andrelândia (Figura 2). A associação do embasamento do Sistema de Empurrão Superior é composta por ortogranulitos e rochas ortognaisse do Complexo Juiz de Fora que é tectonicamente intercalado com as fácies distais do Grupo Andrelândia, conhecido como Grupo Raposos (e.g, Trouw *et al.* 2000; Ribeiro *et al.*, 2003; Heilbron *et al.*, 2004; Noce *et al.*, 2003; 2006; Barbosa *et al.*, 2019; Almeida *et al.*, 2021; Degler *et al.*, 2017; Heilbron *et al.* 1998; 2010, Noce *et al.* 2007; Degler *et al.*; 2018) (Figura. 2).

O domínio autóctone do Orógeno Ribeira contém as nappes retrabalhadas da parte sul do antigo Sistema Orogênico Brasília (SOB), desenvolvido como produto do fechamento do Oceano Goianides (e.g. Alkmim *et al.*, 2017). As nappes externas de verga E deste sistema orogênico foram retrabalhadas pelo encurtamento NW imposto pela evolução tectônica do Orógeno da Ribeira.

Figura 1 - Mapa de esboço tectônico simplificado modificado de Trouw *et al.* (2013) e Kuster *et al*



Legenda: a) Localização na América do Sul dos crâtons AM-Amazônia, WA- Oeste Africano, SF-São Francisco, PP- Paranapanema e RP- Rio da Prata. b) Localização da principal área de afloramento do Grupo Andrelândia e do embasamento do Complexo Juiz de Fora em relação ao Cráton do São Francisco e aos orógenos Neoproterozóicos. Retângulos vermelho e preto: a área de estudo.

Fonte: Trouw *et al.* (2013) e Kuster *et al.* (2020).

## 1.2 As unidades da Bacia Andrelândia na Faixa do Ribeira: síntese e subdivisão simplificada adotada

O Grupo Andrelândia ou Megassequência tem sido interpretado como a margem passiva Neoproterozóica da margem sul e SSE do SFC envolvendo tanto as unidades de impulso do SOB meridional quanto o Orógeno Ribeira do AROS (Paciullo *et al.*, 2000; Heilbron *et al.*, 2017). A maior dificuldade encontrada é que a maioria dos autores tenta integrar as pilhas estratigráficas tectônicas observadas dentro de dois sistemas orogênicos neoproterozóicos

diferentes, ou seja, o mais antigo (ca. 650 – 630 Ma) segmento leste da Faixa Brasília e o mais jovem (ca. 620 – 530 Ma) Orógeno da Ribeira com confluência NW (Figura 1).

Parte das unidades do Grupo Andrelândia aflora na zona de superposição entre esses dois orógenos, denominada zona de interferência, embora os limites entre esses dois cinturões sejam motivo de debate. Parte dos autores considerou a zona de interferência como parte do Orógeno Brasília (Trouw *et al.* 2000; 2013; Campos Neto; Caby, 2000; Campos Neto *et al.*, 2020; Frugis *et al.*, 2018; Kuster *et al.*, 2020; Marimon *et al.*, 2020), enquanto outros consideram que a zona de interferência é representada pelo retrabalhamento do Orógeno Brasília pelo Orógeno Ribeira (Valladares *et al.* 2004; Heilbron *et al.*, 2017, Valeriano *et al.*, 2004).

Diferentes subdivisões estratigráficas foram propostas, como a tentativa de reconstrução das seis unidades agrupadas em duas sequências por Paciullo *et al.* (2000) ou unidades tectônicas compostas conforme relatado por Heilbron *et al.* (2019) e Campos Neto *et al.* (2020). A primeira subdivisão estratigráfica integrada do Grupo Andrelândia foi proposta por Paciullo (2000), considerando tanto as napas mais meridionais do Orógeno Brasília quanto o Sistema de Empurrão Superior do terreno Ocidental do Orógeno Ribeira (Figuras 1 e 2). Esses autores subdividiram o Grupo Andrelândia em duas sequências principais:

- a) Sequência Inferior Carrancas incluindo paragnaisse bandados de biotita com camadas pelíticas e anfibolitos (A1 e A2); camadas de quartzito com mica branca (A3); e intercalações de filito/xisto ricas em grafite e ortoquartzitos (A4).
- b) A Sequência Superior Serra do Turvo compreende um pacote de xistos/gnaisses ricos em plagioclásio-biotita com camadas pelíticas e quartzitos (A5) e xistos pelíticos e gnaisses (A6).

É importante ressaltar que as unidades A3 e A4 mapeadas no Orógeno Brasília Sul não são reconhecidas no segmento distal do Grupo Andrelândia (SEI) e no Grupo Raposos (UTS), no Segmento Central do Orógeno da Ribeira. Para o propósito da contribuição, focada nas rochas metabásicas intercaladas, uma subdivisão litológica simplificada é adotada e tentativamente correlacionada com a subdivisão proposta anteriormente por Paciullo *et al.* (2000). As unidades estratigráficas adotadas são baseadas em mapas geológicos detalhados das unidades da bacia de Andrelândia no lado da Faixa Ribeira Central, integrados a mapas geológicos em escala 1:100.000 (9 folhas) e publicados pelo Serviço Geológico ([www.rigeo.cprm.gov.br](http://www.rigeo.cprm.gov.br)).

Outras contribuições (e.g, Westin *et al.*, 2016), trabalhando na mesma região (LTS), propuseram que as unidades inferiores do Grupo Andrelândia de Paciullo *et al.* (2000), A1+A2, são mais antigas (ca. 2.1Ga,), classificadas como Unidade São Vicente, pertencentes às unidades de embasamento do Craton do São Francisco. Esta proposição é baseada na proveniência unimodal paleoproterozóica obtida para amostras de gnaisses bandados das unidades A1+A2, embora zircões detriticos jovens neoproterozóicos tenham sido encontrados em todas as unidades de Andrelândia (Belém *et al.*, 2011; Santos *et al.*, 2011; Lobato, 2018; Heilbron *et al.*, 2019). No entanto, nossos estudos mostraram que os contatos entre paragnaisses bandados de biotita A1+A2 com quartzitos interlaminares e xistos de quartzo no Sistema de Empurrão Inferior (Domínio Andrelândia) são gradacionais e não tectônicos. Não há rochas miloníticas detectadas ao longo desses contatos. Por outro lado, no topo da pilha, próximo às unidades de alta pressão, lascas de embasamento (ortognaisses plutônicos) foram intercaladas dentro das Unidades de topo de Andrelândia (A5 e A6), com feições miloníticas ao longo dos contatos. Mais referências com Trouw *et al.* (2000; 2013), Heilbron *et al.* (2000; 2004; 2008; 2017) e Cioffi *et al.* (2016).

Devido a este debate estratigráfico em curso, uma nomenclatura estratigráfica simplificada é adotada aqui, onde o termo Grupo Andrelândia é usado para as unidades proximais da bacia (incluindo o SEI do Orógeno Ribeira e os nappes do SOB sul) enquanto o termo Grupo Raposos é sugerido para a UPS do Orógeno da Ribeira, representando associação mais distal da bacia (e.g, Heilbron *et al.*, 2017; 2019; 2020).

Os Grupos Andrelândia e Raposos, no Orógeno Ribeira Central, compreendem um espesso pacote de metassedimentos siliciclásticos Neoproterozóicos intercalados com rochas metabásicas que sugerem estágios magmáticos atribuídos a pulsos tectônicos da evolução da Bacia de Andrelândia (Paciullo *et al.*, 2000). A distribuição da sedimentação foi disposta na borda sudeste do Paleocontinente São Francisco (Paciullo *et al.*, 2000; 2003) e os metabasitos interlamelares e corpos meta-ultrabásicos, que ocorrem paralelamente à foliação principal da rocha hospedeira, sugerem episódios tectono-magmáticos durante a bacia (Paciullo *et al.*, 2000; Ribeiro *et al.*, 1995; Gonçalves; Figueiredo, 1992; Marins, 2000; Heilbron *et al.*, 2019; Queiroga, 2010). Conforme relatado por vários autores, os contatos entre as rochas metabásicas e as rochas metassedimentares são acentuados e nenhum sinal de texturas miloníticas foi detectado. As rochas metabásicas apresentam a mesma deformação e fácie metamórfica das rochas metassedimentares de base

Na região proximal, aflorando no SEI (Domínio Andrelândia), três unidades foram individualizadas no Grupo Andrelândia: os gnaisses bandados de biotita com intercalação de

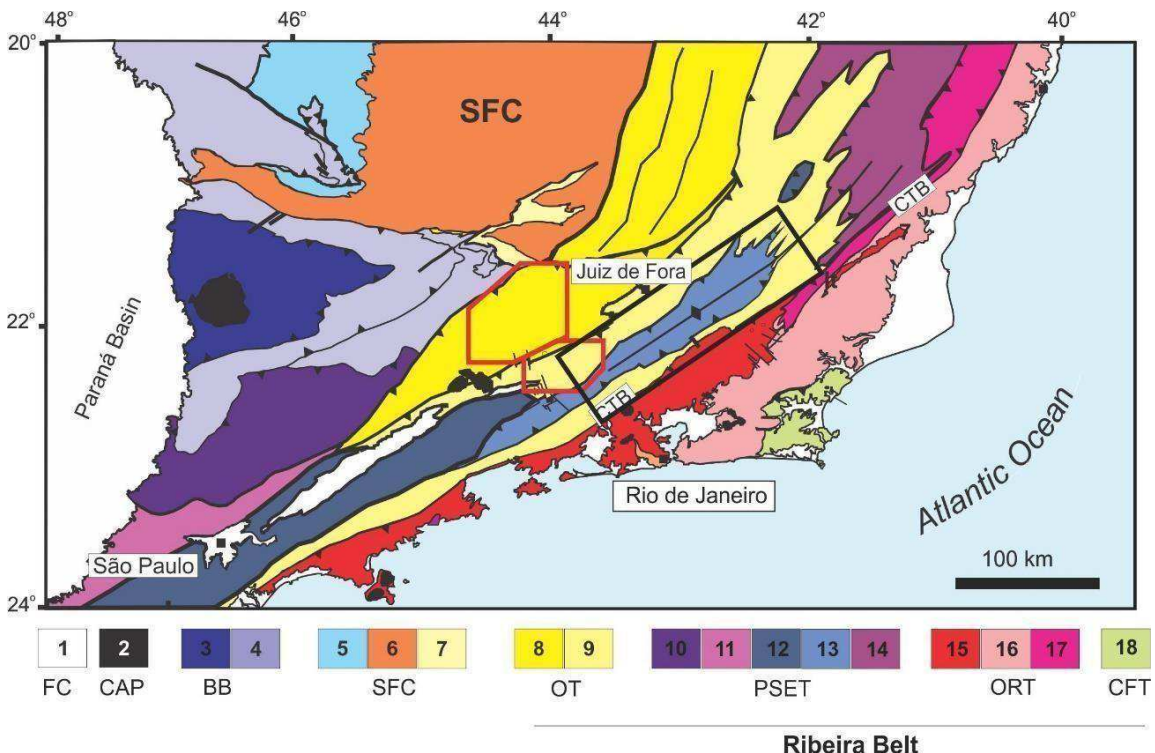
quartzitos e xisto-gnaisses (equivalente a A1+A2 de Paciullo *et al.*, 2000), plagioclásio gnaisses xistosos ricos (biotita xisto equivalente a A5) e biotita pelítico xistas e gnaisses ricos granada, com quartzitos, calcisilicaticas e rochas ricas em Mn e Fe (equivalentes a A6). Na parte distal da bacia SES (Domínio Juiz de Fora), apenas duas unidades foram mapeadas dentro do grupo Raposos, A1 + A2 e A6. Outras diferenças entre os Grupos Andrelândia e Raposos são a evolução tectono-metamórfica e o estilo estrutural:

- a) No Sistema de Empurrão Inferior, as rochas do grupo Andrelândia exibem um gradiente metamórfico invertido com rochas de alta pressão e um estilo estrutural complexamente dobrado acoplado a rochas do embasamento (Trouw *et al.*, 2000; 2013).
- b) No Sistema de Empurrão Superior, as rochas do grupo Raposos exibem fácies granulítica de soleira de alta temperatura paragênese, com poucos relictos de alta pressão. O estilo estrutural é caracterizado por uma intensa interdigitação tectônica entre unidades metassedimentares e rochas do embasamento do Complexo de Juiz de Fora (Heilbron *et al.*, 1998; 2000; 2017; Duarte *et al.*, 1997; Heilbron *et al.*, 2019; Araújo *et al.*, 2019; maior detalhe próxima seção).

Dados anteriores de U-Pb sobre as rochas metabásicas produziram idades de cristalização propostas muito conflitantes, variando de ca. 1,4-1,5 Ga e 2,1-2,2 Ga (Coelho *et al.*, 2017; Frugis *et al.*, 2018; Pinheiro *et al.*, 2019), mais antigos que as rochas hospedeiras metassedimentares. Conforme relatado por Gonçalves e Figueiredo (1992) no SEI, as rochas metabásicas registram magmatismo intraplaca e sinal E-MORB para as porções inferior e superior, respectivamente. Esses corpos toleíticos apresentam idades modelo TDM de 1,2 a 1,05 Ga, com valores de  $\delta\text{Nd}(1,0)$  de +4,8 e +3,1, refletindo reservatórios mantélicos esgotados com curto tempo de residência crustal (Gonçalves; Figueiredo, 1992; Figueiredo *et al.*, 1995; Paciullo, 1997). Para as unidades intermediárias do grupo Andrelândia, LTS, rochas metabásicas retroeclogíticas registraram idades U-Pb em torno de 1,4-1,5 e foram interpretadas como tendo sido relacionadas a episódios de intrusões de paleodiques antes da abertura da Bacia de Andrelândia ou blocos exóticos calimianos dentro do prisma acrecional (Coelho *et al.*, 2017; Frugis *et al.*, 2018). As idades Paleoproterozóicas fundadas por Pinheiro *et al.* (2019) para essas rochas colocadas no LTS foram interpretadas como um evento magmático Riaciano relacionado a configurações de suprasubducção no paleocontinente sul do SF. No entanto, poucas idades U- Pb mais jovens e mais compatíveis ca. de ca. 760, 670 e 645 Ma, juntamente com as idades do modelo TDM de 1,18 a 1,05 são consideradas a melhor estimativa para o magmatismo sin- deposicional (Belém *et al.*, 2011;

1989; 2019; Campos Neto; Caby, 1999; Reno *et al.*, 2009, Trouw, 2009). Neste caso, todas as rochas mais antigas devem ser interpretadas como herança, pois as idades são compatíveis com as unidades do embasamento descritas.

Figura 2 - Mapa tectônico da Faixa Ribeira central modificado de Heilbron *et al*



Legenda: Os polígonos vermelhos abertos marcam a localização da área de estudo. 1: Cobertura Fanerozóica; 2: rochas alcalinas K-T; 3: nappes relacionadas à margem passiva; 4: nappes relacionadas ao arco; 5: embasamento cratônico; 6: Cobertura Bambuí; 7: Unidades rifte-a-sag Mesoproterozóicas; 8-9: Terreno Ocidental com 8 - Andrelândia (Empurrão Inferior) e 9 - Juiz de Fora (Empurrão Superior). Terrenos acrescidos do arco cordilheiro, com 10: Apiaí; 11: Socorro; 12: Embú; 13: Paraíba do Sul; 14: Rio Doce; 15: Arco do Rio Negro; 16: Arco de Italva; 17: metassedimentos de alto grau; 18: Terreno Cabo Frio. PC- Cobertura Fanerozóica; Províncias CAP-Cálcio-Alcalinas; Faixa BB-Brasília, SFC- Craton do São Francisco; OT- Terreno Ocidental; PSET-Terreno Paraíba do Sul-Embu, ORT-Terreno Oriental; CFT- Terreno Cabo Frio. CTB-Central Tectonic Boundary.

Fonte: Heilbron et al. (2017a).

### 1.3 Complexo Juiz de Fora

No Sistema de Empurrão Superior (Figura 2), a unidade metassedimentar Neoproterozóica distal equivalente é denominada Grupo Raposos (equivalente distal do Grupo Andrelândia, Heilbron *et al.*, 2013; 2021), que é tectonicamente intercalada com as rochas granulíticas do embasamento de composições químicas variadas pertencentes ao Complexo

Juiz de Fora (e.g., Trouw *et al.* 2000; Heilbron *et al.*, 2004; Noce *et al.*, 2003; 2007; Degler *et al.*, 2018).

O Complexo de Juiz de Fora foi previamente descrito como uma série de rochas formadas sob uma configuração de arco intra-oceânico (por exemplo, Noce *et al.*, 2007; Heilbron *et al.*, 1998; 2010), porém estudos recentes (Araújo *et al.*, 2021; Almeida *et al.*, 2021), incluem rochas de arco magmático evoluídas e interpretadas como resultado de ciclos tectônicos complexos.

As rochas mais antigas têm assinaturas em forma de arco e são representadas por magmatismo toleítico de baixo K em ca. 2445 Ma, seguido por magmatismo TTG-sanukitóide moderadamente juvenil a evoluído em ca. 2200-2070 Ma, seguidos por toleítos de arco insular de 2200-2040 Ma e rochas granítóides colisionais híbridas em ca. 2030-2010 Ma; e uma associação bimodal de E-MORB e charnockitos em torno de ca. 1,9 Ga, com magmatismo e granítóides pós-colisionais híbridos sendo encaixados em ca. 2,04 a 1,9 Ga (Araújo *et al.*, 2021; Almeida *et al.*, 2021). Em estudos recentes, alguns dados indicam o registro de herança arqueana nos ortogranulitos do Complexo de Juiz de Fora como mostram por idades modelo Hf TDM de 3,45 a 2,75 Ga e idades modelo Nd T DM de 3,20 a 2,75 Ga (Silva *et al.*, 2002; Degler *et al.*, 2018; Araújo *et al.*, 2019; 2021; Kuribara *et al.*, 2019; Almeida *et al.*, 2021).

Idades Paleoproterozóicas mais jovens de cerca de 1,7-1,6 Ga também foram relatadas para maficas granulitos de tendência alcalina, ocorrendo no setor noroeste do estado do Rio de Janeiro (Heilbron *et al.*, 2010). Essas rochas maficas mais jovens foram interpretadas como relacionadas ao evento de rifteamento Espinhaço do paleocontinente São Francisco (Brito Neves, 1995; Martins-Neto, 2000).

As condições metamórficas Brasilianas registradas nos ortogranulitos do Complexo de Juiz de Fora foi estimado em 700 - 850°C, em pressões de 4 a 7 kbar, associado a um caminho P-T-t no sentido horário. Esta estimativa foi baseada em assembléias minerais e inclusões fluidas (Duarte, 1998; Nogueira *et al.*, 2004; Medeiros-Junior *et al.*, 2017). Semelhante resultados também foram obtidos por Kuribara *et al.* (2019) para os ortognaisses com estimativas de 680–770 °C e 6,0–7,7 kbar obtidos usando alumínio em hornblenda como geobarômetro e o par hornblenda-plagioclásio como um geotermômetro (Hammarstrom; Zen, 1986; Holland; Blundy, 1994). Embora raro, poucos autores têm sugerido o metamorfismo pré-Brasiliano para as rochas do Complexo de Juiz de Fora com base na textura granoblástica dos ortogranulitos que se formou antes da principal foliação penetrativa no evento metamórfico Brasiliiano (Duarte, 1998) ou em texturas e morfologias de zircões (Araujo *et al.*, 2021).

As

condições metamórficas pré-Brasiliano foram estimadas por Duarte *et al.* (2000), usando o termômetro Opx+Cpx produzindo um T max de 895 °C e pressões intermediárias.

## 2 METODOLOGIA

A metodologia aplicada no projeto inclui um levantamento bibliográfico de dados preexistentes e a integração de 1: 50.000 cartas geológicas presentes no acervo do Tektos Research Group. Este levantamento também abrange teses e dissertações anteriores, que contêm informações detalhadas sobre a geologia de fundo da área do campo. Foi realizado mapeamento de campo na área alvo que contempla as rochas metabásicas do Grupo Andrelândia-Raposos, bem como as rochas básicas do Complexo Juiz de Fora, visando a descrição geológica detalhada desses corpos máficos. Foram efetuados estudos litogeoquímicos para determinar as séries magmáticas dos corpos metabásicos e o respectivo ambiente tectônico. Para identificar e caracterizar os distintos corpos toleíticos com diferentes histórias evolutivas, é essencial obter idades de cristalização, tempo estimado de extração do manto ou duração da residência crustal ( $\epsilon_{Nd}$ ), se as rochas contêm herança/contaminação crustal e determinar a evolução metamórfica do amostras. Isso será feito usando uma combinação de métodos isotópicos (U-Pb em zircão e rocha total Sm-Nd, Lu-Hf em zircão), bem como elementos principais de rocha total e análise de química mineral, que serão utilizados para determinar as condições P-T. Descrição mais detalhada de cada metodologia utilizada nesta tese está bem descrita na seção dos resultados.

### 3 RESULTADOS

#### 3.1 An example of a Neoproterozoic hyperextended margin: An integrated perspective of the basic magmatism recorded in the Andrelândia Basin, central Ribeira Orogen, SE-Brazil

Talitta Nunes Manoel <sup>a,\*</sup>, Monica Heilbron <sup>a</sup>, Kathryn Cutts <sup>a,b</sup>, Ivo Dussin <sup>a</sup>, Gloria Marins <sup>a</sup>, Jailane <sup>a</sup>, Marcela Lobato <sup>a</sup>, Claudio de Morisson Valeriano <sup>a</sup>, Henrique Bruno <sup>a</sup>

*a Rio de Janeiro State University, Programa de Pós-Graduação, Faculdade de Geologia (FGEL) – TEKTOS. UERJ, São Francisco Xavier Street, 524-Maracaná, Rio de Janeiro, Brazil*

*b Geological Survey of Finland, P.O. Box 96, FI-02151 Espoo, Finland*

#### ABSTRACT

#### ARTICLE INFO

##### Keywords:

Central Ribeira Belt Neoproterozoic magmatism  
Hyperextended Passive margin U-Pb geochronology  
Sm-Nd isotopes

Deformed amphibolite to granulite-facies metasedimentary rocks of Andrelândia and Rapos Group, associated metabasic rocks witnessed the evolutionary stage of the Andrelândia sedimentary basin, within Central Ribeira orogen, bordering the southern São Francisco Craton. Despite detailed geological maps and provenance studies, there is still a knowledge gap and debate on the stratigraphic pile and the age of sedimentation in the Andrelândia basin. New data regarding metabasic rocks interlayered in Andrelândia basin is presented, including detailed geological mapping, lithogeochemistry, Sm-Nd and Rb-Sr isotopes and LA-ICPMS U-Pb zircon geochronology. The metabasic rocks occur as centimetric to metric lenses with sharp contacts with the meta-sedimentary country rocks, displaying the same ca. 620–580 Ma age span of metamorphism and deformation. Geochemical results indicate high-TiO<sub>2</sub> within-plate to low-TiO<sub>2</sub> MORB to E-MORB signatures for lower and upper units of the distal Rapos Group. Additionally, only low-titanium MORB-like metabasites were found in the most proximal unit, Andrelândia Group. One sample within the Rapos Group yielded crystallization age of ca. 653 Ma, metamorphic overprint at ca. 579 Ma and Paleo to Mesoproterozoic inherited zircon grains. The metabasic rocks interleaved in the Andrelândia Group, Nd TDM model ages are between 1.10 and 1.90 Ga, with εNd (653 Ma) varying between -8 to +2.1 and <sup>87</sup>Sr/<sup>86</sup>Sr (653 Ma) values between 0.7144 and 0.7033. Nd TDM model ages are between 1.80 and 2.0 Ga, with negative εNd (653) -14 to -0.2 and initial <sup>87</sup>Sr/<sup>86</sup>Sr between 0.7157 and 0.7043. The results indicate an isotopic similarity with the biotite schists of the Santo Antônio Unit, previously considered as arc-derived in an active margin setting. Together with previously published isotopic and geochronology data, and with the structural distribution of the units and tectonic interleaved basement slices in the distal Rapos Group, we envisage a tectonic model with *syn-to-late* depositional basic magmatism between ca. 760 to 653 Ma. The proposed model compares the evolution of Andrelândia-Rapos basin with modern hyper-extended magma poor rifted continental margin sedimentary basins as plausible tectonic setting. Finally, the results are compared with those from the Araçuaí orogen, the Northern part of the Araçuaí-Ribeira Orogenic System, displaying similarities in ages and composition.

#### 1. Introduction

Intercalations of tholeiitic basic rocks interlayered within sedimentary strata are very common in various tectonic settings, from continental rifts to passive margins and oceanic plateaus in extensional regimes, and also in convergent settings, such as magmatic arcs and back-arc settings, as well as in post-collisional phases of orogenic belts

(Pearce and Cann, 1973; Pearce et al., 1975; Pearce, 1983, 1987; Wilson, 1989; Saccani, 2015).

In many high-grade metamorphic units exposed in deeply eroded orogenic belts of Western Gondwana (Ganade de Araújo, 2014; Coelho et al., 2017; Tedeschi et al., 2017; Kuster et al., 2020; Fig. 1), the original tectonic setting of the precursor basin commonly remains unclear because high temperature recrystallization and deformation obliterate

most features of the metasedimentary rocks. The U-Pb age of detrital zircon technique for provenance studies of supracrustal units normally yield imprecise sedimentation ages, since often the youngest detrital zircon is much older than depositional ages especially in rift to passive margin settings developed in older cratonic areas of paleocontinents (Bel’em et al., 2011; Santos., 2011; Coelho et al., 2017; Frugis et al., 2018; Kuster et al., 2020). In these cases, the study of interlayered basic rocks, concerning both geochemical-isotopic signatures and geochronology can be an important tool to constrain depositional ages and tectonic environments.

Other interesting aspect for past rift to passive margin sedimentary basins is the investigation of the possible development between magma poor (hyperextended) and magma rich rifted continental margins, the two end-members that have been recognized in the present-day passive margins (Sutra and Manatschal, 2012; Zalan et al., 2011; Dore and Lundin, 2015; Peron-Pindivic and Manatschal, 2019).

The Ribeira Orogen (RO), southeast Brazil, integrates the Araquáí-Ribeira Orogenic System (AROS), that represents one of the Neoproterozoic to Early Paleozoic network of Brasiliano orogenic belts that resulted from the amalgamation of Western Gondwana (Fig. 1). In Brazil, the AROS makes up a 300 km wide and 600 km long deeply eroded orogenic system that runs roughly parallel to the country southeastern coast (Trouw et al., 2000, 2013; Campos Neto et al., 2000, 2004; Heilbron et al., 2004, 2008, 2017a; Pedrosa-Soares et al., 2008; Alkmim et al., 2017; Fig. 1b). The external zone of this orogenic system comprises the reworked Neoproterozoic passive margin of the São Francisco paleocontinent. Because of deformation and metamorphism related to the Brasiliano collage, the metasedimentary units together with syn-depositional magmatic rocks occur out as high-grade gneisses, that were tectonically interleaved with highly deformed basement slivers during the collisional orogeny.

The Andrelândia Group or Megasequence (Paciullo et al., 2000; Heilbron et al. 2017) has been regarded as representative of a Neoproterozoic passive margin basin developed around the southern margin of the São Francisco Craton (SFC). In this area, units of the Andrelândia basin were involved in the convergence of two orogenic episodes both related with the amalgamation of the Gondwana supercontinent: the older (640 to 600 Ma), E-verging, southern Brasília Orogen (Valeriano., 2017), and the younger (600–565, and 535–510 Ma) NW verging

Ribeira Orogen (e.g., Heilbron et al., 2017). Many previous works using U-Pb, Nd and Sr, and more recently Lu-Hf isotope data (e.g., Frugis et al., 2018; Lobato, 2018; Kuster et al., 2020; Marimon et al., 2020) have contributed to discuss the sources and maximum depositional ages for the Andrelândia Group between Tonian and Cryogenian times (900 to 670 Ma, e.g., Belém et al., 2011; Santos., 2011; Frugis et al., 2018; Kuster et al., 2020). On the other hand, relatively few works focused on basic magmatism. As highlighted by Heilbron et al. (2019), it has proved an essential tool to reveal Tonian to Cryogenian magmatic episodes that help untangle the tectonic evolution of the Andrelândia basin, as possible sources for the younger zircons detected by the U-Pb studies in the metasedimentary units.

This work brings new petrographic, geochemical, Nd-Sr isotopic, and U-Pb geochronological data as well as a geological mapping of the metabasic rocks integrated published U-Pb studies of the Andrelândia Group, including its most distal equivalent the Raposos Group, in order to understand the tectonic setting and processes involved during the basin evolution. The obtained dataset is discussed together with provenance data for the proximal metasedimentary units and associated metabasic rocks, to build an integrated overview of basin evolution. Finally, data is correlated with similar studies reported in the Araquáí Orogen northwards, to constrain the overall Neoproterozoic passive margin evolution of the ESE border of the SF paleocontinent.

## 2. The Ribeira Orogen tectonic organization

The amalgamation of Western Gondwana led to the formation of several Neoproterozoic-Cambrian orogenic systems surrounding Archean and Paleoproterozoic cratons (Fig. 1). The Ribeira-Araquáí Orogenic System (AROS) developed as the result of the closure of the Adamastor ocean, involving diachronic collisions of different tectono-stratigraphic terranes including a micro paleocontinent and magmatic arcs (e.g., Heilbron et al., 2017; Pedrosa-Soares et al., 2008, 2011; Alkmim et al., 2017; Degler et al., 2017; Campos Neto et al., 2004), (Fig. 1).

The tectonic organization of the central segment of the Ribeira Orogen comprises four tectono-stratigraphic terranes from NW to SE: the Occidental, Central, Oriental and Cabo Frio terranes (Fig. 2), which progressively docked against the southern tip of the SF paleocontinent

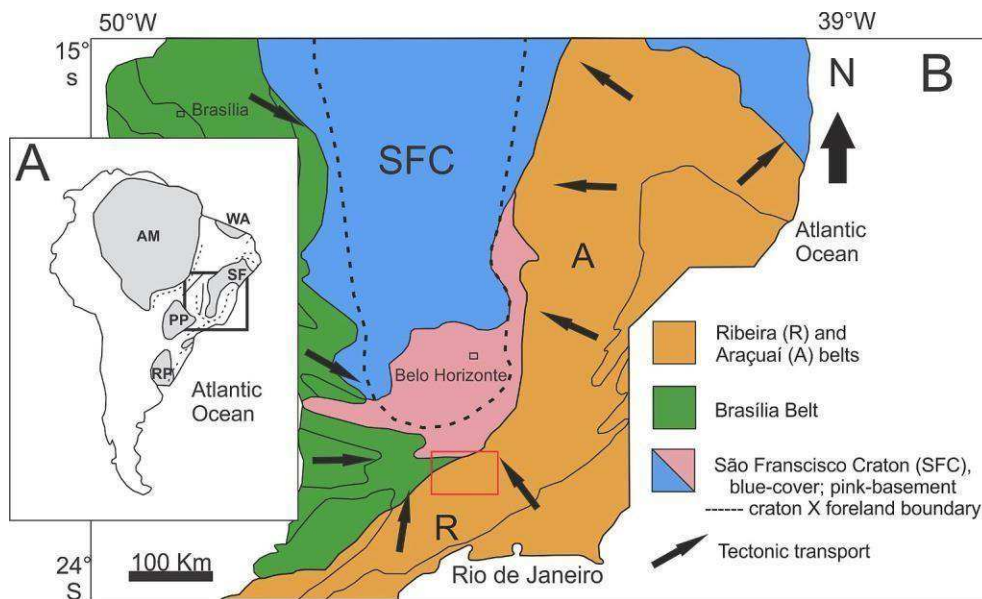


**Fig. 1.** a) Location in South America of the AM-Amazonian, WA- West African, SF-S~ão Francisco, PP- Paranapanema and RP- Rio de la Plata cratons. b) Location of the Andrelândia Group main outcrop area in relation to the São Francisco Craton and Neoproterozoic orogens. Red rectangle: the study area. Simplified tectonic sketch map modified from Trouw et al. (2013) and Kuster et al. (2020).

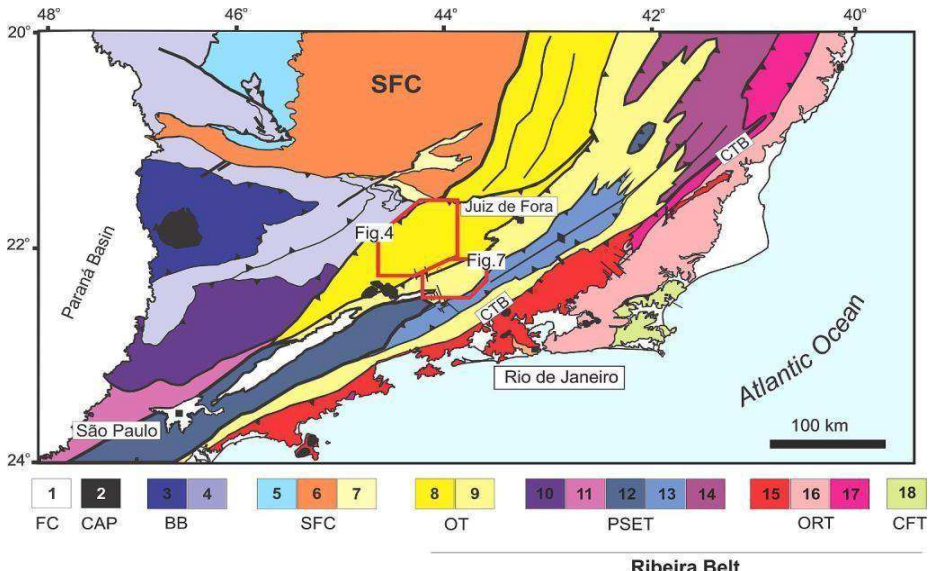


**Fig. 2.** Tectonic map of central Ribeira Belt modified from Heilbron et al. (2017a). The open red polygons mark the location of Figs. 4 and 7. 1: Phanerozoic cover; 2: K-T alkaline rocks; 3 and 4 east-verging units of the Brasília Belt, including the Guaxupé nappe and lower nappes; 5: cratonic basement; 6: Bambuí cover; 7: Mesoproterozoic rift-to-sag units; 8–9: Occidental Terrane with 8 - Andrelândia (lower thrust) and 9 - Juiz de Fora (upper thrust). Cordilleran arc accreted terrane, with 10: Apiaí; 11: Socorro; 12: Embú; 13: Paraíba do Sul; 14: Rio Doce; 15: Rio Negro arc; 16: Itáva arc; 17: high-grade metasediments; 18: Cabo Frio Terrane. PC- Phanerozoic cover; CAP-Calc-Alkaline Provinces; BB-Brasília Belt, SFC- São Francisco Craton; OT- Oriental Terrane; PSET-Paraíba do Sul-Embu Terrane, ORT- Oriental Terrane; CFT-Cabo Frio Terrane. CTB-Central Tectonic Boundary.

(Heilbron et al., 2008, 2017, 2020). The OcT (Occidental Terrane) encompasses the Neoproterozoic passive margin (Andrelândia Group- Paciullo et al. 2000) and reworked cratonic basement (Heilbron et al., 2010; Degler et al., 2017; Cutts et al., 2019; Bruno et al., 2020, 2021). It is structurally subdivided into two crustal thrust sheet systems, the Lower Thrust System (LTS) (Andrelândia Domain), and the Upper Thrust System (UTS) (Juiz de Fora Domain) (Heilbron et al., 1998, 2000, 2010).

In the Lower Thrust System, the Piedade microcontinent and Mantiqueira Complex (Heilbron et al., 1998, 2010; Duarte et al., 2004; Bruno et al., 2020, 2021) represent Archean to Paleoproterozoic basement units that folded together with the Andrelândia Group cover (Fig. 2). In Upper Thrust System, the basement association is composed of orthogranulites and orthogneisses rocks of the Juiz de Fora Complex which is tectonically interlayered (Fig. 2) with the distal facies of the Andrelândia Group, known as the Raposos Group (e.g., Trouw et al., 2000; Ribeiro et al., 2003; Heilbron et al., 2004; Noce et al., 2003, 2006; Barbosa et al., 2021; Almeida et al., 2021, Degler et al., 2017; Heilbron et al., 1998, 2010; Noce et al., 2007; Degler et al. 2018) (Fig. 2).

The autochthonous domain of the Ribeira Orogen contains the reworked nappes of the southern part of the older Brasília Orogenic System (BOS), developed as the product of the closure of the Goianides Ocean (e.g., Alkmim et al., 2017). The E-verging external nappes of this orogenic system were reworked by the NW-verging shortening imposed by the tectonic evolution of the Ribeira Orogen.

### 3. The Andrelândia basin units in the Ribeira belt: Previous work and a simplified subdivision

The Andrelândia Group or Megasequence has been interpreted as the Neoproterozoic passive margin of the southern and SSE margin of the SFC involving both the thrust units of the southern BOS and the Ribeira Orogen of the AROS (Paciullo et al., 2000; Heilbron et al., 2017). One major problem is that most authors tried to integrate the tectonic-stratigraphic piles of the Andrelândia Group in two different Neo-proterozoic Orogenic Systems, i.e., the older (ca. 650 – 630 Ma) E-verging Brasília Orogen and the younger (ca. 620 – 530 Ma) NW-verging Ribeira Orogen (Fig. 1).

Part of the Andrelândia Group crops out in the superposition zone between these two orogens although the limits between these two belts

is still a matter of debate. Part of the authors considered this “interference zone” as part of the Brasília Orogen (Trouw et al., 2000, 2013; Campos Neto and Caby, 2000; Campos Neto et al., 2020; Frigis et al., 2018; Kuster et al., 2020; Marimon et al., 2020) while others consider that the “interference zone” represents the reworked portion of the Brasília Orogen by the Ribeira Orogen (Valladares et al., 2004; Heilbron et al., 2017, Valeriano et al., 2004, 2017; Ebert et al., 1958).

Different stratigraphic subdivisions have been proposed, such as the tentative reconstruction of the six lithostratigraphic units grouped in two sequences by Paciullo et al. (2000) or composite tectonic units as reported by Heilbron et al. (2019) and Campos Neto et al. (2020). The first integrated stratigraphic subdivision of the Andrelândia Group was proposed by Paciullo et al. (2000), considering both the southernmost nappes of the Brasília Orogen and the LTS of the Occidental terrane in the Ribeira Orogen (Figs. 1 and 2). These authors subdivided the Andrelândia Group into two main sequences:

i) The basal Carrancas Sequence: biotite banded paragneiss with pelitic layers and amphibolites (A1 and A2); micaceous quartzite layers (A3); and intercalations of graphite-rich phyllite/schist and ortho-quartzites (A4).

ii) The upper Serra do Turvo Sequence: plagioclase-biotite rich biotite schist/gneiss with metapelitic layers and quartzite (A5) and meta-pelitic schists and gneisses (A6).

It is important to emphasize that units A3 and A4 mapped in the Southern Brasília Orogen cannot be recognized in the distal segment of the Andrelândia Group (LTS) and in the Raposos Group (UTS), in the central segment of the Ribeira Orogen. For the purpose of this contribution, which is focused on the interlayered metabasic rocks, a simplified lithostratigraphic subdivision is adopted and tentatively correlated with the previously proposed subdivision of Paciullo et al. (2000), (Fig. 3). It is important to stress that adopted lithostratigraphic units adopted here (see Fig. 3) are based on detailed geological maps of the Andrelândia basin units on the Central Ribeira belt, integrated with 1:100.00 scale geological maps (up to 9 sheets) published by the Brazilian Geological Survey ([www.rigeo.cprm.gov.br](http://www.rigeo.cprm.gov.br)).

Other contributions (e.g., Westin et al., 2016), working within the same region (LTS), have proposed that the lower units of the Andrelândia Group of Paciullo et al. (2000), A1 + A2, classified as São Vicente Unit, are older (ca. 2.1 Ga), thus belonging to the basement s of the São Francisco Craton. This proposition is based on the

Andrelândia Sequence Units	Brasília Orogen Nappes			Ribeira Belt Orogen	Ribeira Belt Orogen
	Main collisional episode	Authochthonous		β	Upper Thrust System
	Stratigraphic nomenclature	ca. 650-630 Ma	Andrelândia Group	ca. 620-580 Ma	ca. 620-580 Ma
	Lithostratigraphic Units			Andrelândia Group	Raposos Group
Rio do Turvo Sequence	A6-Garnet rich schists gneisses	A6		A6-Upper pelitic Unit (758Ma*, a), β	
	A5-plagioclase rich schist gneisses	A5	A5	A5-plagioclase rich schist-gneisses (680-640* Ma, b)	
Carrancas Sequence	A4-Quartzites and graphite schists	A4	A4		
	A3-green micaquartzites and schists	A3			
	A2-banded gneisses with schists and quartzites	A2	A1+A2	A1+A2-lower biotite banded gneiss , (950Ma*, c), β	A1+A2-lower biotite banded (766Ma**,d), gneiss
	A1-A2-banded gneisses	A1			
Basement Units	1.7 to 1.3 magmatism Pre-1.8 Ga	SFC, Mineiro belt	Mineiro belt, Piedade	X	X
				Mantiqueira Complex	Juiz de Fora Complex

a Frugis et al. (2018)

References b Belém et al. (2011); Santos (2011); Westin & Campos Neto. (2013); Frugis et al. (2018); Kuster et al. (2020); Campos Neto et al. (2020)

c Belém et al. (2011)

d Heilbron et al.(2019)

\* Maximum depositional age U-Pb

\*\* Crystallization age U-Pb

**Fig. 3.** Andrelândia Group lithological units according to this paper, and the correlation with the units described by Belém et al. (2011); Campos Neto et al. (2020) Santos (2011); Frugis et al. (2018) and Westin and Campos Neto (2013).

Paleoproterozoic unimodal detrital zircon U-Pb ages obtained from banded gneiss samples of units A1 + A2 units, even though Neo- proterozoic young detrital zircons have been found throughout the Andrelândia units (Belém et al. 2011; Santos., 2011; Lobato., 2018; Heilbron et al. 2019). However, our studies have shown that the contacts between banded biotite paragneisses A1 + A2 with interlayered quartzites and quartz schists in the Lower Thrust System (Andrelândia Domain) are gradational and not tectonic. There are no mylonitic rocks detected along these contacts. On the other hand, at the top of the pile (Units A5 and A6), close to the overlying high-pressure units, basement slices of plutonic orthogneisses were tectonically interleaved within the Andrelândia with mylonitic features along the contacts (Trouw et al., 2000,2013; Heilbron et al., 2000, 2004, 2008, 2017; Cioffi et al., 2016). A simplified stratigraphic nomenclature is adopted here, where the term Andrelândia Group is used for the proximal units of the basin, including the LTS of the Ribeira Orogen and the nappes of the southern BOS, whereas the term Raposos Group is suggested for the UTS of the Ribeira Orogen, representing more distal association of the basin.(Heilbron et al., 2017, 2019) (Fig. 3).

The Andrelândia and Raposos Groups in the Central Ribeira Origen comprise a massive pile of Neoproterozoic siliciclastic metasedimentary rocks intercalated with metabasic rocks (Paciullo et al., 2000). The sedimentation distribution was disposed along the southeastern margin of the São Francisco Paleocontinent (Paciullo et al., 2000, 2003) and the intercalated metabasites and meta-ultrabasic bodies, that occur parallel to the host rock's main foliation, suggest tectono-magmatic episodes during basin development (Gonçalves and Figueiredo., 1992; Ribeiro et al., 1995; Marins., 2000; Paciullo et al., 2000; Queiroga, 2010; Heilbron et al., 2019).

As reported by many authors, the metabasic rocks display the same deformational and metamorphic features of the enclosing metasedimentary rocks, and their contacts with the metasedimentary rocks are sharp and devoid of any mylonitic textures.

In the LTS (Andrelândia Domain), three proximal units were individualized in the Andrelândia Group have been identified: the banded biotite gneisses with quartzite and schist-gneisses intercalation (equiv- alent to A1 + A2 of Paciullo et al., 2000), plagioclase rich schists to gneisses (biotite schist equivalent to A5) and garnet-rich metapelitic biotite schists and gneisses, with quartzite, calcsilicate and Mn-and- Fe rich intercalation (equivalent to A6).In the distal part of the basin UTS (Juiz de Fora Domain), two units are mapped within the Raposos Group: A1 + A2 and A6. Other differences between the Andrelândia and Raposos Groups are the tectono- metamorphic evolution and the structural style:

i) In the LTS, rocks of the Andrelândia Group display an inverted metamorphic gradient with high-pressure rocks and a complexly folded structural style coupled with basement rocks (Fig. 4; Trouw et al., 2000, 2013).

ii) In the UTS, the rocks of the Raposos Group display high- temperature sillimanite-garnet parageneses of granulites, with few high-pressure relicts minerals. The structural style is characterized by an intense tectonic interleaving of metasedimentary units and with the basement rocks of the (Juiz de Fora complex (Heilbron et al., 1998, 2000,2017; Duarte et al., 1997, Heilbron et al., 2019; Araujo et al., 2019).

Previous U-Pb data regarding the metabasic rocks yielded conflicting interpreted crystallization ages, varying from ca. 1.4–1.5 Ga to 2.1–2.2 Ga (Coelho et al., 2017; Frugis et al., 2018; Pinheiro et al., 2019), all older than the metasedimentary hosts rocks. As reported by Gonçalves and Figueiredo. (1992) in the LTS, the metabasic rocks are composi- tionally characterized as representing intraplate magmatism with E- MORB signatures for the lower and upper portions. These bodies of tholeiitic affinity yield  $T_{DM}$  model ages of 1.20 to 1.05 Ga, with  $\Sigma Nd_{(1.0)}$  values of + 4.8 and + 3.1, reflecting depleted mantle reservoirs with short crustal residence time (Gonçalves and Figueiredo, 1992; Figueiredo et al., 1995; Paciullo, 1997). For the intermediate units of the Andrelândia Group, LTS, retroeclogitic metabasic rocks records U-Pb ages around 1.54–1.4 Ga and were interpreted as have been related to episodes of paleodyke intrusions before the development of the Andrelândia Basin, or alternatively representing Calymmian exotic blocks within an accretionary prism (Coelho et al., 2017; Frugis et al., 2018). The Paleoproterozoic ages found by Pinheiro et al. (2019) for these rocks placed in the LTS were interpreted as a Rhyacian magmatic event related to suprasubduction settings in the southern SF paleo- continent. However, few younger and more compatible U-Pb ages of ca. 760, 670 and 645 Ma together with ca. 1.18 to 1.05 Ga  $T_{DM}$  model ages are considered the best estimates for the syn-depositional magmatism (Belem et al., 2011, Campos Neto et al. 2007; Heilbron et al., 1989, 2019; Campos Neto and Caby, 2000;Reno et al., 2009 ). In this case, all older dated zircon grains should be interpreted as inherited, since their ages are compatible with those of basement units (e.g. Almeida et al., 2021; Araujo et al., 2021).

This work brings a detailed study of the metabasic rocks and geometric relations with the country rocks included within the metasedi- mentary units of the Andrelândia and Raposos Group. An integration of geochemical compositions and isotopic signatures, together with new U- Pb ages aimed to include the metabasic rocks in a broader tectonic evolutionary model for the basin.

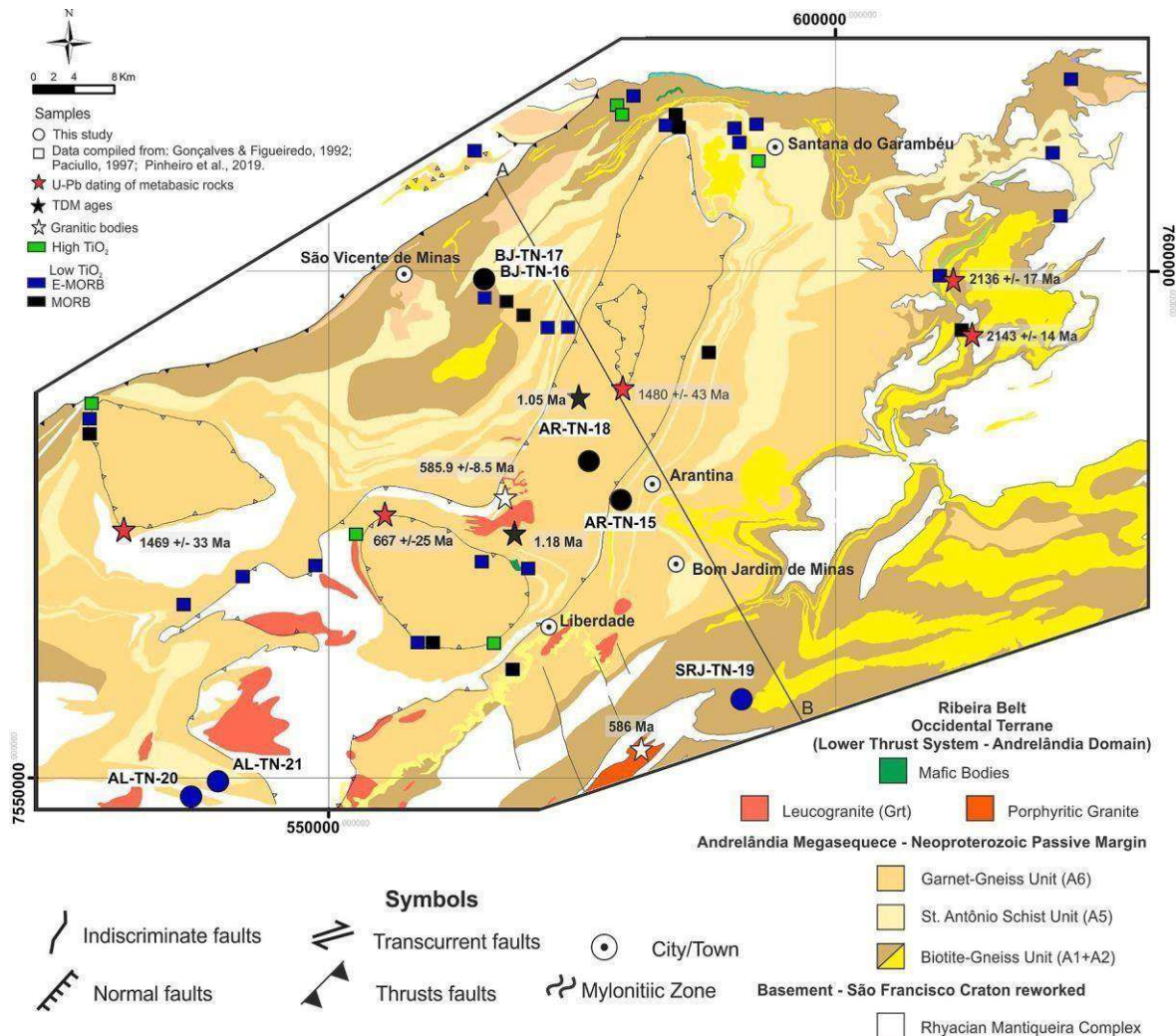


**Fig. 4.** Geological map of the study area showing the all-available geochemical and age data for the metabasic rocks within Andrelândia Group.

#### 4. Methods

Field excursions were carried out in the study area (Fig. 2) for sample collection and geological characterization of the mafic bodies. An initial step was made in the southwestern Raposos Group, Upper Thrust System, compiling the pre-existing geochemical data (Marins., 2000) with the new mafic bodies integrating a total of 19 samples within this segment. The second step consisted of investigating the mafic bodies interleaved in the proximal segment of the Andrelândia Group, within the Lower Thrust System.

##### 4.1. Lithogeochemistry

The selected samples were prepared for analyses of major and trace elements composition analyses, including Rare-Earth Elements – REE. Samples were crushed and milled at the LGPA laboratory (“Laboratorio Geologico de Processamento de Amostras”) of the Rio de Janeiro State University.

Whole rock geochemical analyses were carried out at the Activation Laboratories (Actlabs, Ancaster, Canada), following their 4Litho proto- col, a combination of packages Code 4B (lithium metaborate/tetraborate fusion ICP), Code 4B2 (trace element ICP/MS) and Code 4B (major elements and Ba, Sc, Sr, V, Y and Zr) where samples are prepared and analyzed in a batch system. Each batch contains a method reagent blank, certified reference material and samples with 6 % replicates. Samples

are mixed with lithium metaborate and lithium tetraborate and fused in an induction furnace. The melt is immediately poured into a solution of 5 % nitric acid containing an internal standard and mixed continuously until completely dissolved (~45 min). The samples are run for major oxides and selected trace elements (4B) on a combination simultaneous/ sequential Thermo Jarrell-Ash ENVIRO II ICP or a Varian Vista 735 ICP. Calibration is performed using 14 prepared USGS and CANMET certified reference materials. One of the 14 standards is used during the analysis for every group of ten samples. Weight % sum of major elements should stay between 98.5 % and 101 %. Further details of the analytical techniques used by this laboratory are available at <https://www.actlabs.com>. Previous geochemical data from mafic granulites obtained by Marins (2000) were integrated to cover a larger spatial distribution of the Andrelândia Group within the study area (Fig. 2). Treatment of the geochemical data used the GeoChemical Data ToolKIT (GCDkit) soft- ware of Janousek et al. (2006).

##### 4.2. U-Pb geochronology

The sample preparation for the U-Pb systematics involved crushing and manual panning, followed by density and magnetic separation in the LGPA, of the UERJ. The zircon grains mounted in polished sections and were then imaged by cathodoluminescence (CL) and by back-scattered electron (BSE), using Scanning Electron Microscope (SEM) at the MULTILAB, facilities of UERJ. Images were used to recognize

morphological features, internal structures, and the presence of inclusions, cracks or damaged areas.

The U-Pb data for the mafic granulite samples was obtained at the Laboratório de Geocronologia of the Departamento de Geologia da Universidade Federal de Ouro Preto (Brazil) and analyzed using a ThermoScientific Element II sector field (SF) ICP-MS coupled to a CETAC UV Nd-YAG 213 nm laser system (using spot diameter of = 30 µm). The data reduction was performed using the Glitter software (Van Achterbergh et al., 2001). To test the validity of the applied methods and the accuracy and external reproducibility of the obtained U-Pb age data, it was used the BB-9 zircon reference material (562 ± 1 Ma; Santos et al., 2017) was used as primary standard and the Plesovice zircon (337.3 ± 0.4 Ma; Slama et al., 2008) and GJ-1 (608 ± 1 Ma; Jackson et al., 2004) reference materials were used as secondary standards.

The age calculations and plots were performed with the Isoplot 4.15 software (Ludwig, 2008). Uncertainties of individual ages are quoted at 2σ for the sample NSA-FT-02A. Among the performed laser spots analyses, only those with less than 10 % of analytical errors and discordance were considered for age calculations. The complete dataset for the samples and standards can be found in the [Supplementary Material](#).

#### 4.3. Sm-Nd and Sr isotope analysis

For Sm-Nd and Sr isotopes analyses, thirteen mafic granulites samples were selected from the Andrelândia and Raposos Group samples, among those used for the geochemistry study. Sm-Nd and Sr isotopic analyses were conducted in the Laboratory of Geochronology and Radiogenic Isotopes (LAGIR) of the Universidade do Estado do Rio de Janeiro(<https://www.lagir.com.br>). Chemical procedures were carried out in clean rooms with use of Milli-Q® water purifier and of sub-boiling distillation of PA Merck® acids. Between 25 and 50 mg of the pulverized samples were subjected to digestion in Savigex® vessels on hot plates, after the addition of proportional amounts of a double 149Sm-150Nd tracer solution. A mixture of concentrated HF and HNO<sub>3</sub> 6 N was applied for 3 days, followed by further digestion with HCl 6 N for 2 days. Separation of Sr and REE used cation exchange following conventional techniques described in Cardoso et al. (2019).

## 5. Results

### 5.1. Geology and petrographic studies

In this section is provided the main features described during the field mapping and the context of metabasites within the metasedimentary units as well the petrographic characterization the mineralogical diversity of metabasic rocks from both LTS and UTS.

#### 5.1.1. Metabasic rocks of the lower thrust System – Andrelândia Group (Andrelândia Domain - Occidental Terrane)

The studied metabasic rocks are represented by metric to centimetric lenses and boudins within the metasedimentary units that comprise the Andrelândia Group, at the lower thrust system. Mafic rocks display the regional foliation, parallel to the host rocks, and crop out in various stratigraphic positions within the Andrelândia Group. The maps in Figs. 4 and 5 shows that the metabasic rocks occur within the banded biotite-gneiss unit (basal unit equivalent to A1 + A2), hosted in the feldspar-rich biotite schists/gneisses (A5) and in the garnet-biotite-gneiss unit (A6). The contacts of the metabasic rocks with the meta-sedimentary host rocks are sharp (Fig. 6), but not tectonic, as sign of mylonitic textures were detected. The metabasic rocks are parallel to subparallel to the transposed metasedimentary S0 stratification.

The metabasites are amphibolites with a fine-grained granonematoblastic texture, and a pervasive foliation defined by amphibole grains (Fig. 6a, c, e and g). Some few occurrences of retroeclogitic metabasites were described by Coelho et al. (2017) and Reno et al. (2009). The main mineralogy common to all studied samples comprises hornblende, plagioclase, titanite, quartz, and opaque minerals such as ilmenite and magnetite (Fig. 6b, d, f and g). Regarding the presence of biotite and epidote, the studied rocks were subdivided into two groups:

a) epidote amphibolites (samples BJ-TN-17, BJ-TN-18, AL-TN-20, AL-TN-21) and biotite-amphibolite (sample SRJ-TN-19; Fig. 6d). The previously identified retroeclogitic samples were not targeted in this study. In most of the epidote–amphibolite samples, the epidote crystals show hypidioblastic to xenoblastic morphologies and occur between plagioclase and hornblende crystals. Only in sample AL-TN-20 does epidote exhibit euhedral to subhedral grain shapes in association with nematoblastic hornblende crystals and plagioclase (Fig. 6h). Titanite presents xenoblastic morphologies commonly occurring together with opaque phases, often at the borders of hornblende crystals. Quartz can be found as small grains included in hornblende (Fig. 6f) and spread throughout the matrix of the samples along with plagioclase.

In the biotite amphibolite sample (SRJ-TN-19), granoblastic textures predominate, and the biotite occurs as flakes at the edges of coarse-grained nematoblastic hornblende, the sample contains suggesting formation during a retrograde phase. Besides biotite and hornblende, plagioclase, titanite, quartz and opaque phases. As reported for the epidote amphibolites, titanite together with opaque phases occurs at the borders of hornblende. Plagioclase, quartz and titanite together define a granoblastic texture, with titanite growing at the edges of the mafic minerals (Fig. 6c, d). Opaque minerals are rare.

#### 5.1.2. Metabasic rocks of the upper thrust System – Raposos Group (Juiz de Fora Domain - Occidental Terrane)

The Raposos Group crops out in the UTS of the Occidental terrane in

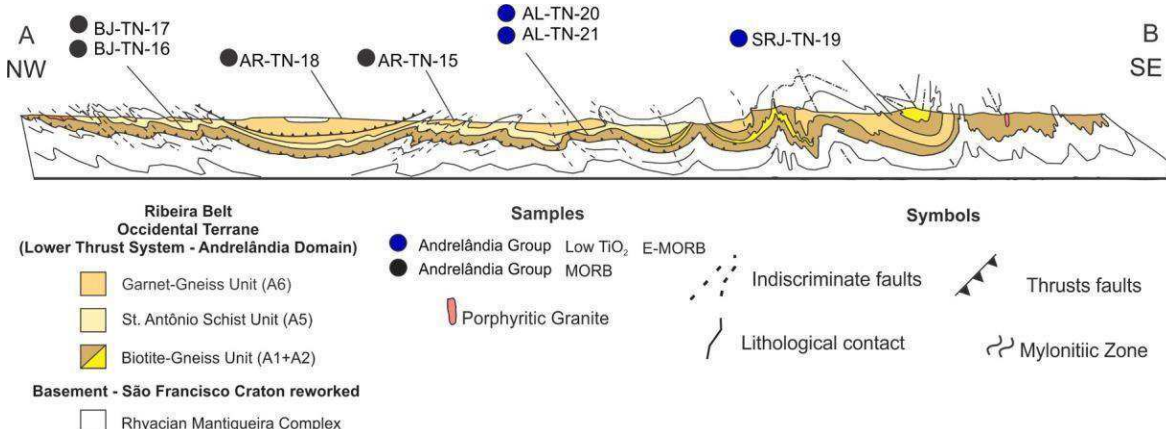
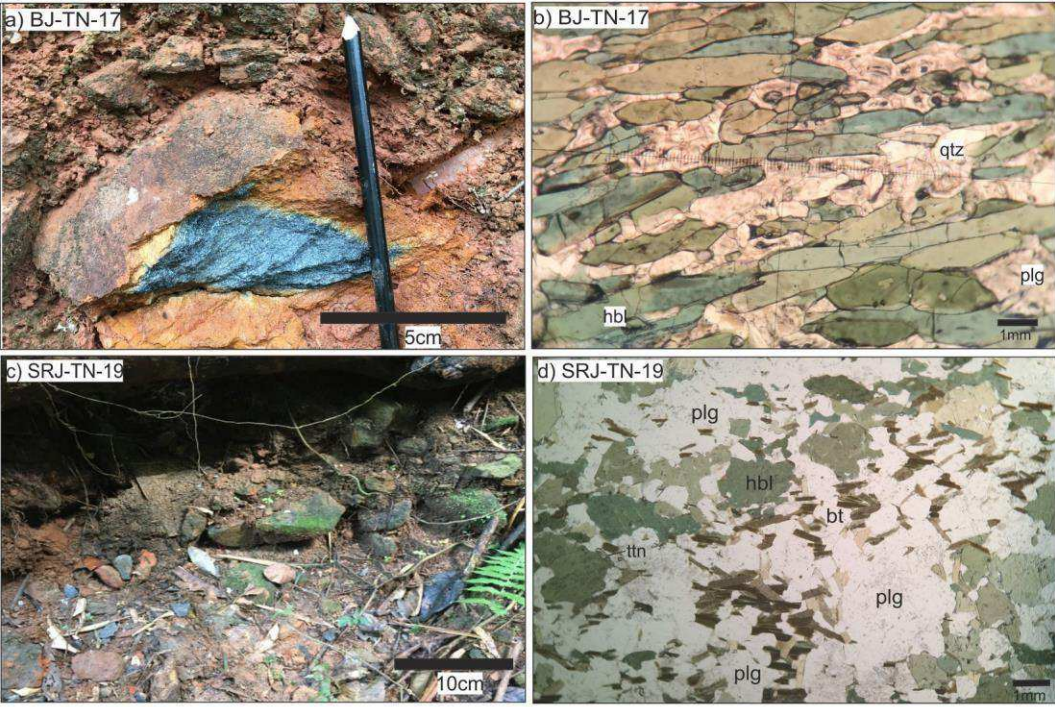


**Fig. 5.** A-B cross-section of the Andrelândia Group showing the positions of the samples identified geochemical signature.

### Biotite-Gneiss Unit



### Garnet-Gneiss Unit

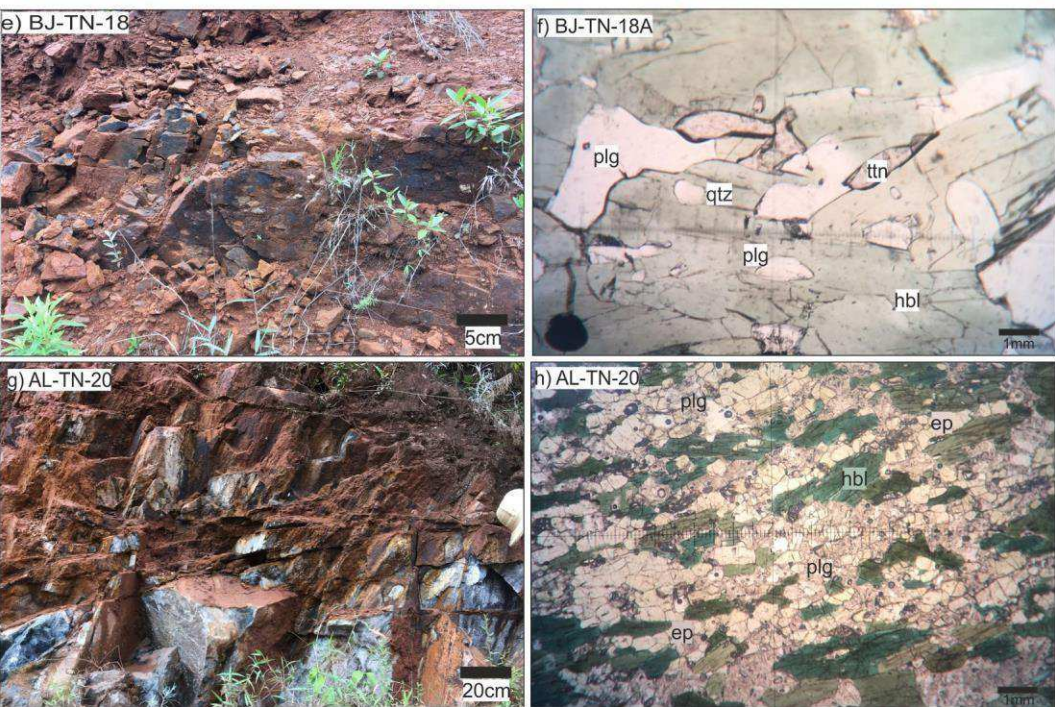


**Fig. 6.** Outcrop images of the basic rocks interlayered within Andrelândia Group metasediments: (a) BJ-TN-17, (c) SRJ-TN-19, (e) AL-TN-20 and BJ-TN-18A. Photomicrographs of mafic rocks: (b) foliated amphibolite showing the stretched hornblende defining the rock orientation, (d) biotite amphibolite with titanite and quartz inclusions, (f) foliated amphibolite with stretched hornblende and epidote stripes, (h) epidote–amphibolite showing the titanite along the hornblende edges. Hbl:hornblende, qtz:quartz, pl: plagioclase, ttn: titanite, ep: epidote.

the studied area (Fig. 7). The metasedimentary units are tectonically interleaved with the basement Paleoproterozoic orthogranulites of the Juiz de Fora Complex (Fig. 8). The cross section shown in Fig. 8 illustrates the two units and the intense tectonic imbrication of the Raposos Group with the rocks of the JFC. Two metasedimentary units crop out, consisting of biotite-rich gneisses and garnet-bearing gneisses. The cross section also indicates the location of samples selected for geochronology

within the studied area. The Raposos Group have a pervasive strong foliation, which is mylonitic on the contacts between the metasedimentary units and the Paleoproterozoic orthogranulites rocks. These are mainly detected at the tectonic contacts of the upper thrust system. However, the contacts between the metabasites and the enclosing tectonic rocks are sharp (Fig. 9), but not tectonic.

Both units contain metric to centimetric layers of impure feldspathic

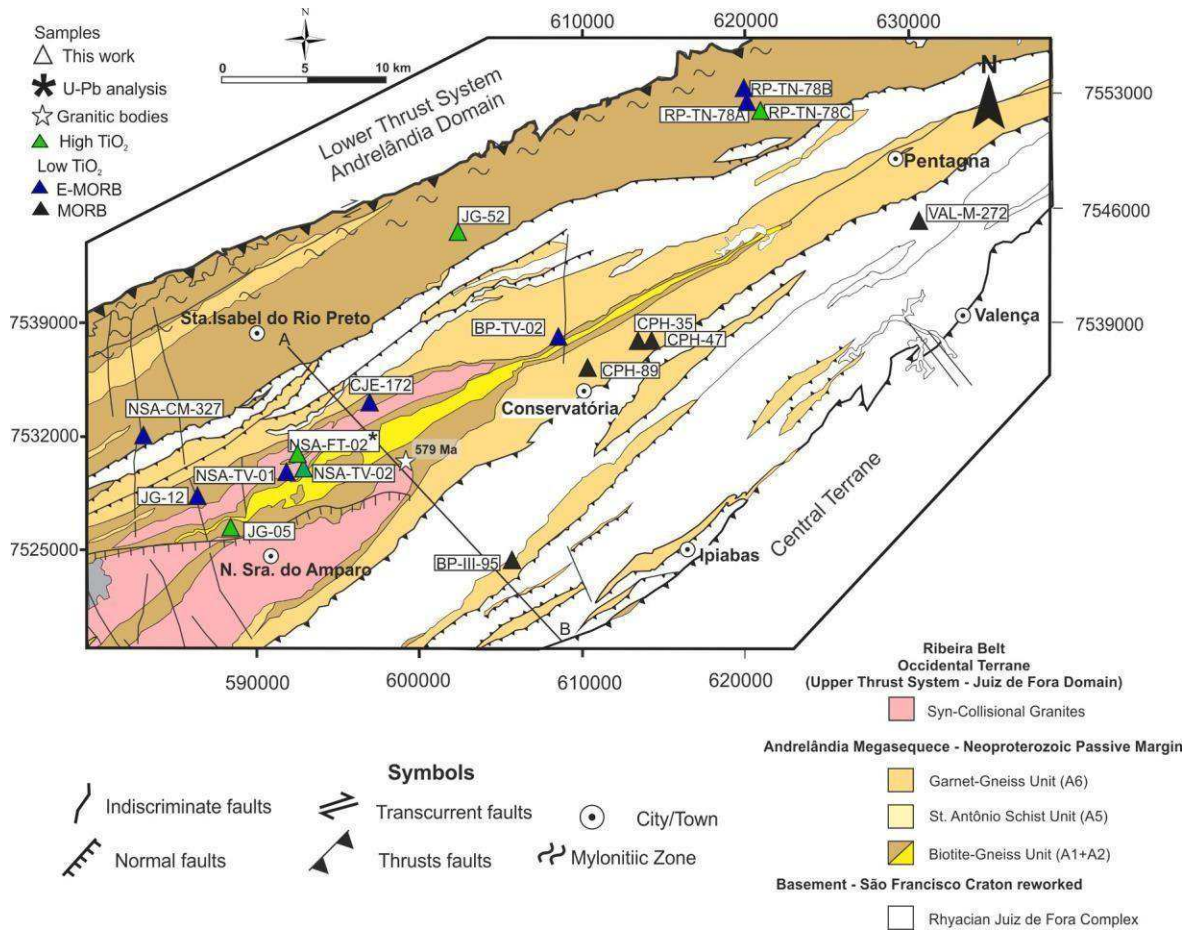


Fig. 7. Geological map of the Raposos Group in studied area with the sample location.

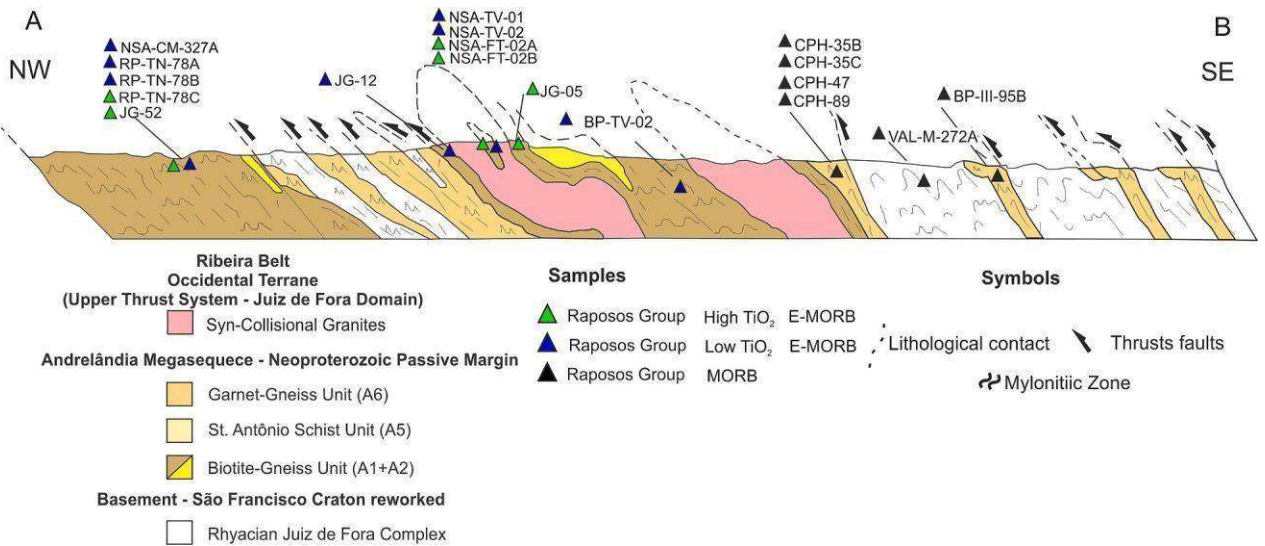


Fig. 8. A-B cross-section of the Raposos Group showing the positions of the samples identified and geochemical signature.

quartzites, calcsilicate rocks and Mn-rich rocks (gondites), but these are more common within the garnet-bearing gneisses, and metabasites. The metabasites lenses are present in both biotite-rich gneisses and the garnet-bearing gneisses.

The metabasic rocks occur as dark lenses or boudins, from several centimeters to a few meters thick. They occur parallel to the host rock foliation throughout the stratigraphic pile always with sharp contacts

(Fig. 9). Since the metabasites present similar deformation and metamorphism as experienced by the Neoproterozoic host rocks, and they occur as thin layers parallel to the sedimentary stratification, they are preliminarily interpreted to represent *syn-sedimentary* magmatism, either representing flows, deformed sills and/or dikes.

The metabasites interlayered with the metasedimentary units of the Raposos Group have a fine-grained granonematoblastic texture,

## Biotite-Gneiss Unit

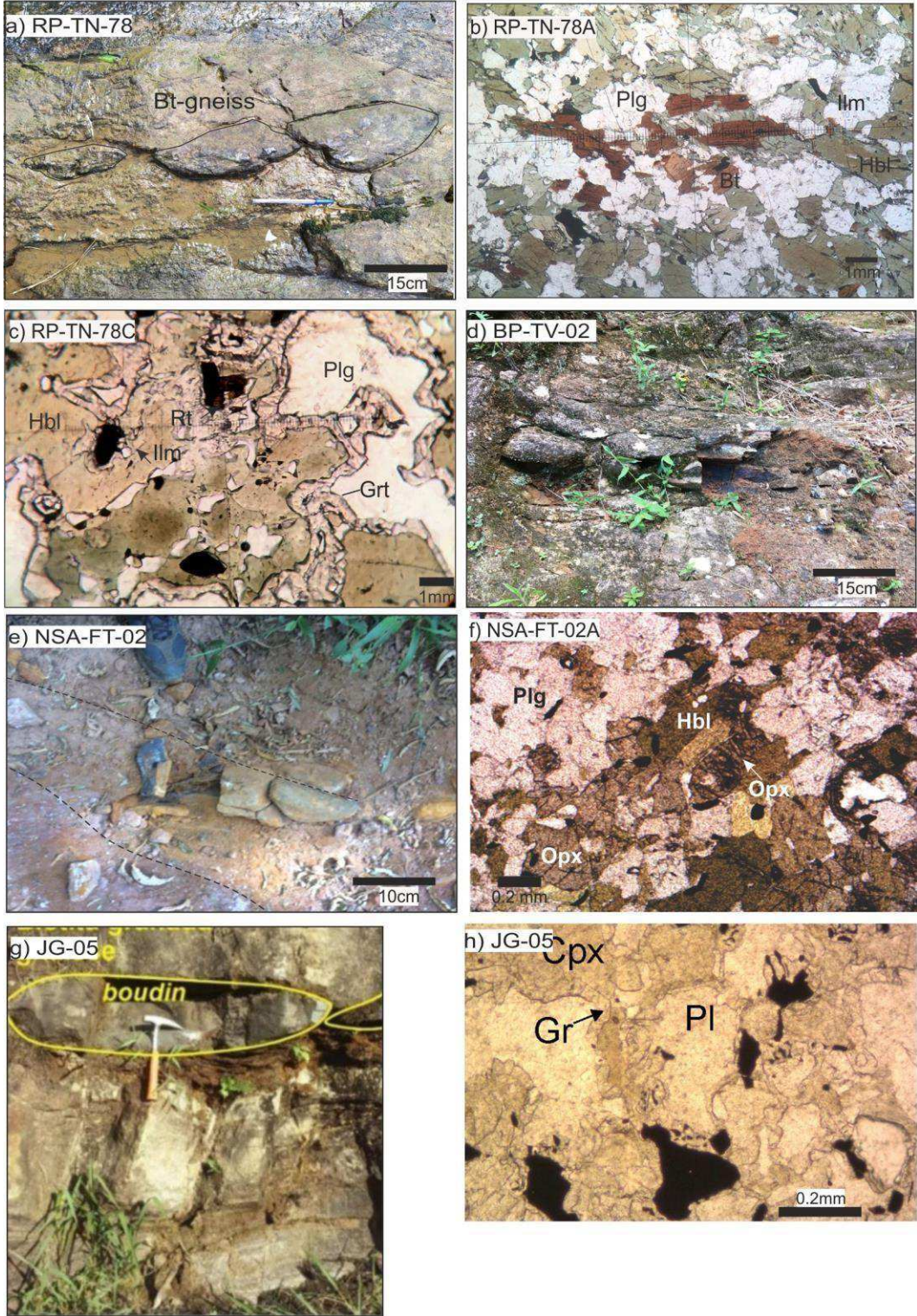


**Fig. 9.** Outcrop images of the basic rocks interlayered within Raposos Group. Biotite-Gneiss Unit: (a) RP-TN-78, (d) BP-TV-02, (e) NSA-FT-02 and (g) JG-05. Photomicrographs of mafic rocks. Biotite-Gneiss Unit: (b) foliated Biotite-granulite, (c) granulite with coronitic garnet texture, (f) fine-grained orthopyroxene- amphibolite. (h) granulite with coronitic garnet texture and ilmenite. Bt, biotite, Grt, garnet, Hnb, hornblende, IIm, ilmenite, Opx, orthopyroxene, Pl, plagioclase, Qtz, quartz, Rt, rutile.

consisting of hornblende, clinopyroxene, orthopyroxene, garnet, plagioclase, biotite, quartz, and ilmenite. According to their mineralogy, the metabasites were classified as orthopyroxene granulites, biotite granulites, and garnet granulites (Fig. 9).

The biotite mafic granulite has a stronger foliation when compared with the orthopyroxene-mafic granulites (Fig. 9a). In one biotite- granulite sample (RP-JC-78B), biotite grows at the edges and along the cleavage of the coarse-grained nematoblastic hornblende, suggesting

that it may relate to a late metamorphism or a retrogression phase. Plagioclase, quartz, clinopyroxene and orthopyroxene are granoblastic texture. Discontinuous layers rich in hornblende and biotite define the main foliation of the sample. Ilmenite is usually located along the boundaries of both hornblende and biotite grains. Quartz and plagioclase appear also as inclusions in hornblende and biotite grains (Fig. 9b).

In the garnet mafic granulite (sample RP-JC-78C), garnet occurs both as individual grains or as symplectitic coronas intergrown with fine-grained plagioclase and ilmenite that develop between coarse hornblende and plagioclase grains (Fig. 9c). Rutile appears as acicular grains in association with hornblende and ilmenite. Clinopyroxene and orthopyroxene grains constitute minor phases in the matrix (Fig. 9c). Hornblende crystals, grow along the edges of clinopyroxene, and along with the coronitic garnet likely represent retrograde metamorphism in this sample.

The sample JG-05 is a fine to coarse grained garnet-bearing mafic granulite that presents garnet coronas that growth between plagioclase and ilmenite grains. Plagioclase and ilmenite also occur as small millimetric symplectitic textures included within the garnet coronas. Plagioclase and clinopyroxene grains show granoblastic textures. Hornblende occurs at the edges of clinopyroxene and together with the symplectitic and garnet corona texture likely belongs to the retrograde evolution of the sample. Quartz grains occur dispersed in the sample, constituting a minor phase (Fig. 9g, h).

The orthopyroxene-mafic granulites (samples NSA-FT-02A, BP-TV-02) contain hornblende and plagioclase with minor quartz and orthopyroxene, and are fine to medium grained, weakly foliated rocks (Fig. 9d, e and f). Clinopyroxene is absent in these samples. Opaque minerals are present (ilmenite), normally in association with hornblende that exhibits a dark brown color and a nematoblastic to granoblastic shape. Plagioclase occurs as disseminated small grains within the matrix or as millimetric porphyroblasts, with albite-twinning (Fig. 9).

## 5.2. Lithogeochemistry

Eight samples from the Andrelândia Group of the LTS and nineteen samples from the UTS of the Occidental Terrane, including those 8 samples reported by Marins (2000), were selected for geochemical analyses. As described above, the metabasites occur as lenses and boudins interlayered with the metasedimentary units of the Andrelândia Group (circle symbols), and the Raposos Group (triangle symbols). Results are presented in Supplementary Table 1.

As the samples sometimes represent small lenses within the

metasedimentary units, first they were tested several ortho and para derived discrimination diagrams, and present in Fig. 10 a, b. Diagrams used were Zr/Ti versus Ni FeOt versus TiO<sub>2</sub> from Winchester et al. (1980) and Pellogia and Figueiredo (1992), respectively. In both diagrams the analyzed metabasic rocks clearly plot in the igneous field, excluding the presence of metamorphosed marls.

The next step used diagrams to detect spilitization (albitization process of primary plagioclase) and weathering alteration (Fig. 10 c and d), this was done because some rocks present high LOI values. All the samples show low Na<sub>2</sub>O/CaO ratios, suggesting low ionic mobility for Na<sub>2</sub>O (wt%) and K<sub>2</sub>O (wt%) as well as for the trace elements such as Rb, Cr, Ba, Ni (ppm, Mullen, 1983). The metabasic rocks reveal no signs of spilitization but show some degree of weathering alteration (Fig. 10d), although modifications are not substantial.

The TiO<sub>2</sub> rate criteria was adopted due to the low Ti-mobility during alteration or metamorphic processes (Dilek and Furnes, 2011) and in the obtained REE patterns as discriminant indexes. Using these parameters (Fig. 11 a to d), the metabasic samples from both the LTS and UTS were subdivided in three geochemical groups:

- i) High TiO<sub>2</sub> (TiO<sub>2</sub> values between 2.13 and 3.2 wt%) with enrichment in the Light Rare Earth Elements (LREE), form a group with a within plate signature (green color in all diagrams). MgO values are between 4.0 and 6.51 wt%. The REE chondrite-normalized profile corresponds to a more fractionated pattern with the highest enrichment of LREE (Fig. 11b, [La/Yb<sub>N</sub> = 1.77–7.11]) and with an average Eu/Eu\* anomaly of 0.94.
- ii) Low TiO<sub>2</sub> (TiO<sub>2</sub> values between 0.85 and 1.96 wt%) with moderate LREE contents (blue color in all diagrams). MgO values are between 5.14 and 13.41 wt%. The REE chondrite-normalized profile corresponds to a fractionated pattern with an enrichment of LREE (Fig. 11c, [La/Yb<sub>N</sub> = 2.3–5.04]) and an average Eu/Eu\* anomaly of 0.88.
- iii) Low TiO<sub>2</sub> (TiO<sub>2</sub> values between 0.7 and 1.9 wt%) with flat REE signature (black color in all diagrams). MgO values are between 6.0 and 11.4 wt%. The REE chondrite-normalized profile corresponds to a near flat pattern (Fig. 11d, [La/Yb<sub>N</sub> = 0.48–2.02]) with a high average Eu/Eu\* anomaly of 0.98.

In the AFM diagram of Fig. 11e, all the studied metabasic rocks belong to the tholeiitic series. For classification using immobile elemental ratios such as the TAS modified by Pearce (1996) Zr/Ti × Nb/Y (Fig. 11f), all the studied samples plot preferentially in the basalt field.

**Table 1**

Synthesis of Sm-Nd and Sr isotopic data of the metabasic rocks.

SAMPLE	Geochemical Group	Group	Sm (ppm)	Nd (ppm)	143Nd/ 144Nd	147Sm/ 144Nd	<sup>87</sup> Sr/ 86Sr	$\epsilon$ (0)	143Nd/ 144Nd(t)	143Nd/ 144Nd(i)	$\epsilon$ (653)	T(DM)* <sup>87</sup> Sr/ 86Sr(i)	
NSA-TV-02	E-MORB	UTS	5.09	20.80	0.51223	0.14801	0.71007	-7.98	0.51160	0.51160	-3.93	1.85	0.70962
NSA-FT-02B	High-TiO <sub>2</sub>	UTS	6.15	25.00	0.51221	0.14878	0.71568	-8.40	0.51157	0.51157	-4.41	1.91	0.71500
NSA-TV-01	E-MORB	UTS	4.46	18.86	0.51220	0.14306	0.70932	-8.57	0.51159	0.51159	-4.11	1.79	0.70875
BP-III-GD-96B	MORB	UTS	11.86	41.38	0.51182	0.17337	0.70524	-15.91	0.51108	0.51108	-13.99	3.98	0.70438
RP-TN-78A	E-MORB	UTS	4.47	18.84	0.51219	0.14349	0.71055	-8.83	0.51157	0.51157	-4.40	1.83	0.70827
RP-TN-78B	E-MORB	UTS	6.71	26.87	0.51217	0.15095	0.71631	-9.08	0.51153	0.51153	-5.27	2.04	0.71454
RP-TN-78C	High-TiO <sub>2</sub>	UTS	4.25	14.45	0.51254	0.17768	0.71173	-1.84	0.51178	0.51178	-0.26	2.00	0.71110
BP-TV-02	E-MORB	UTS	5.30	21.40	0.512184	0.1485	0.70997	-8.86	0.51154	0.51155	-4.95	1.98	0.70941
NSA-FT-02	High-TiO <sub>2</sub>	UTS	6.30	25.00	0.512204	0.1514	0.71617	-8.47	0.51155	0.51156	-4.78	2.01	0.71572
JG-05	High-TiO <sub>2</sub>	UTS	6.50	22.10	0.51257	0.17730	0.73343	-1.31	0.51181	0.51181	0.26	1.92	null
JG-12	E-MORB	UTS	4.30	15.30	0.51251	0.16890	0.70891	-2.50	0.51178	0.51179	-0.27	1.81	0.70789
JG-52	High-TiO <sub>2</sub>	UTS	10.40	50.00	0.51239	0.12540	0.70580	-4.80	0.51185	0.51186	1.12	1.18	null
SRJ-TN-19	E-MORB	LTS	3.83	16.55	0.51197	0.13986	0.71775	-13.12	0.51137	0.51137	-8.40	2.14	0.71456
AL-TN-20	E-MORB	LTS	8.41	37.98	0.51228	0.13380	0.71105	-7.06	0.51170	0.51170	-1.81	1.48	0.71007
AL-TN-21	E-MORB	LTS	4.91	18.45	0.51250	0.16108	0.71091	-2.75	0.51181	0.51181	0.22	1.59	0.70803
AR-TN-18A	MORB	LTS	39.74	172.50	0.51250	0.13927	0.70385	-2.66	0.51191	0.51191	2.13	1.17	0.70354
AR-TN-18B	MORB	LTS	2.00	5.21	0.51317	0.23220	0.70371	10.37	0.51218	0.51218	7.41	0.35	0.70329
BJ-TN-17	MORB	LTS	2.18	7.58	0.51265	0.17379	0.70615	0.23	0.51191	0.51191	2.14	1.52	0.70493

– null is referent to the Sr (ppm) values below the detection limit (see Supplementary Material 3).

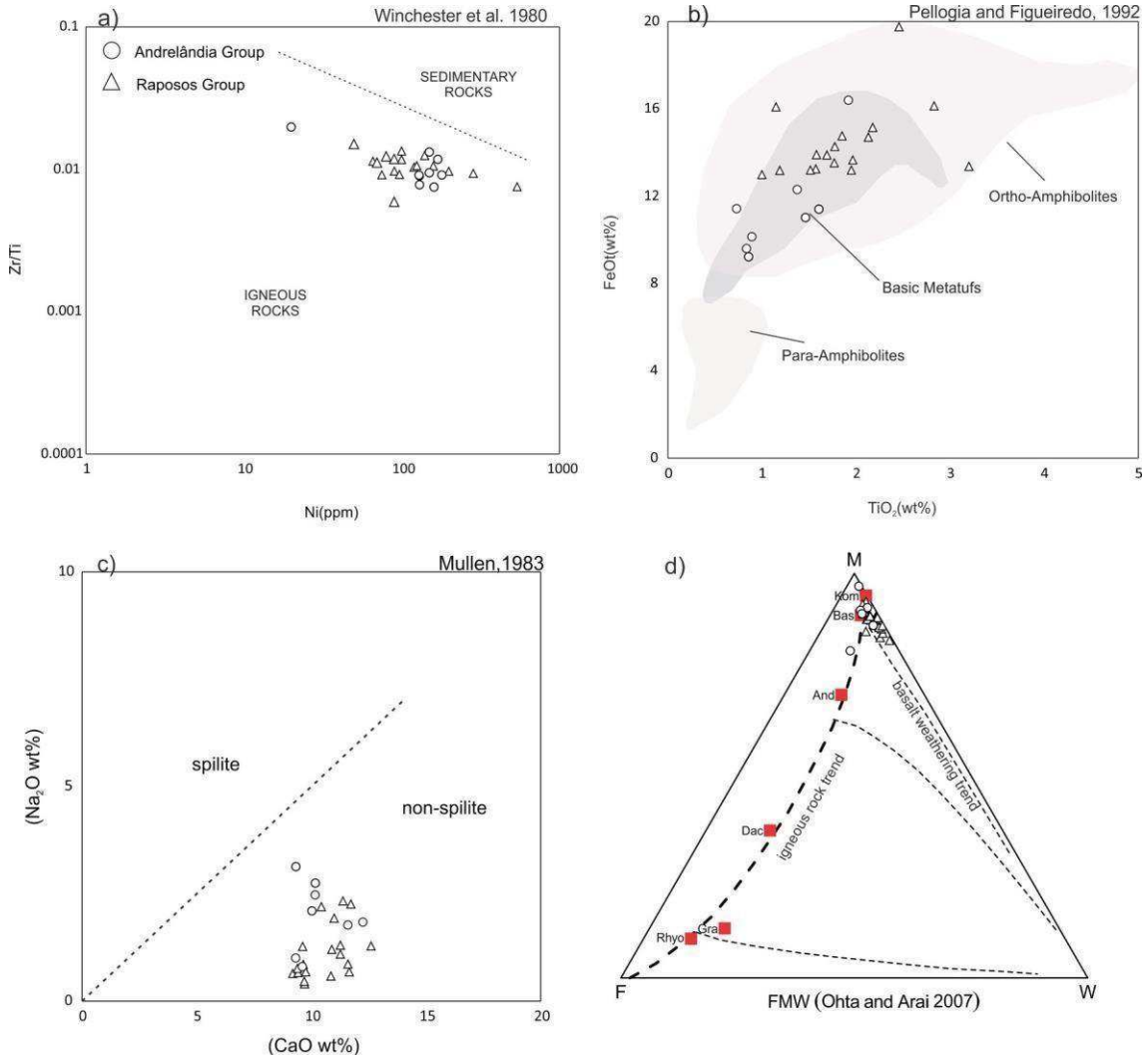


**Fig. 10.** Origin discriminant and alteration index diagrams a) Ni versus Zr/Ti of Winchester et al. (1980); b) FeOt versus TiO<sub>2</sub> from Pellogia and Figueiredo (1992); c) Na<sub>2</sub>O versus CaO, (Mullen, 1983); d) MFW diagram by Ohta and Arai (2007).

The mafic rocks show SiO<sub>2</sub> contents between 43.57 and 50.49 wt%, except for sample SRJ-TN-19, which has a SiO<sub>2</sub> content of 54.37 wt%. The MgO values of all samples are between 4.94 and 13.41 wt%. Fe<sub>2</sub>O<sub>3</sub> values are high, between 9.09 and 21.96 wt% and there are a broad range of TiO<sub>2</sub> contents of 0.73–3.2 wt%. These results are indicative of a basaltic protolith with a low-K tholeiitic trend, with just one sample plotting in the andesitic field.

In the TiO<sub>2</sub> × MgO (wt%) binary diagram shown in Fig. 11a, both Low TiO<sub>2</sub> groups display an inflection point at around 8 to 8.5 wt% of MgO values, suggesting AFC processes (assimilation-fractional crystallization), with sphene and ilmenite as the possible fractionating assemblage.

Using *N*-MORB normalized spidergrams (Fig. 12 a, b and c) the three groups presented above have the following tectonic signatures: a) the high TiO<sub>2</sub> group show within plate signature, and the low TiO<sub>2</sub> groups, display b) E-MORB and c) MORB signatures, respectively.

All the geochemical groups were found in both the lower and upper thrust systems, however in the intraplate high TiO<sub>2</sub> group, commonly found in the lower gneissic unit (A1 + A2, see section and maps of Figs. 4, 5, 7 and 8), was sampled only within the Raposos Group, at Upper Thrust system.

Additionally, to the spidergrams, selected tectonic discrimination diagrams that use trace, immobile and REE elements are presented in Fig. 13. They include: TiO<sub>2</sub> versus Nb/Y (Pearce, 2008; Fig. 13a), Ti/Zr

diagram (Pearce, 1982; Fig. 13b), V/Ti diagram (Shervais, 1982; Fig. 13c), and (La/Nb)<sub>N</sub> versus (La/Yb)<sub>N</sub> (Wilson, 1989, Fig. 13d). All diagrams indicate extensional tectonic scenarios for the presented samples. As expected by the geochemistry, the high TiO<sub>2</sub> group suggests an intraplate setting, whereas the low TiO<sub>2</sub> groups indicate progressive lithospheric thinning during the evolution of the Andrelândia-Raposos passive margin. In the (La/Nb)<sub>N</sub> versus (La/Yb)<sub>N</sub> diagram of Fig. 13d, an enriched mantle source predominates, indicating a major contribution from the SCLM (subcontinental lithospheric mantle). This pattern can be recognized by using *N*-MORB normalized by Sun and McDonough (1989) spidergrams (Fig. 12 a to c), these exhibit extensional patterns and lacking the expected negative anomalies of P and Ti for compressional settings.

### 5.3. U-Pb data

The sample NSA-FT-02A belongs to the intraplate high TiO<sub>2</sub> of metabasites from the Raposos Group (UTS) (Fig. 7). The CL images of zircon grains (Fig. 14a) reveal three different types of textures. Prismatic grains with rounded rims and weak planar internal textures (Corfu et al., 2003), type 1, are consistent with typical primary zircons expected for basic tholeiitic rocks. On the other hand, large zircon with oscillatory to complex internal textures and different shapes and sizes, type 2, possibly represent for inheritance. Finally, rims having homogeneous dark

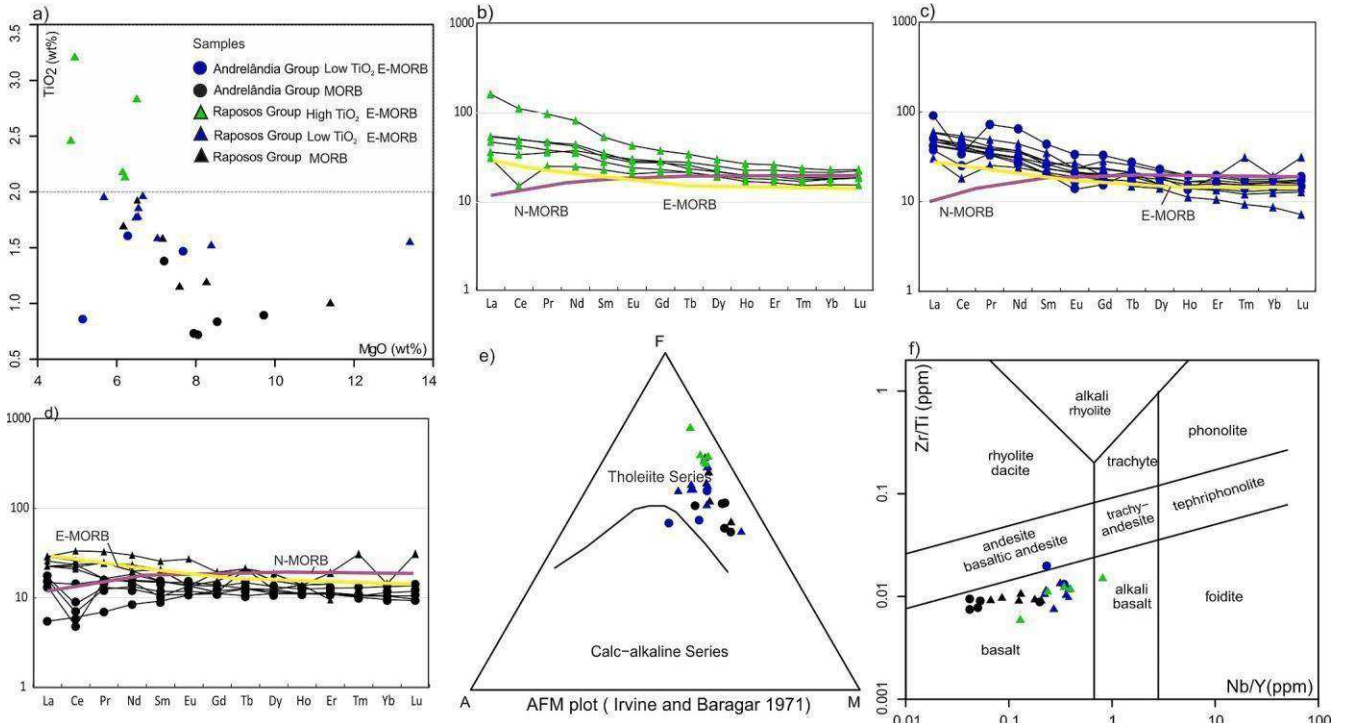


**Fig. 11.** Classification diagrams. a)  $\text{TiO}_2 \times \text{MgO}$  binary diagram; b,c,d) Chondrite-normalized spidergrams for the High- $\text{TiO}_2$ , E-MORB and MORB groups. The spidergrams were normalized using the chondrite composition of Boynton (1984); e) AFM diagram (Irvine and Baragar, 1971), f)  $\text{Zr}/\text{Ti}$  ×  $\text{Nb}/\text{Y}$  (TAS modified by Pearce, 1996). The yellow and purple lines represent, respectively, the E-MORB and N-MORB average compositions from Boynton (1984).

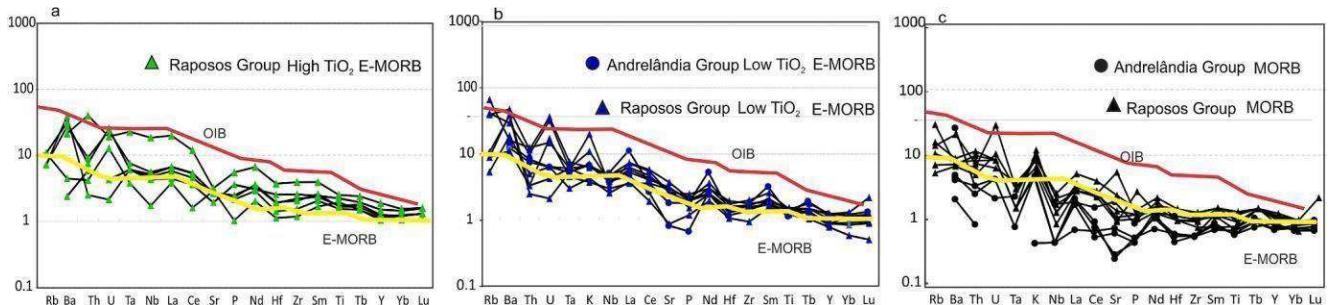


**Fig. 12.** a,b,c) N-MORB -normalized spidergrams for the High- $\text{TiO}_2$ , E-MORB and MORB groups. The spidergrams were normalized using the N-MORB composition of Sun and McDonough (1989). The yellow and red lines represent, respectively, the E-MORB and OIB average compositions from Sun and McDonough (1989).

domains or high to medium CL intensity, together with resorption textures (embayment or truncated domains), type 3, were regarded as representative of the high-grade metamorphic overprint (Fig. 14a).

Fifty-four zircon spots were analyzed from sample NSA-FT-02A (Supplementary Material 2; Fig. 14b). Considering the complexity of dating metabasic tholeiitic rocks, and three types of zircon grains observed, data for each zircon grain type are treated separately.

A set of five analyses from CL-bright prismatic cores with planar zoning, type 1 zircons, yielded a Cryogenian 206Pb/238U weighted average age of  $653 \pm 38$  Ma (Fig. 14c), this age is interpreted as the crystallization age of the metabasite. The Th/U ratios are between 1.44 and 2.39 (Fig. 14a and c).

The inheritance of the metabasic rocks is detected by the type 2 zircon, large grains with CL-bright oscillatory to complex zoning. They yield a Paleoproterozoic 207Pb/206Pb age of  $2482 \pm 30$  Ma (disc. 0 %, Th/U = 9.67; Fig. 14) and a Mesoproterozoic 207Pb/206Pb age of  $1373 \pm 59$  Ma (disc. 0 %, Th/U = 11.83; Fig. 14), both showing Pb-loss to an Ediacaran metamorphic overprint.

Type 3 zircons, encompassing tips and reabsorbed textures yielded a

concordant age of  $578.1 \pm 3.6$  Ma (with variable Th/U ratios between 0.44 and 5.0). These tips and disturbed textures are interpreted to result from the high-temperature metamorphic overprint overgrowing both type 1 (crystallization age zircon grains) and type 2 (inheritance).

#### 5.4. *Sm-Nd and Rb-Sr data*

Eighteen analyses from all geochemical groups of the metabasic rocks were obtained. The sample locations are shown in Figs. 4, 5 (LTS) and in Figs. 7, 8 (UTS). A synthesis of the results is presented in Table 1 below. All Sm-Nd and Rb-Sr analytical results are presented in Supplementary Material 3.

Most of the studied metabasites from the Andrelândia Group yielded Mesoproterozoic TDM model ages ranging from 1.17 to 1.59 Ga and initial  $\epsilon_{\text{Nd}_{(653)}}$  values between +2.1 to -8.4. The younger TDM model ages were found in the MORB group. Just one sample (SRJ-TN-19) of the A1 + A2 unit, with E-MORB signature, yielded a TDM model age of 2.14 Ga and a negative initial  $\epsilon_{\text{Nd}_{(653)}}$  values (Table 1, Fig. 15).

Conversely the results obtained for the metabasites interleaved with

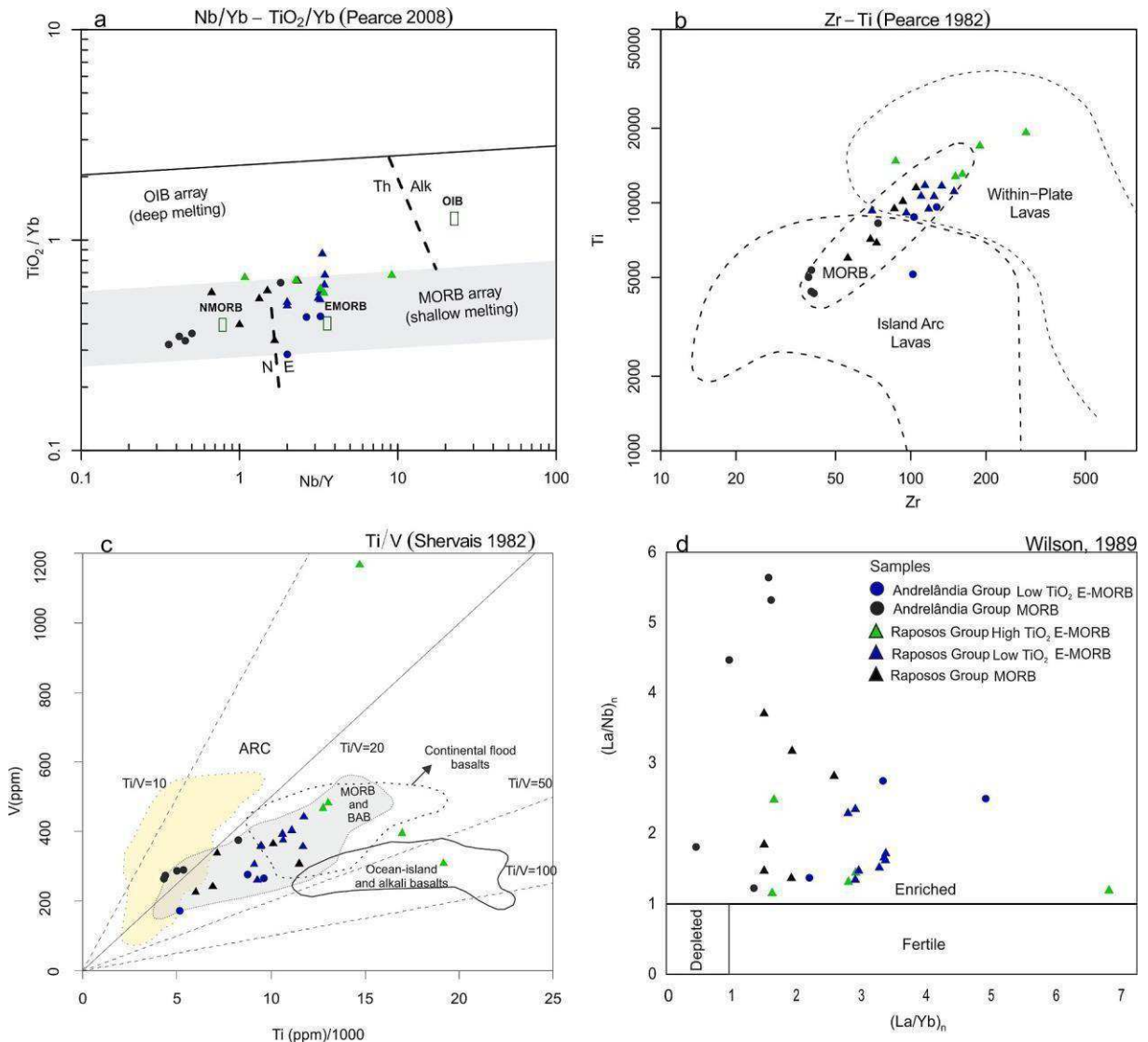


**Fig. 13.** Tectonic diagrams. a)  $\text{TiO}_2\text{-Yb}$  (Pearce, 2008); b)  $\text{Zr-Ti}$  diagram (Pearce, 1982); c)  $\text{Ti/V}$  diagram (Shervais, 1982); d)  $(\text{La}/\text{Nb})_n$  versus  $(\text{La}/\text{Yb})_n$  diagram of Wilson (1989).

the Raposo Group of the Upper Thrust Systems yielded older TDM model ages between ca. 1.79 to 2.04 Ga with  $\varepsilon\text{Nd}_{(653)}$ , values between  $-0.2$  to  $-5.2$ , and only one sample yield TDM model ages of ca. 1.18 Ga and positive  $\varepsilon\text{Nd}_{(653)}$  of  $+1.1$ , representative of the high- $\text{TiO}_2$  group (Table 1, Fig. 15).

The older TDM model ages of the metabasites are concentrated in the Upper Thrust System where slices of basement rocks occur tectonically interleaved with the metasedimentary rocks that host the studied metabasites.

The initial  $^{87}\text{Sr}/^{86}\text{Sr}$  ratios show primitive values from both UTS and LTS metabasites, with data for the Raposo Group metabasites varying from 0.7083 to 0.7157, whereas the Andrelândia Group metabasites vary from 0.7033 to 0.7146.

## 6. Discussion

The Andrelândia Group corresponds to a variety of rocks occurring in several different settings, and the nomenclature (Paciullo et al., 2000; Trouw et al., 2000, 2013) was used for all passive margin sequences around the southeastern and southern margin of the SFC (Fig. 3). This includes rocks occurring in: a) the external E-verging nappes of the Brasília belt at the interference zone between the Brasília and Ribeira

orogens (Trouw et al., 2000, 2013; Westin et al., 2016, 2019, 2021; Kuster et al., 2020); b) the lowermost thrust nappe system of the Occidental Terrane of the Ribeira belt (LTS of the Occidental Terrane); and c) the UTS of the Occidental Terrane of the Ribeira belt, which presents the distal part of the basin represented by the Raposo Group, the focus of this investigation.

In order to make a regional comparison between the eastern and southeastern margins of the SFC, in the discussion items ahead we will compare the magmatism and provenance studies just related to the units that crop out in the AROS. Data from the Andrelândia units that crop out at the Brasília Belt were not considered in this section.

### 6.1. Magmatic constraints of the Andrelândia-Raposo Group

For the LTS of the Occidental Terrane (Andrelândia Group), the metabasic studied rocks did not yield zircons. The available U-Pb data for this region yielded ca. 669 Ma (Campos Neto and Caby, 2000; Reno et al., 2009) for a metabasite sample from the A6 top unit. Geochemical data indicate high and low  $\text{TiO}_2$  groups, ranging from intraplate to E-MORB and MORB, with predominance of the intraplate signature in metabasites interleaved in the lower A1 + A2 biotite banded gneiss unit (Gonçalves and Figueiredo, 1992; Paciullo et al., 2000). Older Nd data

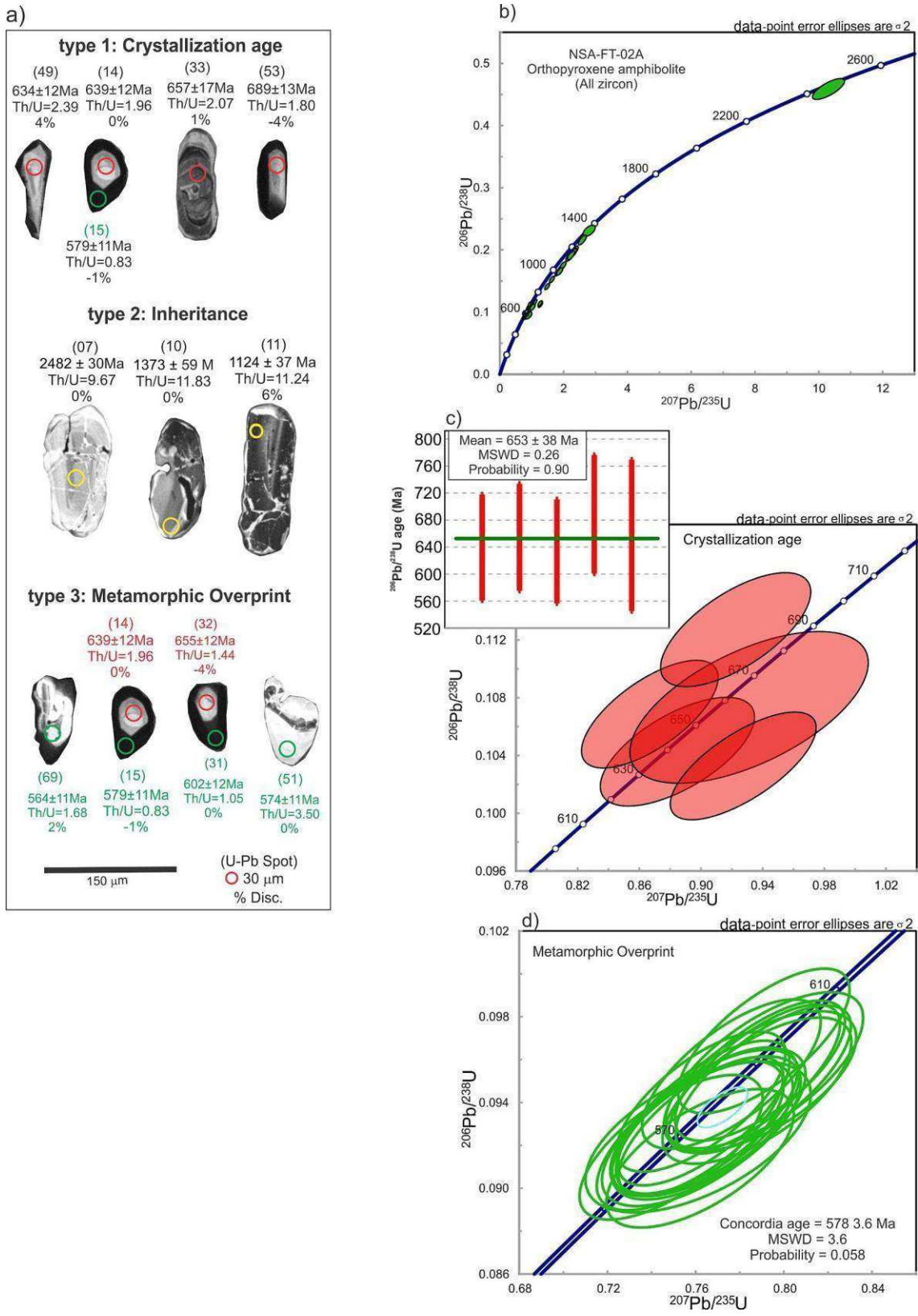


**Fig. 14.** Zircon U-Pb data from the metabasite sample (NSA-FT-02A) interlayered within paragneisses of the Raposos Group. a) the identified group types of zircon: type 1- crystallization age; type 2- inheritance and type 3- metamorphic overprint; b) concordia diagram for all analyzed zircons, indicating the Mesoproterozoic and Paleoproterozoic inheritance; c) concordia diagram referent to the crystallization age and weighted average age of 653 Ma; d) calculated metamorphic overprint at 578 + -3.6 Ma.

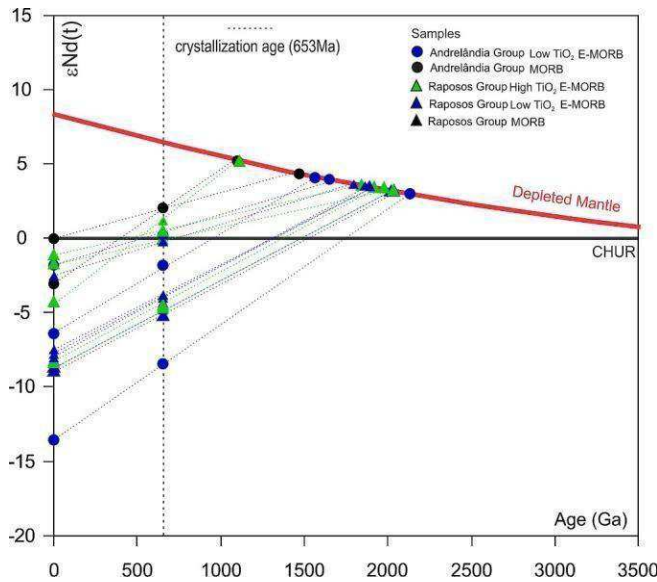


Fig. 15.  $\epsilon\text{Nd}(653)$  versus age diagrams of the metabasic rocks of this work.

for metabasites interlayered within the A6 Andrelândia Group yield TDM model ages of 1.20–1.05 Ga, with  $\epsilon\text{Nd}(1.0)$  values of +4.8 and +3.1, reflecting depleted mantle reservoirs with short crustal residence time, and constraining the depositional age in the Neoproterozoic (Heilbron et al., 1989). Altogether the data suggest a juvenile contribution from the SCLM and some degree of crustal contamination from country rocks. The older Mesoproterozoic and Paleoproterozoic ages (Coelho et al., 2017; Frugis et al., 2018; Pinheiro et al., 2019), common in the base- ment units are interpreted as inheritance. The ca. 1.0–1.10 Ga TDM model ages of Heilbron et al (1989) corroborate this interpretation. It is important to reinforce again the absence of mylonitic foliation combined with the lack of tectonic contacts between the amphibolites and the metasedimentary country rocks also reinforces the interpretation that these ages represent in fact different sources inherited by the mafic magmatism.

For the UTS, one sample rendered zircon grains for the U-Pb study. The sample mafic granulite with an intraplate signature (NSA-FT-02A),

hosted in the Biotite-Gneiss Unit of the Raposo Group, yielded a Cryogenian age of a ca. 653 Ma (weighted average age), which is interpreted to be the magmatic age of the protolith (crystallization age, see red analyses in Fig. 14). The zircon age results also indicate inherited zircon grains of Paleoproterozoic (ca. 2.48 Ga) and Mesoproterozoic (ca. 1.37 Ga), ages, corroborated by the older Paleoproterozoic TDM model ages, presented by some samples, such as the TDM model age of 2.0 Ga with a negative  $\epsilon\text{Nd}(653)$  values of –4.5.

The likely pathways for xenocrystic zircon grains in the basic magma could have been achieved by incorporation several ways: (1) unmelted zircons from the source, (2) incorporation of zircons from the basement during magmatic ascent or (3) from zircons hosted in the Neo- proterozoic sediments during its final emplacement. Usually, low-TiO<sub>2</sub> volcanic tholeiitic basic rocks are not suitable to crystallize zircon because of their low zirconium content increasing the probability that these older zircon grains have been inherited from basement units.

The geochemical zoning detected on the UTS have revealed the predominance of the low TiO<sub>2</sub> groups in the upper A6 unit, suggesting larger degree of extension of the lithosphere in the distal sector of the basin. Additionally, the TDM model ages have yielded values from 1.77 to of 2.03 Ga with negative  $\epsilon\text{Nd}(653 \text{ Ma})$  values (-5.3 to –0.2, Table 3), showing some degree of crustal contamination.

To solve this question an integrated epsilon Nd versus age diagram is presented (Fig. 16a), with samples from the metabasic rocks of this study were combined with previous data from other published metabasic rocks (Heilbron et al., 2019) and with data from the metasedimentary units of the Andrelândia basin (Santos, 2001; Frugis et al., 2018), and from the basement complexes (Cioffi et al., 2016; Araújo et al., 2019; Bruno et al., 2020; Almeida et al., 2021).

It is clear that the metabasites display juvenile signatures with discrete contributions from the basement rocks, as detected by the inherited zircon grains in the U-Pb systematics. Nevertheless, the isotopic signature of the metabasites are striking similar with previously isotopic signature of the Santo Antonio unit (A5), see Fig. 16a.

The results show that the A5 unit display similar isotopic signatures with the metabasites (Fig. 16b). Together the geometry, isotopic signature and obtained Cryogenian ages reinforces the interpretation of coeval magmatism with the development of the Andrelândia-Raposo basin in passive margin setting.

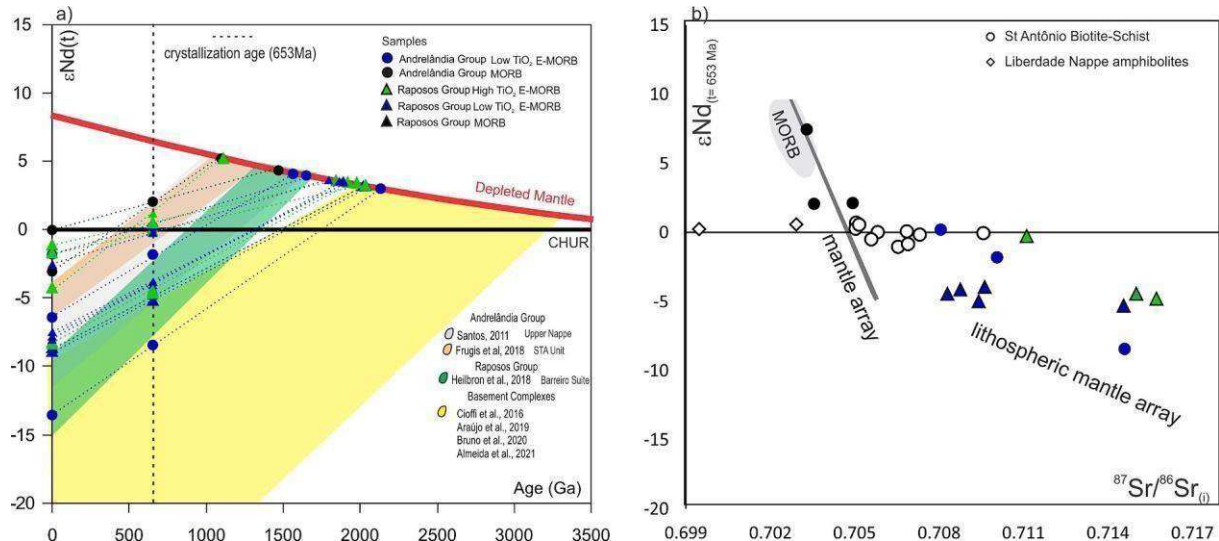


Fig. 16. a)  $\epsilon\text{Nd}(653)$  versus age diagrams of the metabasic rocks of this work and for comparison, the metasedimentary of from Santos (2011) and Frugis et al (2018) together with the basement complexes by Cioffi et al. (2016); Araújo et al. (2019), Bruno et al. (2020); Almeida et al. (2021). b) Nd-Sr correlation diagram of Andrelândia-Raposo Group rocks at 653 Ma with the combined data of Santo Antônio Unit of Frugis et al. 2018. Uniform Reservoir data extracted from DePaolo (1988).

## 6.2. Magmatic episodes within the passive margin sequences of the AROS

The Andrelândia-Raposos basin development is intimately connected with the Neoproterozoic passive margin evolution surrounding the São Francisco-Congo paleocontinent (e.g., Heilbron et al., 2017). During extensional events in the early Tonian the passive margins in the AROS are represented by the Macaúbas Group, in the Araçuaí Belt (e.g. Pedrosa-Soares et al. 2008, Alkmim et al. 2017), to the north, and possibly by the Andrelândia Group, in the south (e.g., Pedrosa-Soares et al., 2008, Alkmim et al., 2017).

In the Barreiro Tholeiitic suite, which occurs at the connection between the Araçuaí Orogen, in the northeast of Rio de Janeiro State, metabasites placed within the top successions of the Raposos Group record an intraplate magmatism. The Barreiro suite presents an age of  $\sim 766$  Ma suggesting that the distal portion of the Andrelândia basin was under development since the Tonian period (Heilbron et al., 2019). The intraplate magmatism but also the MORB-like patterns recorded in these lithotypes are very similar to the data described here and testify the continental extension associated with development of the Neo-proterozoic passive margins around the São Francisco paleocontinent (Heilbron et al., 2019).

In the north of the AROS, in the Araçuaí Orogen, the passive margin units are represented by the Macaúbas Group (Pedrosa-Soares et al., 1992, Pedrosa-Soares et al., 2001, Pedrosa-Soares et al., 2008, Babinski et al., 2012; Kuchenbecker et al., 2015) These authors reported two distinctive intrusive magmatic episodes coeval with the development of the Macaúbas basin. In the proximal sector, intruding basement rocks, the Pedro Lessa mafic dykes ( $906 \pm 2$  Ma; Machado et al., 1989) and the younger Salto da Divisa A-type granite ( $875 \pm 9$  Ma; Silva et al., 2002b, 2007) were reported. In the distal segment, one U-Pb age of  $645 \pm 10$  Ma was obtained for a plagiogranite within the Ribeirão da Folha ophiolite, occurring in the northernmost portion of the Araçuaí Orogen. This episode illustrates the advanced stages of the rifting event and the

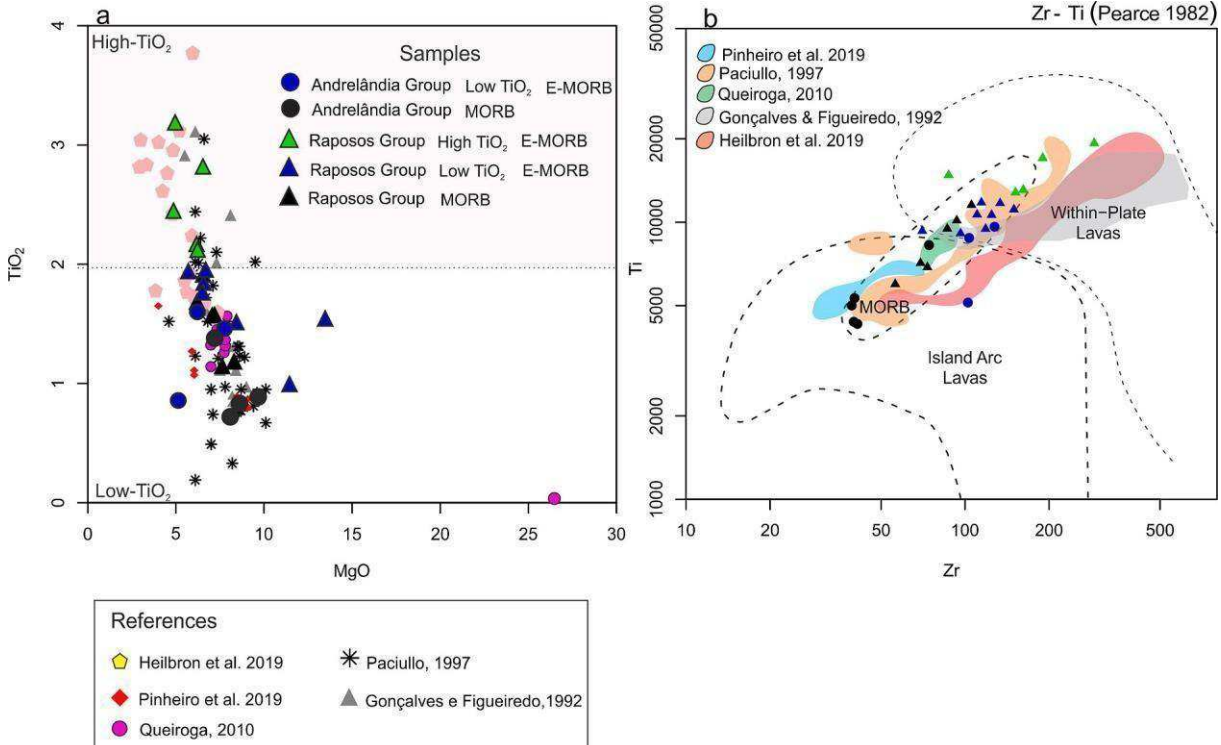
creation of oceanic crust (Pedrosa-Soares et al., 1992, 2001, 2008; Queiroga, 2010; Amaral et al., 2020).

Fig. 17 presents a geochemical compilation of the mafic rocks found within the AROS. Altogether, the data supports what is expected in the development of a passive margin, with initial bimodal magmatism and mafic rocks with intracontinental signatures, followed by intraplate to MORB-like mafic rocks with the progression of extension, and finally with rocks with ocean floor tectonic signatures (ophiolitic slivers).

In the West Congo Belt, the African counterpart of the Araçuaí belt, the continental rifting process is marked by the Zadianian- Mayumbian Groups, where an age of  $999 \pm 7$  Ma is obtained for the Noqui peralkaline granite (Tack et al., 2001) and an age of ca. 920 Ma for the upper Mayumbian Group. These rocks record bimodal magmatism, but with no evidence of ophiolitic slivers (Tack et al., 2001; Frimmel et al., 2006; Pedrosa-Soares et al., 2008).

## 6.3. Provenance studies encompassing the Andrelândia Group

The provenance studies encompassing the Andrelândia Group suggest that the lower units are strongly associated with the Macaúbas extensional event (1000–900 Ma) of the São Francisco Paleocontinent (Ribeiro et al., 1995; Westin et al., 2019) as shown by detrital zircon ages of quartzite samples from the Andrelândia Group that yield maximum depositional ages of ca. 1.0 Ga and a metamorphic age of 588 Ma (Valeriano et al., 2004). Similar results were also found by Valladares et al. (2004), for a quartzite placed at the base of the Andrelândia sequence (A1 + A2 units), which yielded a maximum depositional age of ca. 1.0 Ga, with a main contribution from Paleoproterozoic sources spanning from (1.8–1.9 Ga) to (2.0–2.1 Ga). A paragneiss hosted in the A1 + A2 units of the lower Andrelândia thrust system also recorded similar maximum depositional ages around 950 Ma, with a wide contribution from Mesoproterozoic to Archaean sources (Belem et al., 2011).



**Fig. 17.** A comparison of new data and previously published data for mafic rocks in the region of the Andrelândia deformed basin units. This compilation includes Paciullo (1997), Gonçalves and Figueiredo (1992), Pinheiro et al. (2019), Queiroga, (2010), Heilbron et al. (2019), compared with our data for the Andrelândia- Raposos Groups. (A)  $\text{TiO}_2 \times \text{MgO}$  diagram showing that both proximal and distal samples can be divided into the same groups, and (B) plot in the  $\text{Zr}-\text{Ti}$  tectonic diagram of Pearce (1982).

For the upper units, besides Archean, Paleoproterozoic and Mesoproterozoic source rocks, Neoproterozoic ages ranging from 900 to 640 Ma have been assigned as an important contribution, defining the maximum depositional ages for the Andrelândia Group (e.g., [Belem et al., 2011](#); [Santos, 2011](#); [Frugis et al., 2018](#); [Kuster et al., 2020](#)). The previous authors suggest that in the deepest section of the basin, the sediments were dominated by Tonian sources probably marking the extensional period, whereas in the uppermost segment the major contribution was the magmatic arcs of the Brasília Belt and the active margin of the Paranapanema paleocontinent (e.g., [Bel' em et al., 2011](#); [Frugis et al., 2018](#); [Santos, 2011](#); [Kuster et al. 2020](#)). However, the Tonian Barreiro Suite (766 Ma) and other Neoproterozoic mafic rocks, such as the ages obtained here, cannot be ruled out as a potential source for upper units, especially the most differentiated andesite-basaltic amphibolites with intraplate signatures.

### 6.3.1. Raposos Group

For the distal segment of the Andrelândia basin, however, limited geochronological data available. [Valladares et al. \(2008\)](#) dated detrital zircon from two high-grade quartzites by LA-ICPMS that yielded a maximum depositional age of ca. 1.1 Ga. The main age group are within the 1.80–2.20 Ga interval, suggesting the erosion of old Paleoproterozoic orogens and a small contribution of a 2.50–3.60 Ga old Archean crustal sources. [Belem et al. \(2011\)](#) obtained similar U-Pb results as the upper units of the Andrelândia Group for the top of the Raposos Group that crops out in the UTS. They have sampled high-grade paragneisses (biotite-schist, A5 unit), with major Tonian sources ranging from ca. 645 to 800 Ma.

### 6.3.2. Possible source candidates

The wide age spectra displayed by the metabasic rocks found in the Andrelândia-Raposos Group seem to reflect the multisource nature of the Andrelândia-Raposos basin, spanning from the Archean to the Early Neoproterozoic period ([Fig. 18](#)). The Mesoproterozoic and Paleo-proterozoic inherited zircon grains are the most expressive in all

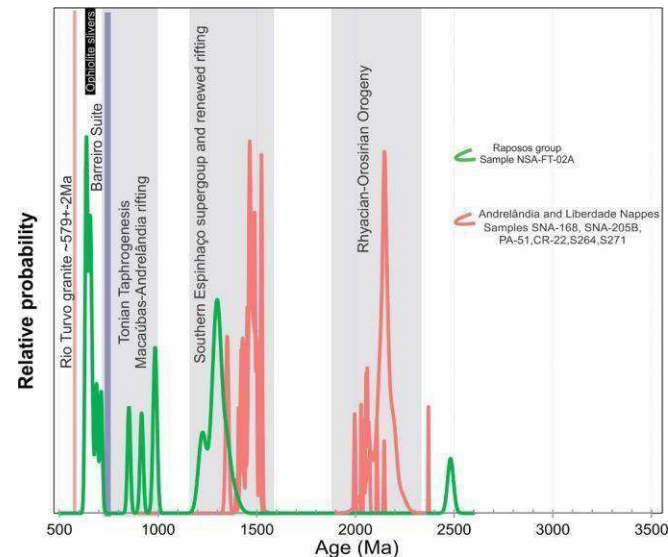


**Fig. 18.** Probability density plots for the mafic rocks. The sample NSA-FT-02 from Raposos group (green) and the metabasic rocks of the Andrelândia Group (light pink, [Coelho et al. 2017](#); [Frugis et al. 2018](#); [Pinheiro et al. 2019](#)) and main tectonic events recorded in the southern edge of São Francisco Craton, in light gray. The red bar represents the Rio Turvo Suite granitoid (~579 Ma, [Machado et al. 1996](#)); the black bar illustrates the ophiolitic slivers placed in the Araçuaí Orogen ([Queiroga, 2010](#); [Amaral et al. 2020](#)) and the purple one marks the intraplate magmatism recorded by the Barreiro Suite (~766 Ma, [Heilbron et al. 2019](#)).

samples, suggesting contamination from basement complexes during emplacement. This behavior can be explained by rift development process. Following the extensional processes, as the exhumation of older lithotypes advances, the supply of younger source material decreased (e.g., [Babinski et al., 2012](#); [Kuster et al., 2020](#)). The Tonian-Cryogenian age interval (1.0 Ga to 635 Ma) observed in this study can be related to significant Neoproterozoic basic magmatic events coeval with basin formation that supplied the sedimentary filling of the Andrelândia-Raposos basin (e.g., [Heilbron et al., 2019](#)).

As described in [Kuster et al. \(2020\)](#), the Mesoproterozoic ages interval, between 1.5 and 1.0 Ga, are related to Espinhaço rift expansion. The reworking of supracrustal rocks such as quartzites and diamictites or basic lithologies could represent expressive contribution to the Andrelândia-Raposos Group (e.g., [Babinski et al., 1999](#); [Danderfer et al., 2009](#); [Chemale Jr. et al., 2012](#); [Guadagnin et al., 2015](#); [Fonte-Boa et al., 2017](#)).

Among the main sources, the Rhyacian-Orosirian rocks from the basement orthogneiss made the major peak with ages ranging from ca. 1.8 Ma to 2.3 Ga (e.g., [Machado et al., 1996](#); [Silva et al., 2002](#); [Noce et al., 2007](#); [Heilbron et al., 2010](#)). These Rhyacian-Orosirian source rocks have been assigned to the Piedade, Mantiqueira, the Juiz de Fora and Pocrane complexes ([Caxito et al. 2015](#); [Degler et al. 2017](#); [Bruno et al. 2020a, b](#); [Barbosa et al., 2021](#) and references therein). Older TTG orthogneisses (ca. 2.4 Ga) occur as intrusions within the Mineiro Belt, southern São Francisco Craton ([Moreira et al. 2016](#); [Barbosa et al., 2021](#)).

### 6.4. Towards a tectonic model

The results obtained in this study improve the geotectonic framework envisaged for the evolution of Andrelândia-Raposos basin: a continental rift phase evolving to passive margin setting with strong crustal extension (hyperextended margin-type, [Fig. 19](#)). The occurrence of the metasedimentary units with enclosed metabasic rocks ascribed for the Andrelândia-Raposos extends for ca. 300 km (after the Brasiliano shortening). This large passive margin, together with the occurrence of basement inliers (previous highs) in the distal Raposo Distal Segment, and with the time and compositional evolution of the magmatism presented in the contribution are suggestive of a Neoproterozoic equivalent of a magma-poor hyperextended margin, as suggested for the Iberia and Alps passive margins ([Sutra and Manatschal, 2012](#); [Dore' and Lundin, 2015](#); [Peron-Pindivic and Manatschal, 2019](#)).

The geochemical, geochronology and isotopic data obtained for the Andrelândia-Raposos metabasites, reveal at least two episodes of mafic magmatism, evolving in time and space. The older episode with intra-plate Tonian high-TiO<sub>2</sub> metabasites was only found at the distal Raposo segment. It is followed by Cryogenian basic rocks with predominantly E to MORB signatures, with more juvenile compositions pointing to the maximum extension period of the basin development, coeval with the generation of oceanic crust, currently only found in the Araçuaí Orogen. Additional evidence for coeval magmatism with the deposition of the upper metasedimentary units (A6) is the similar isotopic composition between the studied metabasic rocks and the Santo Antonio plagioclase-rich schist (A5; [Fig. 16](#)). Additionally, the ultramafic inliers in the internal thrust sheets of the proximal domain (Andrelândia Group, LTS) are suggestive of SCLM exposition during the exhumation phase of evolution of a hyperextended margin, as proposed by [Sutra and Manatschal \(2012\)](#); [Dore' and Lundin \(2015\)](#); [Peron-Pindivic and Manatschal \(2019\)](#); [Zalán et al. \(2011\)](#); [Evain et al. \(2015\)](#).

### 7. Conclusions

The analyzed metabasic rocks are interpreted as examples of extensional mafic magmatism contemporaneous with distinct evolutionary stages of the Andrelândia-Raposos basin evolution. These can be correlated with similar ages and chemistry of mafic magmatic rocks

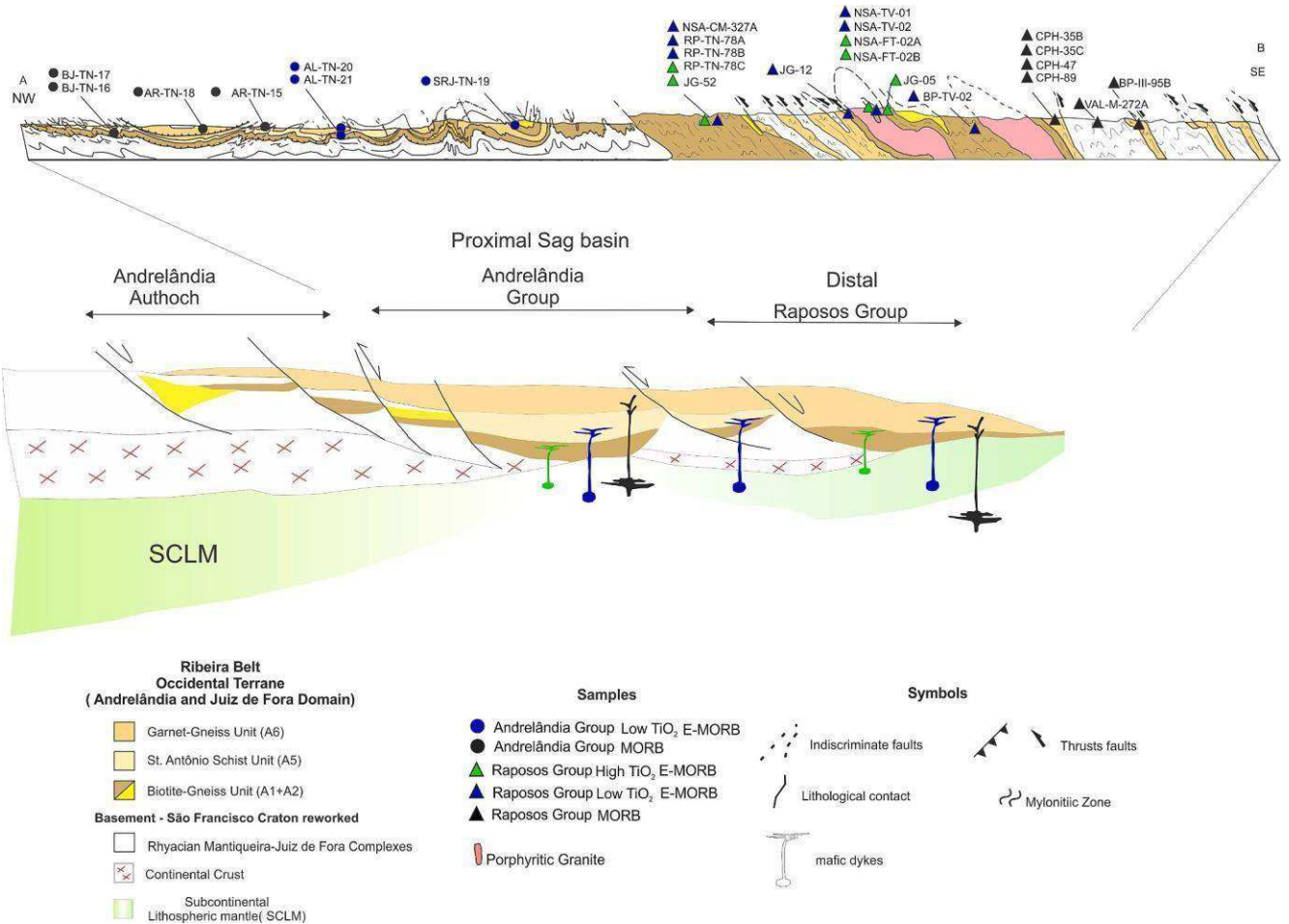


**Fig. 19.** a) geological cross section of the Occidental Terrane and sample locations. b) Tectonic reconstruction of the Neoproterozoic hyperextended margins of the Andrelândia-Raposos Groups.

described for the Araçuaí Orogen, to the north. Presently, three events between the Tonian and the Cryogenian were detected for the entire AROS segment at ca. 900, 766 and 660–650 Ma.

The obtained age of ca. 653 Ma from one example of metabasite with intraplate signatures constrains the final evolution of the basin in the late Cryogenian period. This evaluation is guided by zircon internal textures, high TiO<sub>2</sub> (2.1 %) and Zr (161 ppm) values and similar ages (~645 Ma) recorded by plagiogranites interleaved in ophiolitic slivers occurring within the Araçuaí Belt. As expected for rocks which have experienced a high temperature metamorphic overprint, zircon the morphology and internal textures are essential to recognize inheritance, crystallization ages and the age of the metamorphic overprint. Additionally, these younger mafic bodies may have acted as a potential source candidate for the upper units of the basin.

The chemistry and isotopic signatures evolve from typical high-TiO<sub>2</sub> intraplate magmatism to MORB-like mafic rocks in the distal parts of the basin, but always with some older inherited zircons and mostly mixed Mesoproterozoic T<sub>DM</sub> model ages. One important conclusion of the contribution is that the plagioclase rich biotite schist (A5 unit) of the Andrelândia-Raposos basin, just detected at the Andrelândia Group presents similar isotopic signatures of the studied mafic magmatism, suggesting that an intrabasinal volcaniclastic origin could be possible.

Data suggests that together the high-TiO<sub>2</sub> samples can be associated with the stage of continental rifting while MORB-like rocks are indicative to a more evolved stage of lithosphere thinning and SCLM exhumation. The prevalence of intraplate signatures in the lower units reinforces the idea that the continental extensional event started during the Tonian triggered the SF paleocontinent fragmentation, and that

extensional episodes with coeval magmatism may have lasted until Cryogenian times. Conversely, as deep marine scenario prevailed during depositional of the upper units, the MORB-like magmatism illustrates the severe extensional phase, with SCLM exhumation triggering some partial melt by decompression, generating the MORB-like metabasites until the break-up phase with inception of oceanic crust eastwards.

Finally, the envisaged tectonic model indicates a kind of hyperextend Neoproterozoic margin, with basement highs in the distal part of the basin, relatively poor magmatism, and occurrence of ultramafic slivers within the metasedimentary units. The proposed tectonic model is very similar with recent description of phanerozoic magma-poor hyper-extended margins such as the Santos Basin in the South Atlantic, the offshore Galicia basin at the North Atlantic, and part of the Alpine Tethys related passive margin sections in the Eastern Alps.

#### CRediT authorship contribution statement

**Talitta Nunes Manoel:** Conceptualization, Software, Data curation, Writing – original draft, Investigation, Writing – review & editing. **Monica Heilbron:** Investigation, Supervision, Project administration, Writing – review & editing. **Kathryn Cutts:** Supervision, Writing – re-view & editing. **Ivo Dussin:** Methodology, Software, Data curation. **Gloria Marins:** Sample preparation, Data curation. **Jailane de Sousa Gomes:** Sample preparation, Data curation. **Marcela Lobato:** Methodology, Data curation, Software. **Claudio Valeriano:** Supervision, Writing – review & editing. **Henrique Bruno:** Supervision, Writing – review & editing

## Declaration of Competing Interest

The authors declare that they have no known competing financial interests or personal relationships that could have appeared to influence the work reported in this paper.

## Data availability

Data will be shared as [supplementary materials](#)

## Appendix A. Supplementary data

Supplementary data to this article can be found online at <https://doi.org/10.1016/j.precamres.2022.106863>.

## References

- Alkmim, F.F., Teixeira, W., 2017. The Paleoproterozoic Mineiro Belt and the Quadrilátero Ferrífero. In: Heilbron, M., Cordani, U., Alkmim, F.F. (Eds.), São Francisco Craton, Eastern Brazil: Tectonic Genealogy of a Miniature Continent. Springer, Regional Geology Reviews, pp. 71–94.
- Almeida, R., Elizeu, V., Bruno, H., Bersan, S.M., Araújo, L.E.D.A.B., Dussin, I., Valeriano, C.d.M., Neto, C., Heilbron, M., 2022. Rhyanian-Orosirian tectonic history of the Juiz de Fora Complex: Evidence for an Archean crustal reservoir within an island-arc system. *Geoscience Frontiers* 13 (5), 101292.
- Amaral, L., Caxito, F.d.A., Pedrosa-Soares, A.C., Queiroga, G., Babinski, M., Trindade, R., Lana, C., Chemale, F., 2020. The Ribeira do Folha ophiolite-bearing accretionary wedge (Araçuaí orogen, SE Brazil): New data for Cryogenian plagiogranite and metasedimentary rocks. *Precambrian Res.* 336, 105522.
- Araújo, L.E.D.A.B., Heilbron, M., Valeriano, C.D.M., Teixeira, W., Aguiar Neto, C.C., 2019. Lithogeochemical and Nd-Sr isotope data of the orthogranulites of the Juiz de Fora complex, SE-Brazil: insights from a hidden Rhyanian Orogen within the Ribeira belt. *Brazilian Journal of Geology* 49 (3).
- Babinski, M., Van Schmus, W.R., Chemale Jr, F., 1999. Pb-Pb dating and Pb isotope geochemistry of Neoproterozoic carbonate rocks from the São Francisco basin, Brazil: implications for the mobility of Pb isotopes during tectonism and metamorphism. *Chemical Geology* 160 (3), 175–199.
- Babinski, M., Pedrosa-Soares, A.C., Trindade, R.I.F., Martins, M., Noce, C.M., Liu, D., 2012. Neoproterozoic glacial deposits from the Araçuaí orogen, Brazil: Age, provenance and correlations with the São Francisco craton and West Congo belt. *Gondwana Res.* 21, 451–465. <https://doi.org/10.1016/j.gr.2011.04.008>.
- Barbosa, N.S., Teixeira, W., Ávila, C.A., Montecinos, P.M., Bongiolo, E.M., Vasconcelos, F.F., 2019. U-Pb geochronology and coupled HF-Nd-Sr isotopic- chemical constraints of the Cassiterita Orthogneiss (2.47–2.41-Ga) in the Mineiro belt, São Francisco craton: geodynamic fingerprints beyond the Archean–Paleoproterozoic Transition. *Precambrian Res.* 326, 399–416.
- Bel'ém, J., Pedrosa-Soares, A.C., Noce, C.M., Silva, L.C., Armstrong, R., Fleck, A., Gradim, C.T., Queiroga, G.N., 2011. Bacia precursora versus bacias orogênicas: exemplos do Grupo Andrelândia com base em datações U-Pb (LA-ICP-MS) em zircão e análices litogênicas. *Geonomos* 19 (2), 224–243. <https://doi.org/10.18285/geo nomos.v19i2.55>.
- Boynton, W.V., 1984. Cosmochemistry of the rare earth elements; meteorite studies. In: Henderson, P. (Ed.), Rare earth element geochemistry. Publ. Co., Amsterdam Elsevier Sci, pp. 63–114.
- Bruno, H., Elizeu, V., Heilbron, M., de Morisson Valeriano, C., Strachan, R., Fowler, M., Bersan, S., Moreira, H., Dussin, I., Guilherme do Eirado Silva, L., Tupinambá, M., Almeida, J., Neto, C., Storey, C., 2020. Neoarchean and Rhyanian TTG-Sanukitoid suites in the southern São Francisco Paleocontinent, Brazil: evidence for diachronous change towards modern tectonics. *Geoscience Frontiers* 11 (5), 1763–1787.
- Bruno, H., Heilbron, M., Strachan, R., Fowler, M., de Morisson Valeriano, C., Bersan, S., Storey, C., 2021. Earth's new tectonic regime at the dawn of the Paleoproterozoic: Hf isotope evidence for efficient crustal growth and reworking in the São Francisco craton. *Brazil. Geology* 49 (10), 1214–1219.
- Campos Neto, M.C., Caby, R., 2000. Lower crust extrusion and terrane accretion in the Neoproterozoic nappes of southeast Brazil. *Tectonics* 19, 669–687.
- Campos Neto, M.C., Janasi, V.A., Basel, M.A.S., Siga Jr, O., 2007. Sistema de nappes Andrelândia, setor oriental: litotestratigrafia e posição estratigráfica. *Rev Bras Geociênc.* 37, 47–60.
- Cardoso, C.D., Ávila, C.A., Neumann, R., Oliveira, E.P., Valeriano, C.M., Dussin, I., 2019. A Rhyanian continental arc during the Evolution of the Mineiro belt, Brazil: constraints from the Rio Grande and Brumado metadiorites. *Lithos* 326–327, 246–264. <https://doi.org/10.1016/j.lithos.2018.12.025>.
- Chemale, F., Kawashita, K., Dussin, I.A., Ávila, J.N., Justino, D., Bertotti, A., 2012. U-Pb zircon in situ dating with LA-MC-ICP-MS using a mixed detector configuration. *An. Acad. Bras. Cienc.* 84, 275–295.
- Cioffi, C.R., Neto, M.D.C.C., Moeller, A., Rocha, B.C., 2016. Paleoproterozoic continental crust generation events at 2.15 and 2.08 Ga in the basement of the southern Brasília Orogen. SE Brazil. *Precambrian Research* 275, 176–196.
- Coelho, M.B., Trouw, R.A.J., Ganade de Araújo, C.E., Vinagre, R., Mendes, J.C., Sato, K., 2017. Constraining timing and P-T conditions of continental collision and late overprinting in the Southern Brasília Orogen (SE-Brazil): U-Pb zircon ages and geothermobarometry of the Andrelândia Nappe System. *Precambrian Research* 292, 194–215. <https://doi.org/10.1016/j.precamres.2017.02.001>.
- Corfu, F., Hanchar, J.M., Hoskin, P.W.O., Kinny, P., 2003. *Atlas of Zircon Textures, Rev. Mineral. Geochem.* 53 (1), 469–500.
- Cutts, K., Lana, C., 2019. The complex tale of Mantiqueira and Juiz de Fora: A comment on “Eoarchean to Neoproterozoic crustal evolution of the Mantiqueira and Juiz de Fora Complexes, SE Brazil: Petrology, geochemistry, zircon U-Pb geochronology and Lu-Hf isotopes”. *Precambrian Research* 332, 105305.
- Danderfer, A., De Waele, B., Pedreira, A.J., Nalini, H.A., 2009. New geochronological constraints on the geological evolution of Espinhaço basin within the São Francisco Craton-Brazil. *Precambrian Res.* <https://doi.org/10.1016/j.precamres.2009.01.002>.
- Degler, R., Pedrosa-Soares, A.C., Dussin, I., Queiroga, G., Schulz, B., 2017. Contrasting provenance and timing of metamorphism from paragneisses of the Araçuaí-Ribeira orogenic system, Brazil: Hints for Western Gondwana assembly. *Gondwana Research* 57, 30–50. <https://doi.org/10.1016/j.gr.2017.07.004>.
- DePaolo, D.J., 1988. Neodymium isotope geochemistry: An introduction. New York, 187pp.
- Dilek, Y., Furnes, H., 2011. Ophiolite genesis and global tectonics: Geochemical and tectonic fingerprinting of ancient oceanic lithosphere. *Bull. Geol. Soc. Am.* 123 (3–4), 387–411.
- Doré, T., Lundin, E., 2015. Research focus: Hyperextended continental margins—knowns and unknowns. *Geology* 43 (1), 95–96.
- Duarte, B., Heilbron, M., Nogueira J.R., Tupinambá, M., Eirado, L.G., Valladares, C., Almeida J.C.H., Guia C., 2003. Geologia das Folhas Juiz de Fora e Chiador. In: Pedrosa-Soares A.C., Noce C.M., Trouw R., Heilbron M. (coords.). Projeto Sul de Minas. Belo Horizonte, COMIG/SEME, v. 1, p. 153–258.
- Duarte, B.P., Figueiredo, M.C.H., Campos, N.M., Heilbron, M., 1997. Geochemistry of the granulite facies orthogneisses of Juiz de Fora Complex, Central Segment of the Ribeira Belt. Southeastern Brazil. *Revista Brasileira de Geociências* 27 (1), 67–82.
- Ebert, H., 1984. Aspectos da Geologia da região de São João del Rei. In: SBG-SP (Ed.), Os Paraiabides entre São João del Rei e Itapira e a Bifurcação entre Paraiabides e Araxáides (in memoriam), pp. 114 São Paulo.
- Evain, M., Afiflido, A., Rigoti, C., Loureiro, A., Alves, D., Klingelhoefer, F., Aslanian, D., 2015. Deep structure of the Santos basin-são Paulo plateau system, SE Brazil. *Journal of Geophysical Research: Solid Earth* 120 (8), 5401–5431.
- Fonse-Boa, T.M.R., Novo, T.A., Pedrosa-Soares, A.C., Dussin, I., 2017. Records of Mesoproterozoic taphrogenic events in the eastern basement of the Araçuaí Orogen, southeast Brazil. *Braz. J. Genet.* 47 (3), 447–466.
- Frimmel, H.E., Tack, L., Basei, M., Nutman, A., Boven, A., 2006. Provenance and Chemostratigraphy Of the Neoproterozoic West Congolian Group In The Democratic Republic Of Congo. *Journal of African Earth Sciences* 46, 221–239.
- Frugis, G.L., Neto, M.D.C.C., Lima, R.B., 2018. Eastern Parapananema and Southern São Francisco orogenic margins: records of enduring Neoproterozoic oceanic convergence and collision in the Southern Brasília Orogen. *Precambr. Res.* <https://doi.org/10.1016/j.precamres.2018.02.005>.
- Ganade de Araújo, C.E., 2014. Evolução Tectônica da Margem ativa Neoproterozoica do Orogono Gondwana Oeste na Província Borborema (NÉ-Brasil). Universidade de São Paulo, p. 243. PhD Thesis.
- Gonçalves, M.L., Figueiredo, M.C.H., 1992. Geoquímica dos Anfibolitos de Santana do Garambá (MG): Implicações Tectônicas sobre a Evolução do Grupo Andrelândia. *Geoquímica Brasileira* 6 (2), 127–140.
- Guadagnin, F., Chemale, F., Magalhães, A.J.C., Santana, A., Dussin, I., Takehara, L., 2015. Age constraints on crystal-tuff from the Espinhaço Supergroup – insight into the Paleoproterozoic to Mesoproterozoic intracratonic basin cycles of the Congo-São Francisco Craton. *Gondwana Res.* 27, 363–376. <https://doi.org/10.1016/j.gr.2013.10.009>.
- Heilbron, M., Duarte, B.P., Nogueira, J.R., 1998. The Juiz de Fora Complex of The Central Ribeira Belt, Se Brazil: A Segment of Paleoproterozoic Granulitic Crust Thrust During The Panafrikan Orogeny. *Gondwana Research* 1 (3), 373–382.
- Heilbron M.; Soares, A.C.P.; Campos N.; Silva, L.C.; Trouw, R.; Janasi, V., 2004. Província Mantiqueira. In: Mantesso-neto, Virginio; Bartorelli, Andreia; Carneiro, Celso Dal R'e; Brito Neves, Benjamin Bley De. (Org.). *Geologia Do Continente Sul Americano: Evolução da Obra De Fernando Flávio Marques De Almeida*. São Paulo: Beira Produções Culturais, V. I, P. 203–234.
- Heilbron, M., Valeriano, C.M., Tassinari, C.C.G., Almeida, J.C.H., Tupinamba, M., Siga, O., Trouw, R., 2008. Correlation of Neoproterozoic terranes between the Ribeira Belt, SE Brazil and its African counterpart: comparative tectonic evolution and open questions. *Geological Society of London, Special Publication*, p. 294.
- Heilbron, M., Duarte, B.P., Valeriano, C.M., Simonetti, A., Machado, N., Nogueira, J.R., 2010. Evolution of reworked Paleoproterozoic basement rocks within the Ribeira belt (Neoproterozoic, SE-Brazil, based on U-Pb geochronology: Implications for paleogeographic reconstructions of the São Francisco-Congo paleocontinent. *Precambrian Research* 178, 136–148.
- Heilbron, M., Mohriak, W., Valeriano CM, Milani E, Almeida JCH, Tupinambá M., 2000. From collision to extension: the roots of the South-eastern continental margin of Brazil. In: Talwani, Mohriak (Eds.), *Atlantic Riffs and Continental Margin*. AGU Geophysical Monograph Series, vol. 115, 354 pp.
- Heilbron, M., Ribeiro, A., Valeriano, C.M., Paciullo, F.V.P., Almeida, J.C.H., Trouw, R.A. J., Tupinamba, M., Silva, L.G.E., 2017. The Ribeira belt. In: Heilbron, M., Cordani, U. G., Alkmim, F.F. (Eds.), São Francisco Craton, Eastern Brazil: Tectonic Genealogy of a Miniature Continent. *Regional Geology Reviews*. Springer International Publishing Co., Switzerland, pp. 277–304. <https://doi.org/10.1007/978-3-319-01715-0>.
- Heilbron, M., Oliveira, C., Lobato, M., Valeriano, C.M., Dussin, I., Dantas, E., Simonetti, A., Bruno, H., Corrales, F., Socoloff, E., 2019. The Barreiro suite in the central Ribeira Belt (SE Brazil): a late Tonian tholeiitic intraplate magmatic event in

- the distal passive margin of the São Francisco Paleocontinent. *Brazilian Journal of Geology* 49 (2), 1–19. <https://doi.org/10.1590/2317-4889201920180129>.
- Irvine, T.M., Baragar, W.R., 1971. A guide to the chemical classification of common volcanic rocks. *Canadian Journal of Earth Sciences* 8 (5), 523–548. <https://doi.org/10.1139/e71-055>.
- Jackson, S.E., Pearson, N.J., Griffin, W.L., Belousova, E.A., 2004. The application of laser ablation-inductively coupled plasma-mass spectrometry to in situ U-Pb zircon geochronology. *Chem. Geol.* 211, 47–69.
- Janoušek, V., Farrow, C.M., Erban, V., 2006. Interpretation of whole-rock geochemical data in igneous geochemistry: introducing Geochemical Data Toolkit (GCDkit). *Journal of Petrology* 47 (6), 1255–1259.
- Kuchenbecker, M., Pedrosa-Soares, A.C., Babinski, M., Fanning, M., 2015. Detrital zircon age patterns and provenance assessment for pre-glacial to post-glacial successions of the Neoproterozoic Macaúbas Group, Araçuaí orogen, Brazil. *Precambr. Res.* 266, 12–26.
- Kuster, K., Ribeiro, A., Trouw, R.J., Dussin, I., Marimon, R., 2020. The Neoproterozoic Andrelândia group: Evolution from an intraplate continental margin to an early collisional basin south of the São Francisco craton. *Brazil. Journal of South American Earth Sciences* 102666.
- Labot, M.C., 2018. Proveniência das rochas metasedimentares dos diferentes terrenos tectonoestratigráficos da Faixa Ribeira Central, com base em dados U-Pb e Lu-Hf obtidos em grãos de zircão detriticos. Doctoral Thesis. Rio de Janeiro State University.
- Ludwig, K.R., 2008. User's Manual for Isoplot 3.70: A Geochronological Toolkit for Microsoft Excel, 4. Berkeley Geochronology Center Special Publication, p. 76.
- Machado, N., Schrank, A., Noce, C.M., Gauthier, G., 1996. Ages of detrital zircon from Archean-Paleoproterozoic sequences: implications for Greenstone Belt setting, evolution of a Transamazonian foreland basin in Quadrilátero Ferrífero, southeast Brazil. *Earth Planet. Sci. Lett.* 141 (1–4), 259–276.
- Marimon, R.S., Trouw, R.A.J., Dantas, E.L., Ribeiro, A., 2020. U-Pb and Lu-Hf isotope systematics on detrital zircon from the southern São Francisco Craton's Neoproterozoic passive margin: tectonic implications. *J. S. Am. Earth Sci.* 100, 1–20.
- Marins, G., 2000. Petrologia dos Anfíbolitos do Domínio Juiz de Fora e da Klippe Paraíba do Sul, no Setor Central da Faixa Ribeira. MS Dissertation, Programa em Análise de Bacias e Faixas Motrizes, Universidade do Estado do Rio de Janeiro, Rio de Janeiro.
- Moreira, H., Lana, C., Nalini Jr, H.A., 2016. The detrital zircon record of an Archean convergent basin in the Southern São Francisco Craton, Brazil. *Precambrian Research* 275, 84–99.
- Mullen, E.D., 1983. MnO/TiO<sub>2</sub>/P2O<sub>5</sub>: a minor element discriminant for basaltic rocks of oceanic environments and its implications for petrogenesis. *Earth and planetary science letters* 62 (1), 53–62.
- Paciullo, F.V.P., Ribeiro, A., Andreis, R.R., Trouw, R.A.J., 2000. The Andrelândia Basin, a Neoproterozoic intra-plate continental margin, southern Brasília Belt. *Revista Brasileira de Geociências* 30 (1), 200–202.
- Paciullo F.V.P., 1997. A Sequência Depositional Andrelândia. Doctoral Thesis, Instituto de Geociências, Universidade Federal do Rio de Janeiro, Rio de Janeiro.
- Pearce, J.A., 1996. A user's guide to basalt discrimination diagrams. Trace element geochemistry of volcanic rocks: applications for massive sulphide exploration. Geological Association of Canada, Short Course. Notes 12 (79), 113.
- Pearce, J.A., 2008. Geochemical fingerprinting of oceanic basalts with applications to ophiolite classification, The search for Archean oceanic crust. *Lithos* 100 (1), 14–48.
- Pearce, J.A., Cann, J.R., 1973. Tectonic setting of basic volcanic rocks determined using trace element analyses. *Earth and planetary science letters* 19 (2), 290–300.
- Pearce, J.A., 1982. Trace element characteristics of lavas from destructive plate boundaries. In: Thorpe, R.S. (Ed.), Andesites: orogenic andesites and related rocks. Wiley, Chichester, pp. 525–548.
- Pedrosa-soares, A.C., Noce, C.M., Vidal, P., Monteiro, R., Leonards, O.H., 1992. Toward A New Tectonic Model For The Late Proterozoic Araçuaí (Se Brazil)—west Congolian (Sw Africa) Belt. *Journal Of South American Earth Sciences* 6, 33–47.
- Pedrosa-Soares, A.C., Alkmim, F.F., Tack, L., Noce, C.M., Babinski, M., Silva, L.C., Martins-Neto, M.A., 2008. Similarities and differences between the Brazilian and African counterparts of the Neoproterozoic Araçuaí-West Congo orogen. In: Pankhurst, R.J., Trouw, R.A.J., Brito Neves, B.B., De Wit, M.J. (Eds.), West Gondwana: Pre-Cenozoic Correlations Across the South Atlantic Region. Geological Society, Special Publications, London, pp. 153–172.
- Peron-Pinvidic, G., Manatschal, G., 2019. Rifted margins: State of the art and future challenges. *Frontiers. Earth Science* 218.
- Pinheiro, M.A.P., Saita, M.T.F., Lesnov, F.P., Tedeschi, M., Silva, L.C., Medvedev, N.S., Korolyuk, V.N., Pinto, C.P., Sergeev, S.A., 2019. Timing and petrogenesis of metamorphic-metabasic rocks in the Southern Brasília orogen: insights for a Rhyanian multi-system suprasubduction zone in the São Francisco paleocontinent (SE-Brazil). *Precambrian Res.* 321, 328–348.
- Queiroga, G.N., 2010. Caracterização de restos de litosfera oceânica do Oeste do Brasil—West Gondwana: new data from the southern Brasília belt. *Brazil. J. Geol. Soc.* 166 (6), 1013–1032.
- Ribeiro, A., Trouw, R.A.J., Andreis, R.R., Paciullo, F.V.P., Valença, J.G., 1995. Evolução das bacias proterozoicas e o termo-tectonismo brasileiro na margem sul do cráton do São Francisco. *Revista Brasileira de Geociências* 25, 235–248.
- Saccani, E., 2015. A new method of discriminating different types of post-Archean ophiolitic basalts and their tectonic significance using Th-Nb and Ce-Dy-Yb systematics. *Geoscience Frontiers*, 6(4):481–501. <https://doi.org/10.1016/j.gsf.2014.03.006>.
- Santos, M.M., Lana, C., Scholz, R., Buick, I., Schmitz, M.D., Kamo, S.L., Gerdes, A., Corfu, F., Tapster, S., Lancaster, P., Storey, C.D., Basei, M.A.S., Tohver, E., Alkmim, A., Nalini, H., Krambrock, K., Fantini, C., 2017. A new appraisal of Sri Lankan zircons as reference material for in situ U-Pb geochronology, REE analyses and Lu-Hf isotope tracing. *Geostand. Geoanal. Res.*
- Santos, P.S., 2011. Geocronologia, Área Fonte e Ambiente Tectônico da Unidade Santo Antônio – Megasequência Andrelândia. Unpublished Master Thesis. Universidade Federal do Rio de Janeiro, pp. 70.
- Shervais, J.W., 1982. Ti-V plots and the petrogenesis of modern and ophiolitic lavas. *Earth and planetary science letters* 59 (1), 101–118.
- Silva, L.C., Armstrong, R., Delgado, I.M., Pimentel, M., Arcano, J.B., Mello, R.C., Jost, H., Cardoso Filho, J.M., Pereira, L.H.M., 2002. Reavaliação da evolução geológica em terrenos pré-cambrianos brasileiros com base em novos dados U-Pb SHRIMP, Parte I: limite centro-oriental do Cráton São Francisco na Bahia. *Rev. Bras. Geociências* 32 (2), 501–512.
- Slařík, J., Košler, J., Condon, D.J., Crowley, J.L., Gerdes, A., Hanchar, J.M., Horstwood, M.S., Morris, G.A., Nasdala, L., Norberg, N., Schaltegger, U., 2008. Plešovice zircon—a new natural reference material for U-Pb and Hf isotopic microanalysis. *Chem. Geol.* 249, 1–35.
- Sun, S. & McDonough, W.F., 1989. Chemical and isotopic systematics of oceanic basalts: implications for mantle composition and processes. In: Saunders A.D., Norry M.J. (eds.), *Magmatism in the Ocean Basins*. London, Geological Society, p. 313–345.
- Sutra, E., Manatschal, G., 2012. How does the continental crust thin in a hyperextended rifted margin? Insights from the Iberia margin. *Geology* 40 (2), 139–142.
- Tack, L., Wingate, M.T.D., Liégeois, J., Fernández-Alonso, M., Deblond, A., 2001. Early Neoproterozoic magmatism (1000–910 Ma) of the Zadinnian and Mayumbian Groups (Bas-Congo): onset of Rodinia rifting at the western edge of the Congo craton. *Precambr. Res.* 110, 277–306.
- Tedeschi, M., Lanari, P., Rubatto, D., Pedrosa-Soares, A., Hermann, J., Dussin, I., Pinheiro, M.A.P., Bouvier, A.S., Baumgartner, L., 2017. Reconstruction of multiple P-T stages from retrogressed mafic rocks: subduction versus collision in the Southern Brasília orogen (SE-Brazil). *Lithos* 294–295, 283–303.
- Trouw, R.A.J., Heilbron, M., Ribeiro, A., Valeriano, C., Paciullo, F., Almeida, J.C.H., Tupinambá, M., 2000. The Central Segment of the Ribeira belt. In: Cordani U., Milani E., Thomaz-Filho A., Campos D. (eds.), *Geotectonics of South America*. Rio de Janeiro, CPRM, v. 1, p. 287–310.
- Trouw, R.A.J., Peteruel, R., Ribeiro, A., Heilbron, M., Vinagre, R., Duffles, P., Trouw, C.C., Fontainha, M., Kussama, H.H., 2013. A new interpretation for the interference zone between the southern Brasília belt and the central Ribeira belt, SE Brazil. *Journal of South American Earth Sciences* 48, 43–57.
- Valeriano, C.M., Dardenne, M.A., Fonseca, M.A., Simões, L.S.A., Seer, H.J., 2004. A evolução tectônica da Faixa Brasília. In: V. Mantesso-Neto, *Geologia do Continente Sul-Americano: evolução e obra de Fernando Flávio Marques de Almeida, Beca*, São Paulo, pp. 575–593.
- Valladares, C.S., Machado, N., Heilbron, M., Duarte, B.P., Gauthier, G., 2008. Sedimentary Provenance in the Central Ribeira belt based on Laser-Ablation ICPMS 207Pb/206Pb Zircon Ages. *Gondwana Research*, v. 13, p. 516/GR-00196–526.
- Valladares, C.S., Machado, N., Heilbron, M., Gauthier, G., 2004. Ages of detrital zircon from siliciclastic successions south of the São Francisco Craton, Brazil: implications for the evolution of Proterozoic basin. *Gondwana Research* 7 (4), 913–921. [https://doi.org/10.1016/S1342-937X\(05\)71074-1](https://doi.org/10.1016/S1342-937X(05)71074-1).
- Data Reduction Software For La-icp-ms. In *Laser Ablation-icpms In The Earth Science* 29, 2001, 239–243.
- Westin, A., Campos Neto, M.C., 2013. Provenance and tectonic setting of the external nappe of the Southern Brasília Orogen. *Journal of South American Earth Sciences* 48, 220–239.
- Westin, A., Campos Neto, M.C., Cawood, P.A., Hawkesworth, C.J., Dhuime, B., Delavault, H., 2019. The neoproterozoic southern passive margin of the São Francisco craton: insights on the pre-amalgamation of West Gondwana from U-Pb and Hf-Nd isotopes. *Precambrian Res.* 320, 454–471.
- Westin, A., Neto, M.C.C., Hollanda, M.H.B., Salazar-Mora, C.A., Queiroga, G.N., Frugis, G.L., de Castro, M.P., 2021. The fast exhumation pattern of a Neoproterozoic nappe system built during West Gondwana amalgamation: Insights from thermochronology. *Precambrian Research* 355, 106115.
- Westin, A., Campos Neto, M.C., Hawkesworth, C., Cadwood, P., Dhuime, B., Delavault, H., 2016. A Paleoproterozoic intra-arc basin associated with a juvenile source in the southern Brasília Orogen: using U-Pb ages and Hf-Nd isotopic analyses in provenance studies of complex areas. *Precambrian Res.* 276, 178–193.
- Wilson, M., 1989. *Igneous Petrogenesis*. Unwin Hyman, London.
- Winchester, J. A., Park, R. G., & Holland, J. G., 1980. The geochemistry of Lewisian semipelitic schists from the Gairloch District, Wester Ross. *Scottish Journal of Geology*, 16(2–3), 165–179.
- Zalán, P. V., Severino, M. D. C. G., Rigoti, C. A., Magnavita, L. P., Oliveira, J. A. B., & Vianna, A. R., 2011. An entirely new 3D-view of the crustal and mantle structure of a South Atlantic passive margin—Santos, Campos and Espírito Santo basins, Brazil. In AAPG annual conference and Exhibition (Vol. 10, p. 13).
- Zalán, P. V., Severino, M. D. C., Rigoti, C. A., Magnavita, L. P., Oliveira, J. A. B., & Vianna, A. R., 2011. An entirely new 3D-view of the crustal and mantle structure of a South Atlantic passive margin—Santos, Campos and Espírito Santo basins, Brazil. In AAPG annual conference and Exhibition (Vol. 10, p. 13).

## 3.2 The polyphase evolution of the mafic rocks of the Juiz de Fora Complex: The record of two supercontinent cycles

Talitta Nunes Manoel <sup>a,\*</sup>, Kathryn Cutts <sup>b</sup>, Monica Heilbron <sup>a</sup>, George Luvizotto <sup>c</sup>, Henrique Bruno <sup>a</sup>, Cristiano Lana <sup>d</sup>, Ivo Dussin <sup>a</sup>, Claudio de Morrison Valeriano <sup>a</sup>

<sup>a</sup> Rio de Janeiro State University, Programa de Pós-Graduação em Geologia (FGEL) – TEKTOS. UERJ, São Francisco Xavier Street, 524-Maracanã, Rio de Janeiro, Brazil

<sup>b</sup> Geological Survey of Finland, P.O. Box 96, FI-02151, Espoo, Finland

<sup>c</sup> Department of Geology, São Paulo State University, Av. 24A, Rio Claro, 1515, 13506-900, Brazil

<sup>d</sup> Departamento de Geologia, Universidade Federal de Ouro Preto, Ouro Preto, MG, 35400-000, Brazil

### ABSTRACT

#### ARTICLE INFO

##### Keywords:

Juiz de fora complex

Paleoproterozoic arc-related magmatism Zircon U–Pb

geochronology

Lu–Hf isotopes Geothermobarometry

The Juiz de Fora Complex (JFC) in the Araquá-Ribeira orogenic system, southeastern Brazil, is a basement unit displaying a variety of rock types that is tectonically imbricated with the supracrustal rocks of the Raposos Group in the Upper Thrust System of the Occidental Terrane, Ribeira Belt. Here we report new petrological, geochemical, and zircon U–Pb and Lu–Hf isotopic data on mafic garnet-granulites from the JFC with a view to evaluate the timing and P-T conditions of the collisional event as well as protolith formation. This work presents the most comprehensive metamorphic study on the Juiz de Fora Complex rocks to date. Metamorphic P-T estimates for the metamorphic peak conditions of 800–900 °C and 8–9 kbar in basic garnet-bearing granulites were obtained for the JFC, indicating that metamorphism took place at deeper crustal levels. Geochemical, zircon U–Pb geochronology, whole-rock Sm–Nd, Rb–Sr isotopes, and Lu–Hf isotopic data of mafic granulites yielded U–Pb ages of ca. 2201 Ma, and moderately juvenile  $\epsilon_{\text{Nd}}(t) = -0.5$  and were obtained from the JFC marking the timing of volcanic arc magmatism during the Rhyacian period. This arc-related stage was followed by the post-collisional period during the Early Paleoproterozoic with ca. 1.94 Ga E-MORB signature granulites that shows evidence of magma sourced from Neoarchean (~2.8 Ga) crust with addition of juvenile components. The high-grade metamorphism is possibly related to the final collision of the Congo and São Francisco Cratons at 590–560 Ma, which placed the Neoproterozoic metasediments and the JFC rocks at the same level. The integrated information sheds light on two collisional episodes where the oldest is represented by arc-related granulites during the Rhyacian Orogeny and the youngest is the higher-pressure Neoproterozoic overprint during the Brasiliano Orogeny.

## 1. Introduction

Mafic rocks occur in a wide spectrum of tectonic environments throughout time and their study within orogenic belts contributes to development of tectonic models for Precambrian terranes (Sun and McDonough, 1989; Cabanis and Thieblemont, 1988; Vermeesch, 2006; Pearce, 2008; Ross and Bedard, 2009; Pearce, 2014; Saccani, 2015; Xia and Li, 2019). Tectonic environments where mafic rocks occur range from continental and oceanic plateaus (LIPs in intraplate settings), continental rifts to passive margins, and convergent tectonic settings such as magmatic arcs and successor post-collisional magmatism

(Pearce and Cann, 1973; Pearce et al., 1975; Pearce, 1983; Wilson, 1989).

Mafic rocks as mantle-derived magmas, also aid with the understanding of partial melting systems and crustal growth (Foley et al., 2002; Hawkesworth et al., 1994, 2010; Pearce and Parkinson, 1993).

However, in high-grade metamorphic terranes, conditions that are common in Precambrian terranes, recrystallization and deformation could obscure the primary characteristics of mafic rocks, including textures and geometries, which can hamper the interpretation of tectonic settings. In such terranes, the geochemical and isotopic signatures, and the age of mafic rocks are important tools for the determination of their tectonic setting. Geochronology provides additional constraints on

the age of the protoliths and the age of any high-grade metamorphic overprinting event. Within Precambrian terranes, high-grade metamorphism is widely associated with episodes of major continental crust formation and reworking, resulting in polymetamorphic features (Harley, 1989). Pressure-temperature-time (P-T-t) reconstructions in rocks that have experienced amphibolite to granulite facies can be puzzling; however, such rocks have proved an important tool for determining the geodynamic cycles of orogenic belts (e.g. Tedeschi et al., 2017; Kunz and White, 2019; Gutiérrez-Aguilar et al., 2021).

In southeastern Brazil, two major tectonic cycles are responsible for the current configuration of the São Francisco craton and surrounding belts: a) during the Siderian to Rhyacian age at ca. 2.40 to 2.04 Ga, large continental fragments were accreted to the São Francisco paleocontinent (Teixeira et al., 2017; Moreira et al., 2018; Bruno et al., 2020, 2021; Seixas et al., 2012; Noce et al., 2007; Heilbron et al., 2010); b) during the Neoproterozoic between ca. 650-510 Ma, a large network of orogenic systems were amalgamated onto the West Gondwana Supercontinent (Heilbron et al., 2000, 2008, 2010), followed by extensive tectonic collapse during the Late Cambrian to Early Ordovician time (Heilbron et al., 2017).

The focus of this study is the mafic granulites inserted into the Juiz de Fora Complex, which is one of the basement associations (pre-1.8 Ga) of the central segment of the Neoproterozoic Ribeira Belt (Almeida et al., 1977; 1981; Trouw et al., 2000; Heilbron et al., 2017). The Ribeira Belt together with the Northern Araçáí Belt makes up the 1000 km long AROS Orogenic System (Pedrosa Soares et al., 2008; Alkmim et al., 2017), extending along the eastern Brazilian coast. Both the basement and the Neoproterozoic associations experienced high-grade metamorphism as a result of the tectonic stacking during the Brasiliano Orogeny, associated with different stages of the West Gondwana

assembly (e.g. Heilbron et al., 2000, 2017; Duarte et al., 2000; Degler et al., 2018; Cutts et al., 2020; Almeida et al., 2021; Mauri et al., 2022, in press).

The investigated mafic rocks were selected for study because they can provide evidence about the evolving tectonic settings through time during the Rhyacian Orogeny, but they have also experienced high temperature reworking during the Brasiliano Orogeny. The studied rocks contain the assemblage garnet + plagioclase + clinopyroxene + orthopyroxene + amphibole + quartz + ilmenite as the main paragenesis, indicate granulite facies metamorphism (Bucher and Grapes, 2011). In this work we present mineral chemistry data, U-Pb zircon ages coupled with Hf systematics, Sr and Nd isotopes and a petrochronological investigation using quantitative compositional mapping (Lanari et al., 2013, 2014; Lanari and Duesterhoeft, 2019) in an effort to unravel the tectonic setting and evolution of the mafic rocks hosted in the Ribeira Belt. Finally, a discussion of the two major supercontinental stages and the importance of mafic rocks to tectonic models are addressed.

## 2. Regional background geology and the Juiz de Fora complex

The Ribeira Belt, southeast Brazil, comprises a set of orogenic systems resulting from West Gondwana's amalgamation (e.g. Heilbron et al., 2017) and moving up to the north, combined with Araçáí Orogen, illustrates a complex collisional system represented by the Araçáí-Ribeira System (AROS e.g. Pedrosa-Saôres et al., 2008, 2011; Degler et al., 2018).

The tectonic organization of the Ribeira Belt comprises four tectono-stratigraphic terranes (Fig. 1), which are from NW to SE, the Occidental, Central (Paraíba do Sul-Embu), Oriental and Cabo Frio Terranes,

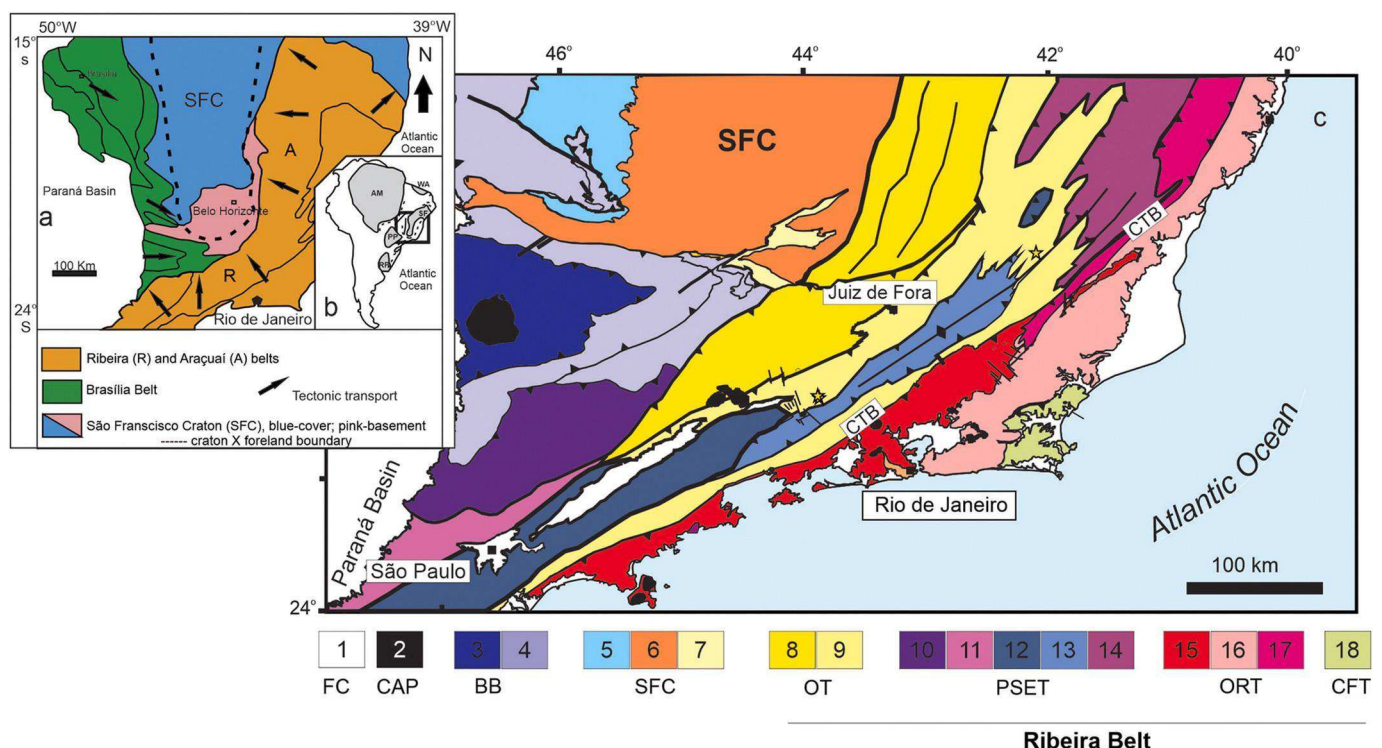


**Fig. 1.** a) Location the studied area (red rectangle) in the context of the São Francisco Craton and Neoproterozoic orogens. b) Location of cratons: AM-Amazonian, WA- West African, SF-São Francisco, PP- Paranapanema and RP- Rio de la Plata cratons. Simplified tectonic sketch map modified from Trouw et al. (2013) and Kuster et al. (2020). c) Tectonic map of the central Ribeira Belt modified from Heilbron et al. (2017). 1: Phanerozoic cover; 2: K-T alkaline rocks; 3: passive margin related nappes; 4: arc-related nappes; 5: cratonic basement; 6: Bambuí cover; 7: Mesoproterozoic rift-to-sag units; 8-9: Occidental Terrane with 8 -Andrelândia (lower thrust) and 9 - Juiz de Fora (upper thrust). Cordilleran arc accreted terrane, with 10: Apiaí; 11: Socorro; 12: Embú; 13: Paraíba do Sul; 14: Rio Doce; 15: Rio Negro arc; 16: Itaíva arc; 17: high-grade metasediments; 18: Cabo Frio Terrane. FC- Phanerozoic cover; CAP-Calc-Alkaline Provinces; BB-Brasília Belt, SFC-São Francisco Craton; OT- Occidental Terrane; PSET-Paraíba do Sul-Embu Terrane, ORT-Oriental Terrane; CFT-Cabo Frio Terrane. CTB-Central Tectonic Boundary. star: sample location.

Heilbron et al. (2008, 2017, 2021). These terranes progressively docked to the southern tip of the SFC. The westernmost tectonic terrane, the focus of the work, is represented by the Occidental Terrane, which encompasses a Neoproterozoic passive margin succession (Andrelândia Group-e.g., Paciullo et al., 2000) and reworked cratonic basement complexes (Heilbron et al., 2010; Degler et al., 2018; Cutts et al., 2020; Bruno et al., 2020).

The Occidental terrane (Fig. 2) includes two crustal-scale thrust sheets that configure the lower thrust sheet (Andrelândia structural Domain), and the upper thrust sheet (Juiz de Fora structural Domain) (Heilbron et al., 2010). In the lower thrust sheet, the Piedade and Mantiqueira complexes (Noce et al., 2003; Heilbron et al., 2010; Degler et al., 2018; Kuribara et al., 2019; Bruno et al., 2020, 2021) represent the Archean to Paleoproterozoic basement unit that are overridden by highly deformed (amphibolite to granulite facies) metasedimentary units of Andrelândia Group (e.g., Heilbron et al., 2010). In the upper thrust system, the equivalent distal Neoproterozoic metasedimentary unit is named the Raposos Group (distal equivalent of the Andrelândia Group, Heilbron et al., 2013; 2021), which is tectonically interlayered with the compositionally diverse, granulite facies basement rocks of the Juiz de Fora Complex (e.g. Trouw et al., 2000; Heilbron et al., 2004; Noce et al., 2003, 2007; Degler et al., 2018). The studied mafic rocks are representative of mafic granulites of the Juiz de Fora Complex.

The Juiz de Fora Complex was previously reported as a series of rocks formed in an intra-oceanic arc setting (e.g. Noce et al., 2007; Heilbron et al., 1998; 2010) but more recently, including evolved magmatic arc rocks, and interpreted to result from complex tectonic cycles. The oldest

rocks have arc-like signatures and are represented by low-K tholeiitic magmatism at ca. 2445 Ma, followed by moderately juvenile to evolved coeval TTG-sanukitoid magmatism at ca. 2200-2070 Ma, then by island arc tholeiites from 2200 to 2040 Ma, and collisional granitoid hybrid rocks at ca. 2030–2010 Ma, and a bimodal association of charnockites and E-MORB mafic rocks at around ca. 1.9 Ga, with magmatism and post-collisional hybrid granitoids being emplaced at 2.04 to 1.9 Ga (Araújo et al., 2021; Almeida et al., 2021). More recently, few data indicate the record of Archean inheritance in the orthogranulites of the Juiz de Fora Complex as shown by Hf  $T_{DM}$  model ages of 3.45 to 2.75 Ga and Nd  $T_{DM}$  model ages of 3.20 to 2.75 Ga (Silva et al., 2002; Degler et al., 2018; Araújo et al., 2019; 2021; Kuribara et al., 2019; Almeida et al., 2021).

Younger late Paleoproterozoic ages of around 1.7–1.6 Ga were also reported for mafic granulites with an alkaline tendency, occurring in the northwest sector of the state of Rio de Janeiro (Heilbron et al., 2010). These younger mafic rocks have been interpreted to be related to the Espinhaço rifting event of the São Francisco paleocontinent (Brito Neves, 1995; Martins-Neto, 2000).

The Brasiliano metamorphic overprint conditions recorded in the orthogranulites of the Juiz de Fora Complex have been estimated to be 700–850 °C, at pressures of 4–7 kbar, associated with a clockwise P-T-t path. This estimate was based on mineral assemblages and fluid inclusions (Duarte, 1998, Nogueira et al., 2004; Medeiros-Junior et al., 2017). Similar results were also obtained by Kuribara et al. (2019) for the orthogneisses with estimates of 680–770 °C and 6.0–7.7 kbar obtained using aluminum-in-hornblende as a geobarometer and the pair

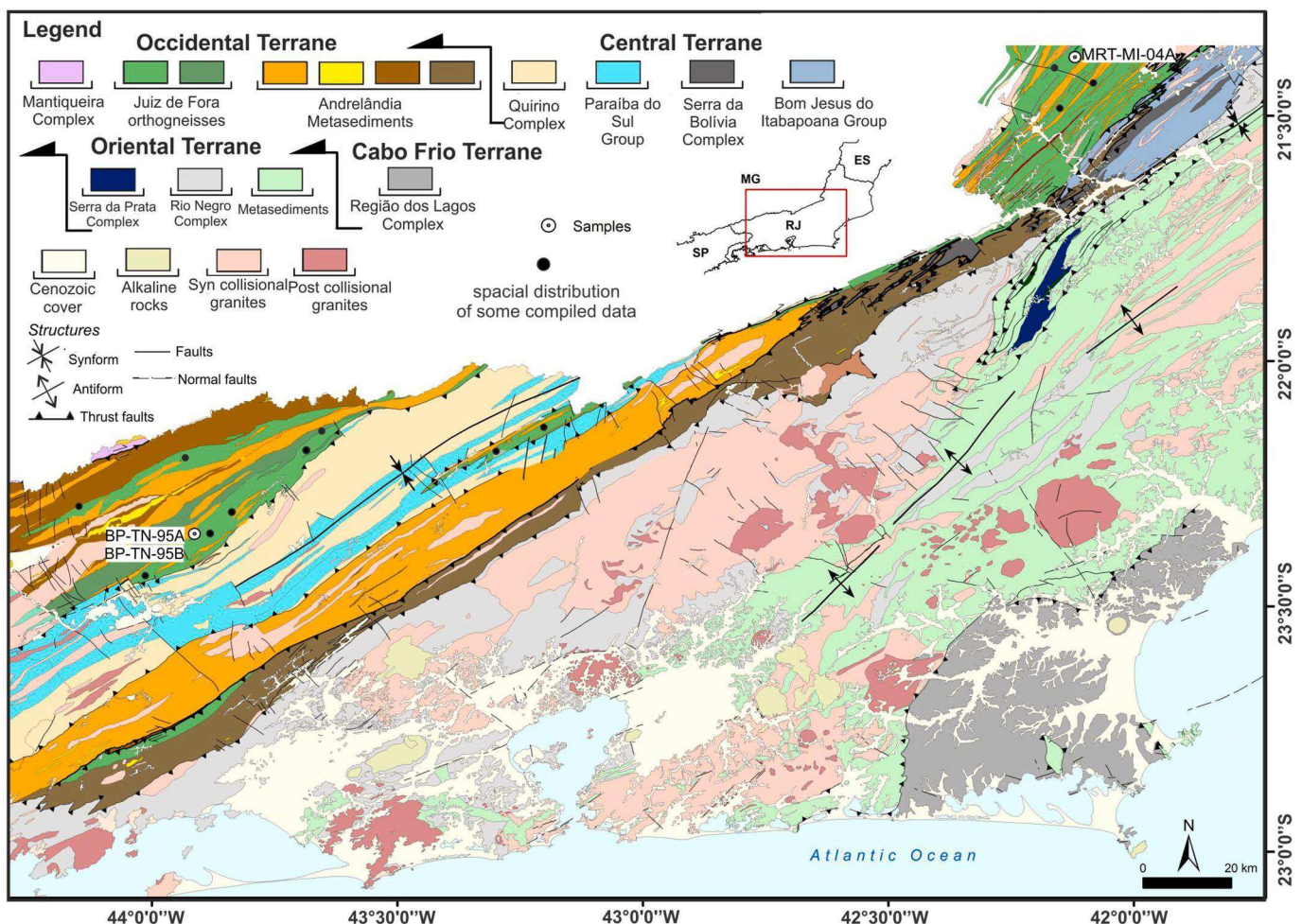


**Fig. 2.** Regional geological map of the studied area with sample location. The black dots correspond to part of the compiled data in order to show the spatial distribution of the Juiz de Fora Complex rocks in the context of this study. References: Duarte et al. (1999; André et al. (2009); Araújo et al. (2019).

hornblende-plagioclase as a geothermometer (Hammarstrom and Zen, 1986; Holland and Blundy, 1994). Although rare, few authors have suggested pre-Brasiliano metamorphism of the rocks of the Juiz de Fora Complex based either on the granoblastic texture of the orthogranulites which was formed prior to the main penetrative foliation in the Brasiliano metamorphic event (Duarte, 1998) or on zircon textures and morphologies (Araujo et al., 2021). The pre-Brasiliano metamorphic conditions were estimated by Duarte et al. (2000), using the Opx + Cpx thermometer producing a  $T_{\max}$  of 895 °C and intermediate pressures.

The collision between the Juiz de Fora and Mantiqueira Complexes took place during the late Rhyacian to Orosirian at 2.05 Ga leading to a metamorphic overprint of the zircon rims in the Mantiqueira Complex (Heilbron et al., 2001; Cutts et al., 2018; Bruno et al., 2020) and reaching granulite facies conditions of 750–800 °C and 6 kbar (Cutts et al., 2018). However, for the Juiz de Fora Complex this collisional period lacks strong evidence, due to the granulite facies overprint of the Brasiliano event on the Juiz de Fora Complex, which only achieved amphibolite facies conditions in the Mantiqueira Complex (Cutts et al., 2018).

To enhance the knowledge of the Rhyacian tectonic environments, and the extent of the Brasiliano metamorphic overprint, we have targeted two samples of garnet-bearing mafic granulites from the Juiz de Fora Complex.

### 3. Methods

#### 3.1. Lithogeochimistry

Three samples were crushed and milled at the Laboratório de Preparação de Amostras (LGPA) of the Universidade do Estado do Rio de Janeiro (UERJ). Geochemical analyses were carried out at the Activation Laboratories (Ontario, Canada). Samples were analyzed for major and trace element determination, including Rare Earth Elements (REE). Details of the analytical techniques used by this laboratory are presented at [www.actlabs.com](http://www.actlabs.com). Previously geochemical data of mafic granulites obtained by Duarte et al. (1997, 2012), Andre' et al. (2009), Heilbron et al. (2013), Araujo et al. (2019), Kuribara et al. (2019) and Almeida et al. (2021), were compiled resulting in a data set of 52 analyses compiled, in order to cover a larger spatial distribution of the Juiz de Fora Complex within the study area (Fig. 2). Treatment of the geochemical data was carried out using the GeoChemical Data ToolKIT (GCDkit) software of Janousek et al. (2006).

#### 3.2. Mineral chemistry

Mineral chemical analysis and elemental maps were performed using a JEOL JXA-8230 EPMA system operated in wavelength-dispersive X-ray spectrometry mode at the Department of Geology, São Paulo State University (UNESP). The matrix correction was performed using the ZAF method. Chemical compositions of garnet, clinopyroxene, orthopyroxene, ilmenite, plagioclase, K-feldspar and amphibole were obtained by EPMA point analyses that were carried out using a focused beam at 15 kV and 20 nA. The total counting times were 10 s peak and 5 s background for major elements and 20 s and 10 s background for minor elements. Natural reference minerals and synthetic oxides were used for calibration; these calibrant materials and detailed EPMA conditions are summarized in Supplementary Table S1, in the electronic supplementary material (ESM). For micro-scale elemental mapping, the EPMA system was operated at 15 kV and 100 nA. The beam size was set to 10 µm and the dwell time per pixel to 180 ms. Data reduction was made using XMapTools 3.2.1 software (Lanari et al., 2014, 2019). Quantitative maps were produced by calibrating X-ray counts using the results of quantitative point analyses placed within the map area (e.g., Lanari et al., 2014).

#### 3.3. P-T modeling

P-T calculations were conducted for two mafic granulite samples, BP-TN-95 A, MRT-MI-04 A (location shown in Fig. 2) using the software package Theriaik/Domino (De Capitani and Petrakakis, 2010) and the database of Holland and Powell (2011; ds62) for the geologically realistic system MnNCFMASHTO ( $\text{MnO}-\text{Na}_2\text{O}-\text{CaO}-\text{FeO}-\text{MgO}-\text{Al}_2\text{O}_3-\text{SiO}_2-\text{H}_2\text{O}-\text{TiO}_2-\text{Fe}_2\text{O}_3$ ) for sample BP-TN-95 and MnNCKFMASHTO ( $\text{MnO}-\text{Na}_2\text{O}-\text{CaO}-\text{K}_2\text{O}-\text{FeO}-\text{MgO}-\text{Al}_2\text{O}_3-\text{SiO}_2-\text{H}_2\text{O}-\text{TiO}_2-\text{Fe}_2\text{O}_3$ ) for sample MRT-MI-04 A. The bulk compositions of both samples were determined by XRF analysis (Table S2). The positions of the X-ray elemental maps were chosen to be representative of the mineral proportions and characteristics of each domain. Utilizing the XRF analysis together with compositional domains determined by mineral modes and compositions allowed us to investigate the bulk composition on different scales from hand specimen (XRF) to fine-grained reaction texture (image analysis; Kelsey et al., 2008).

$\text{K}_2\text{O}$  was not included in the modeling for sample BP-TN-95 A because it unrealistically enhances the stability of biotite such that biotite is present in every assemblage. Biotite is present in small quantities in sample MRT-MI-04 A so this sample was modelled with  $\text{K}_2\text{O}$ .

The ‘metabasite set’ of models from Green et al. (2016), converted to Theriaik-Domino format by Doug Tinkham (see Jørgensen et al., 2019) were applied. These are from White et al. (2014) for orthopyroxene, garnet, biotite, muscovite and chlorite; Green et al. (2016) for clinopyroxene, augite and metabasite melt; Holland and Powell (2011) for olivine and epidote; Holland and Powell (2003) for plagioclase; White et al. (2002) for spinel and magnetite; and White et al. (2000) for ilmenite. Rutile, quartz, and  $\text{H}_2\text{O}$  are also included as pure phases.

Initially,  $T-\text{MH}_2\text{O}$  diagrams were carried out for all the investigated compositions to evaluate how variable  $\text{H}_2\text{O}$  contents impact the P-T conditions of the interpreted peak assemblage. An appropriate value is selected and then a  $T-\text{MFe}_2\text{O}_3$  diagram is conducted to investigate the impact of  $\text{Fe}^{3+}$  content on the peak assemblage field. Following this, P-T pseudosections are calculated. Compositional isopleths for garnet ( $X_{\text{Alm}}$  ( $=\text{Fe}/(\text{Fe} + \text{Ca} + \text{Mg} + \text{Mn})$ )) and  $X_{\text{Grs}}$  ( $=\text{Ca}/(\text{Fe} + \text{Ca} + \text{Mg} + \text{Mn})$ ) and plagioclase ( $X_{\text{Ab}}$  ( $=\text{Na}/(\text{Na} + \text{Ca} + \text{K})$ )) and  $X_{\text{Mg}}$  ( $=\text{Mg}/(\text{Mg} + \text{Fe}^{2+})$ ) of clinopyroxene, orthopyroxene and amphibole, were calculated to further constrain the investigated metamorphic stages. Isopleths for  $X_{\text{Pyr}}$  ( $=\text{Mg}/(\text{Fe} + \text{Ca} + \text{Mg} + \text{Mn})$ ) and  $X_{\text{Sp}}_{\text{ps}}$  ( $=\text{Mn}/(\text{Fe} + \text{Ca} + \text{Mg} + \text{Mn})$ ) were not calculated since they are not abundant in the garnet within these samples, making them less reliable. In addition, mineral abundances (mol) were also calculated for garnet and plagioclase. In the calculated bulk rock compositions,  $\text{Fe}_2\text{O}_3$  was determined based on the amount of  $\text{Fe}^{3+}$  in the recalculated mineral compositions using the method of Droop (1987) for non-hydrous minerals and Tindle and Webb (1994) for amphibole.

#### 3.4. U-Pb geochronology

The preparation for the U-Pb systematics involved crushing and manual panning, followed by density and magnetic separation at the LGPA (Laboratório de Preparação de Amostras), of UERJ. The grains were then imaged by cathodoluminescence (CL) and by backscattered electron (BSE), using Scanning Electron Microscope (SEM) at MULTILAB (facilities of the UERJ) to recognize morphological features, internal structures, and presence of inclusions, cracks or damaged areas.

The U-Pb data for the mafic granulite samples were obtained at the Department of Geology, Federal University of Ouro Preto, Brazil, and analyzed using a ThermoScientific Element II sector field (SF) ICP-MS coupled to a CETAC UV Nd-YAG 213 nm laser system (spot diameter = 30 µm). The data reduction was performed using the Glitter software (van Achterbergh et al., 2001). To test the validity of the applied methods and the accuracy and external reproducibility of the obtained U-Pb age data, reference material BB-9 zircon was used as the primary standard ( $562 \pm 1$  Ma; Santos et al., 2017), and Plesovice zircon ( $337.3 \pm 0.4$  Ma; Sla'ma et al., 2008) and GJ-1 (608 ± 1 Ma; Jackson et al.,

2004) were used as secondary reference material. Plesovice analyses collected over the duration of the study give weighted average results of:  $^{206}\text{Pb}/^{238}\text{U} = 338 \pm 1 \text{ Ma}$ ,  $^{207}\text{Pb}/^{235}\text{U} = 338 \pm 1 \text{ Ma}$  and  $^{207}\text{Pb}/^{206}\text{Pb} = 342 \pm 3 \text{ Ma}$  ( $n = 32$ ).

The age calculations and plots were performed with the Isoplot v4.15 software (Ludwig, 2008). The complete dataset including standard analyses can be found in the Supplementary Material Tables S4 and S5.

The age calculations and plots were performed with the Isoplot v4.15 software (Ludwig, 2008). Among the performed spots, only analysis with less than 10% of analytical errors discordance were considered for ages calculations.

### 3.5. Lu–Hf isotopes

The Lu–Hf isotopic analyses were performed at the Laboratorio Multiusuário of the Rio de Janeiro State University (MULTILAB) using a Neptune Plus MC-ICP-MS. The Lu–Hf dated was collected from 20 previously dated zircons in sample BP-TN-95 A. The laser routine used a spot size of 40  $\mu\text{m}$  in static mode with an ablation time of 60 s and a repetition rate of 6 Hz. The average signal intensity was ca. 10 V for 180 Hf. Data acquisition followed the methods described by Gerdes and Zeh (2006, 2009).

Interference of  $^{176}\text{Lu}$  on  $^{176}\text{Hf}$  was corrected by measuring the in- tensity of the  $^{175}\text{Lu}$  isotope, whereas the interference of  $^{176}\text{Yb}$  on  $^{176}\text{Hf}$  was corrected by simultaneously measuring  $^{173}\text{Yb}$  and  $^{171}\text{Yb}$ , using ra- tios  $^{176}\text{Lu}/^{175}\text{Lu} = 0.02669$  and  $^{173}\text{Yb}/^{171}\text{Yb} = 1.123456$ . The correction for instrumental mass bias utilized an exponential law and a  $^{179}\text{Hf}/^{177}\text{Hf}$  value of 0.7325 (Patchett and Tatsumoto, 1980) for the correction of Hf isotopic ratios. The accuracy and external reproducibility of the Lu–Hf isotopic analyses were verified based on the following primary zircon standard GJ-1 (609 Ma;  $^{176}\text{Hf}/^{177}\text{Hf} = 0.2820000 \pm 0.0000005$ ; Jackson et al., 2004), which yielded  $^{176}\text{Hf}/^{177}\text{Hf}$  of 0.282074  $\pm 0.000710$  ( $n = 46$ ) (all errors are  $\pm 2\sigma$  SD). This pattern was runned two times and the second yielded  $^{176}\text{Hf}/^{177}\text{Hf}$  of 0.282058  $\pm 0.000711$  ( $n = 46$ ) (all errors are  $\pm 2\sigma$  SD). The initial  $^{176}\text{Hf}/^{177}\text{Hf}$  and  $\epsilon\text{Hf}$  were calculated using the  $^{176}\text{Lu}$  decay constant of Soderlund et al. (2004) at the estimated  $^{207}\text{Pb}/^{206}\text{Pb}$  ages of respective zircon domains, and the CHUR parameters:  $^{176}\text{Lu}/^{177}\text{Hf} = 0.0336$ , and  $^{176}\text{Hf}/^{177}\text{Hf} = 0.282785$  (Bou- vier et al., 2008). The complete dataset including standard analyses can be found in the Supplementary Material Table S6.

### 3.6. Sm–Nd–Sr isotopes

For Sm–Nd and Sr analyses, three granulites (BP-TN-95 A, BP-TN-95 B and MRT-MI-04 A) were selected from Juiz de Fora Complex samples used for the geochemistry study. Sm–Nd and Sr isotopic analyses were conducted in the Laboratory of Geochronology and Radiogenic Isotopes (LAGIR) of Universidade do Estado do Rio de Janeiro. Chemical pro- cedures were carried out in clean rooms with the use of sub-boiling distillation of Milli-Q® water and PA Merck® acids (Cardoso et al., 2019). Between 25 and 50 mg of the pulverized samples were subjected to digestion in Savigex® vessels on hot plates, after the addition of proportional amounts of a double  $^{149}\text{Sm}-^{150}\text{Nd}$  tracer solution. A mixture of concentrated HF and  $\text{HNO}_3$  6 N was applied for 3 days, followed by further digestion with HCl 6 N for 2 days. Separation of Sr and REE used cation exchange following conventional techniques.

## 4. Results

Garnet bearing mafic granulites of the Juiz de Fora Complex were targeted to conduct the integrated analyses proposed. The detailed geological map (Fig. 2) shows the location of the analyzed samples, together with available geochemical, geochronological, and isotopic data.

The mafic rocks of the Juiz de Fora Complex crop out as centimetric to metric lenses within the felsic granulites of the unit. Contacts are

sharp, although sometimes mafic rocks show digestion and assimilation textures with the felsic host rocks. The mafic granulites are black to deep green, coarse-grained with granoblastic to mylonitic textures. The main mineralogy consists of clinopyroxene (cpx), orthopyroxene (opx), amphibole, plagioclase and quartz. Garnet occurs only locally as either porphyroblasts or coronas around plagioclase. Zircon, apatite and ilmenite are common accessories. Three garnet bearing mafic samples (samples BP-TN-95 A, BP-TN-95 B and MRT-MI-04 A) from the Upper Thrust System of the Occidental terrane (Juiz de Fora Complex) were selected for geochemistry and Sm–Nd–Sr isotopes. Samples BP-TN-95 A and MRT-MI-04 A were selected for P–T modeling and U–Pb dating of zircon. One of these samples (BP-TN-95 A) was also used for Lu–Hf isotopic analysis.

### 4.1. Sample description and mineral chemistry

#### 4.1.1. Sample BP-TN-95 A

Sample BP-TN-95 A is a well-foliated mafic granulite layer over 1 m thick and 10–20 m long. This sample contains garnet, amphibole, plagioclase, clinopyroxene, orthopyroxene, ilmenite and quartz. Quartz occurs exclusively along grain boundaries (especially along amphibole grain boundaries but also some clinopyroxene grains), there are also a few small inclusions in garnet (Fig. 3).

Garnet grains are usually poikiloblastic with a size up to 0.5 mm, containing inclusions of plagioclase, quartz, orthopyroxene, ilmenite and clinopyroxene (Fig. 3). Garnet grains have a pinkish color and irregularly shaped edges. Plagioclase is always associated with garnet, in some places surrounding the garnet grains. In another sector of the thin section, plagioclase appears to embay the garnet crystals with out- growths of garnet (or perhaps the preserved rim) occurring only where the garnet borders amphibole grains. Plagioclase grains exhibit polyg- onal shape and albite-twinning and usually occur as grain aggregates (aggregates are up to 1 mm in size with individual grains around 300–500  $\mu\text{m}$ ). Amphibole is prismatic, brown - green pleochroic and occurs as coarse grains in the matrix or as bands or grain clumps (in- dividual grains are 1–2 mm in size but clumps are up to 1–2 cm). Amphibole is often associated with ilmenite and plagioclase grains. Clinopyroxene is pale green in color and usually appears in contact with amphibole. Clinopyroxene grains are round, equigranular and occur in small clumps (grains are around 1 mm and grain clumps are 5–10 mm). Orthopyroxene is fine grained (around 500  $\mu\text{m}$ ) and usually surrounded by amphibole.

Garnet is compositionally zoned with higher  $X_{\text{Py}}$  in the cores (0.16) than in the rims (0.11).  $X_{\text{Alm}}$  is lower in the cores (0.62) than in the rims (0.66).  $X_{\text{Grs}}$  is uniformly low throughout the garnet grains (0.19–0.21) but is suddenly enriched right on the rims (up to 0.27). Some grains appear to have garnet cores that are enriched in  $X_{\text{Grs}}$ , however, this may be a sectioning artifact.  $X_{\text{Sp}}$  is lower in the core (0.02) than the rim (0.04).

The composition of the plagioclase is andesine with  $X_{\text{Ab}}$  of 0.52 to 0.42. Lower values occur on the rims of grains. The clinopyroxene is generally diopside (although some core analyses were classified as augite) and has  $X_{\text{Mg}}$  of 0.52–0.6 and has the highest values in grain rims. Amphibole is classified as ferroan pargasitic hornblende with  $X_{\text{Mg}}$  of 0.39–0.44, with the highest values found in grain rims, particularly adjacent to garnet or orthopyroxene. Amphibole has high  $\text{TiO}_2$  contents (1.5–2.51 wt% but usually 2.1 to 2.5 wt%) with the highest values occurring in large grain cores or adjacent to garnet and orthopyroxene grains. Orthopyroxene has  $X_{\text{Mg}}$  of 0.4–0.43 and no apparent compositional zoning.

#### 4.1.1.1. Sample MRT-MI-04 A.

Sample MRT-MI-04 A is a mafic granu- lite occurring within a felsic granulite. This sample contains the minerals garnet, clinopyroxene, orthopyroxene, amphibole, plagioclase, quartz, ilmenite, apatite and K-feldspar. Garnet occurs in a symplectitic texture

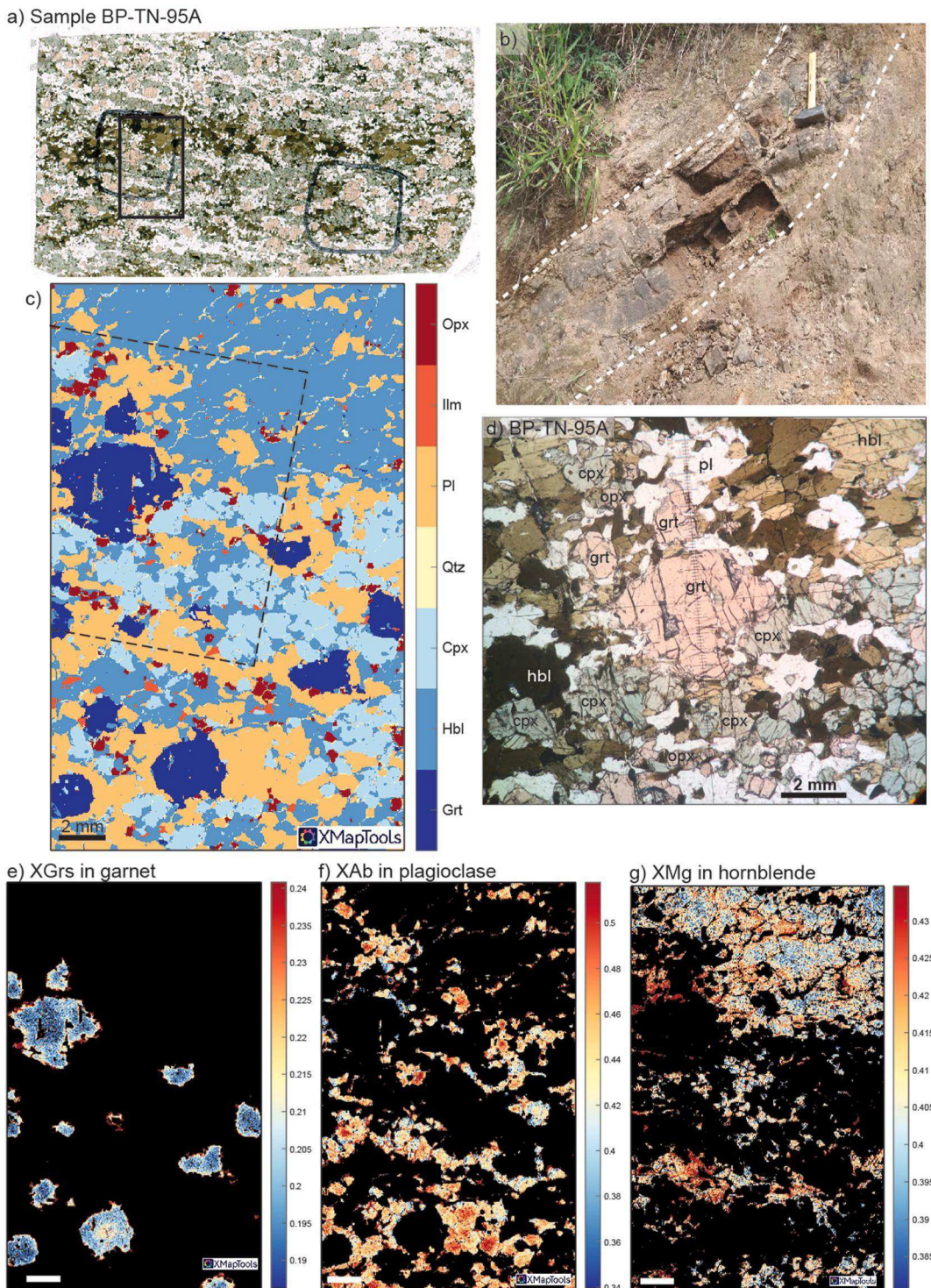


**Fig. 3.** a) Thin section scan of sample BP-TN-95 A with the location of the mapped area shown in Fig. 3c b) Outcrop area where sample BP-TN-95 A was obtained. Mafic boudins are outlined with dashed white lines. c) Mask image showing mineral classification obtained using XMapTools of the mapped area of this sample. The photomicrograph area of the sample is indicated by the dashed black box. d) Photomicrograph of sample BP-TN-95 A. e) X<sub>Grs</sub> content of garnet obtained from the mapped area obtained using XMapTools. f) X<sub>Ab</sub> in plagioclase from the mapped area, obtained using XMapTools. g) X<sub>Mg</sub> in hornblende

with fine inclusions of quartz, clinopyroxene, and amphibole. Garnet also contains rare coarse (100–200 µm) inclusions of orthopyroxene and ilmenite (Fig. 4d). Garnet is surrounded by plagioclase, clinopyroxene, and orthopyroxene with a thin film of K-feldspar commonly occurring on garnet grain boundaries (Fig. 4). Amphibole forms small matrix grains (200–500 µm) and is also found at the edges of clinopyroxene and orthopyroxene, exhibiting a nematoblastic habit. K-feldspar occurs at

the edges of plagioclase and garnet as thin films or as chains of inclusions in orthopyroxene and amphibole. Plagioclase is the most common matrix mineral (mode is 46%) and forms felsic bands (individual grains up to 500 µm) that alternate with the mafic minerals, defining the strong foliation of the sample. Quartz is rare, occurring as isolated grains associated with orthopyroxene or clinopyroxene. Quartz is also present as a symplectitic inclusion within garnet (Fig. 4).

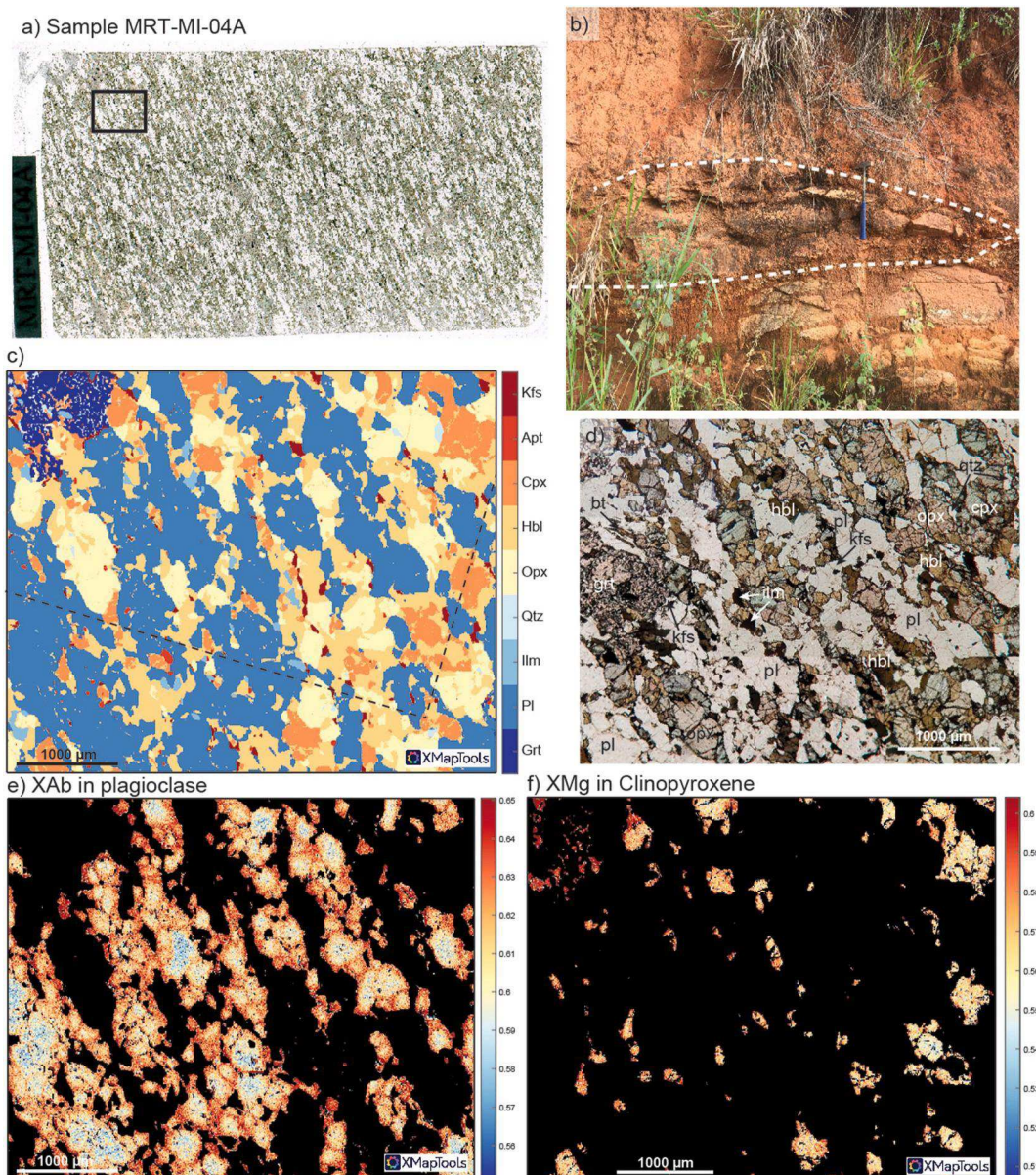


**Fig. 4.** a) Thin section scan of sample MRT-MI-04 A with the location of the mapped area shown in Fig. 5c b) Outcrop area where sample MRT-MI-04 A was obtained. Mafic boudins are outlined with dashed white lines. c) Mask image showing mineral classification obtained by XMapTools of the mapped area of this sample. d) Photomicrograph of sample MRT-MI-04 A. e)  $X_{\text{Gr}}$  content of garnet obtained from the mapped area using XMapTools. f)  $X_{\text{Ab}}$  in plagioclase from the mapped area.

Both ortho and clinopyroxene form large matrix grains (500  $\mu\text{m}$ –1 mm and ca. 500  $\mu\text{m}$  respectively) but these are variably replaced by amphibole (sometimes entirely and in other instances just on grain fractures and rims). Amphibole also occurs commonly as inclusion in plagioclase.

Plagioclase grains are zoned and generally albite rich with  $X_{\text{Ab}}$  of 0.55–0.69, the most albite-rich values occur on grain rims. Ilmenite crystals occur as elongated grains in the matrix and as inclusions within garnet and amphibole, which are generally aligned parallel to the matrix foliation. Garnet grains are slightly zoned with  $X_{\text{Alm}}$  of 0.6–0.67 and the highest values occur on the rims of the grains.  $X_{\text{Sp}}$  is 0.025–0.04 with the highest values appearing on the grain rim.  $X_{\text{Grs}}$  varies from 0.19 to 0.23 and it is generally higher on the grain rim than the core but varies around some inclusions (high values near the inclusion of amph and cpx near the grain core).  $X_{\text{Py}}$  is high in the grain core and low on the rims of grains and varies from 0.1 to 0.16.

Clinopyroxene has  $X_{\text{Mg}}$  of 0.55–0.61 with higher values in grains

adjacent to garnet and the rims of matrix grains.

Amphibole is classified as ferroan pargasitic hornblende with  $X_{\text{Mg}}$  of 0.46–0.49. Amphibole has high  $\text{TiO}_2$  contents (1.9–2.4 wt% but usually 2.1 to 2.3 wt%). Orthopyroxene has  $X_{\text{Mg}}$  of 0.41–0.44 and no apparent compositional zoning.

#### 4.2. Geochemistry

The three new analyzed samples (BP-TN-95 A, BP-TN-95 B, MRT-MI-04 A, see [Supplementary Table S3](#)) show similar  $\text{SiO}_2$  (45.81–50.92 wt%),  $\text{MgO}$  (4.87–5.48 wt %), and  $\text{TiO}_2$  (1.5–1.6%) contents, defining a tholeiitic series ([Fig. 6a](#) and b). New data is integrated with available geochemical data for mafic rocks of the Juiz de Fora complex, compiled from [Duarte et al. \(1997, 2012\)](#), [Andre et al. \(2009\)](#), [Heilbron et al. \(2013\)](#), [Araujo et al. \(2019\)](#), [Kuribara et al. \(2019\)](#) and [Almeida et al. \(2021\)](#), resulting in a data set of 52 analyses compiled.

The metabasic rocks belong to the tholeiitic series in the AFM

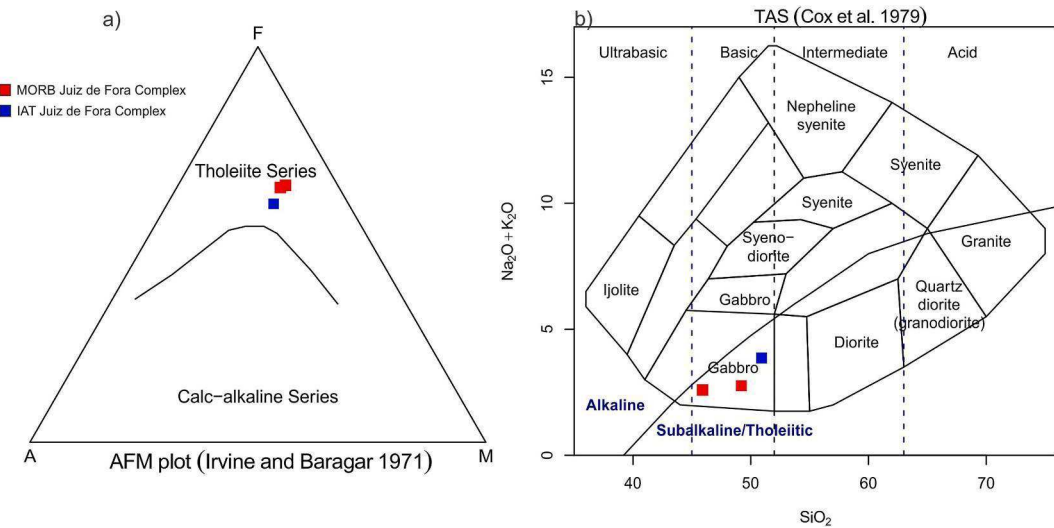


**Fig. 5.** a) classification of sub-alkaline samples into tholeiitic series through AFM diagram (Irvine and Baragar, 1971). b) Protolith classification and magmatic series classification (Cox et al., 1979).

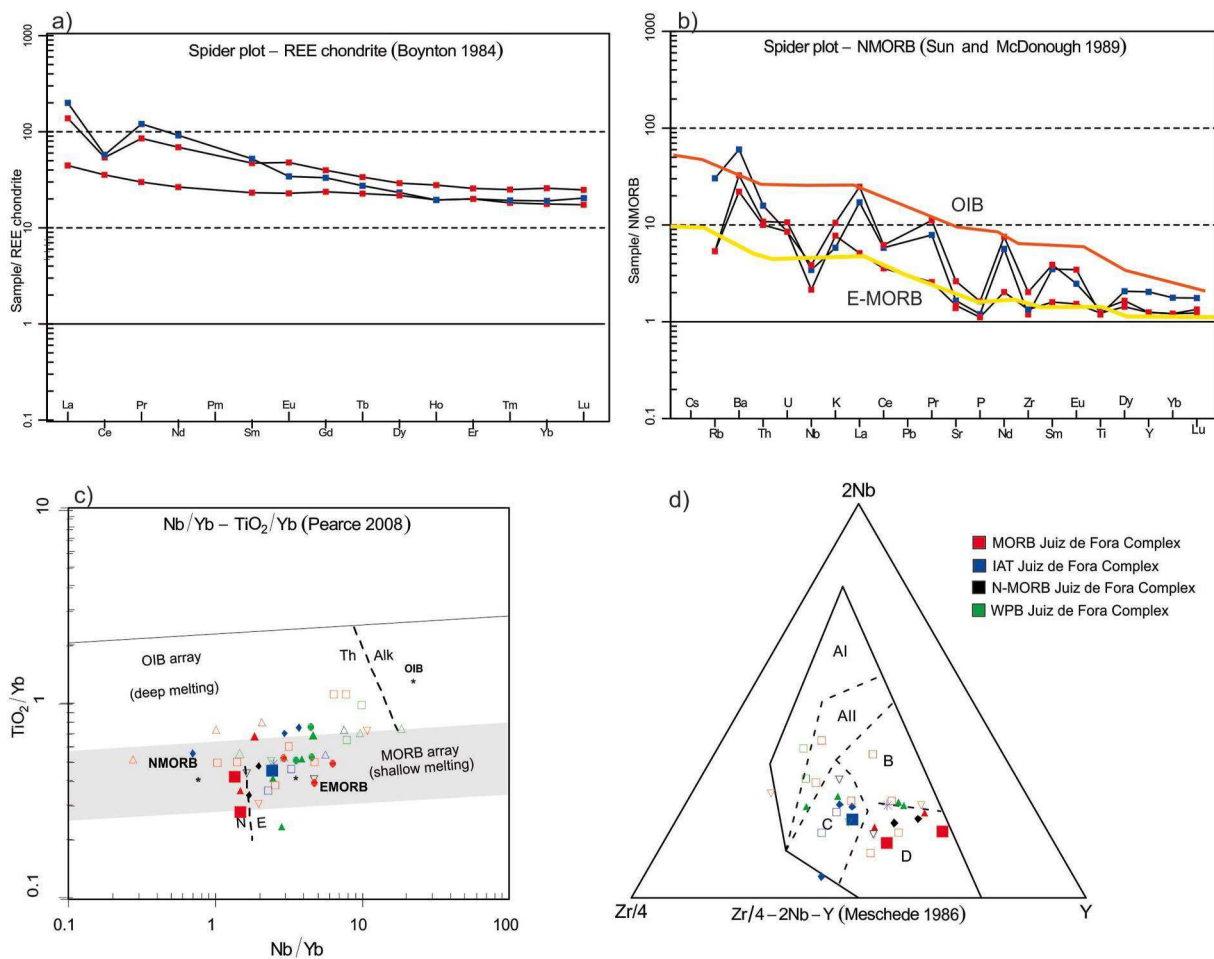


**Fig. 6.** a) Average chondrite-normalized REE patterns normalized after the values from Boynton (1984). b) N-MORB-normalized multielement plots. Yellow and orange lines represent the average composition of E-MORB and OIB, respectively (Sun and McDonough, 1989). c)  $\text{Nb}/\text{Yb}$  vs  $\text{TiO}_2/\text{Yb}$  (Pearce, 2008) with a comparison of new data and previously published data for mafic rocks in the region of the Juiz de Fora Complex. This compilation includes Duarte et al. (1997, 2012), Andre' et al. (2009), Heilbron et al. (2013), Araujo et al. (2019), Kuribara et al. (2019) and Almeida et al. (2021). d) 2Nb-Zr/4-Y diagram (after Meschede, 1986), also including the previously published data. AI: within-plate alkali basalt, All: within-plate tholeiite and within-plate alkali basalt, B: P-type MORB, C: within-plate tholeiite and volcanic arc basalt, D: volcanic arc basalt and N-type MORB.

diagram (Fig. 5a). All samples plot in the subalkaline/tholeiitic field in the TAS diagram (Cox et al., 1979), with SiO<sub>2</sub> and Na<sub>2</sub>O + K<sub>2</sub>O spanning between 45.81 and 50.92 wt% and 2.6–3.86 wt%, respectively (Fig. 5b). Based on the trace elements, the samples were grouped at two groups: E-MORB and IAT (island arc tholeiite).

E-MORB metabasic rocks (BP-TN-95 A and BP-TN-95 B) are characterized by SiO<sub>2</sub> content varying from 45.81 wt% to 49.2 wt% and with REE-chondrite normalized (Boynton et al. 1984) profiles showing relative enrichment of LREE over HREE (2.33 LaN/YbN 5.34) (Fig. 6a). They exhibit intermediate TiO<sub>2</sub> content (~1.5 wt%), Al<sub>2</sub>O<sub>3</sub> (~14.5 wt%) and Fe<sub>2</sub>O<sub>3</sub> (15.4–16.49 wt%).

In the N-MORB normalized multielement spidergram of Sun and McDonough (1989) (Fig. 6b), samples BP-TN-95 A and BP-TN-95 B show

enrichment in incompatible elements such as Ba, K, Pb, Sr and Nd. In the Nb-Zr-Y triangular diagram (after Meschede, 1986) for basaltic rocks, the samples from this group plot in the N-MORB field (Fig. 6c) and also in the N-MORB field on in the tectonic diagram of Pearce (2008) (Fig. 6d).

Sample MRT-MI-04 A, belonged to the IAT group, has SiO<sub>2</sub> content of 50.92 wt%, intermediate TiO<sub>2</sub> content (1.6 wt%), MgO (5.48 wt%) and moderate Fe<sub>2</sub>O<sub>3</sub>(15.76 wt%), CaO (8.82 wt%) and Al<sub>2</sub>O<sub>3</sub>/TiO<sub>2</sub> (8.29) ratios. The REE-chondrite normalized diagram shows an LREE-enrichment relative to HREE (LaN/YbN = 11.28) and shows a slightly negative Ce anomaly (Fig. 6a). Enrichment in incompatible elements such as Rb, Ba, La, Pb and Nd is highlighted in the N-MORB-normalized spidergram (Fig. 6b). This sample plots within the volcanic arc basalt

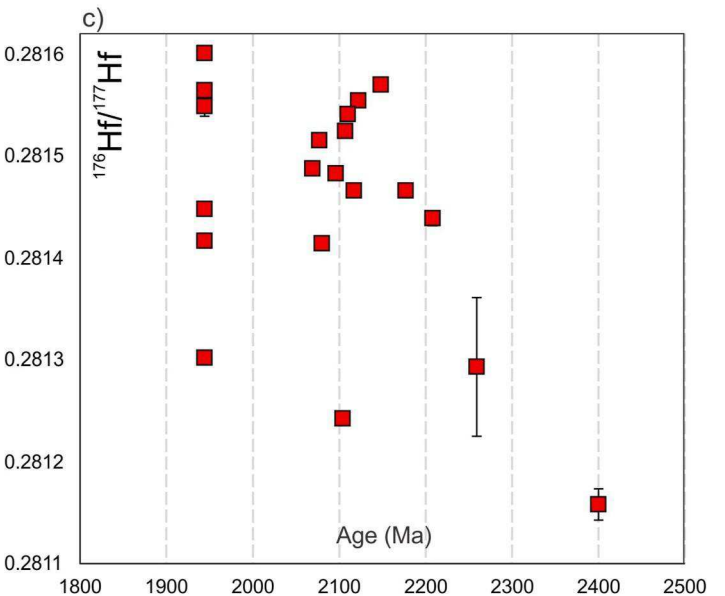
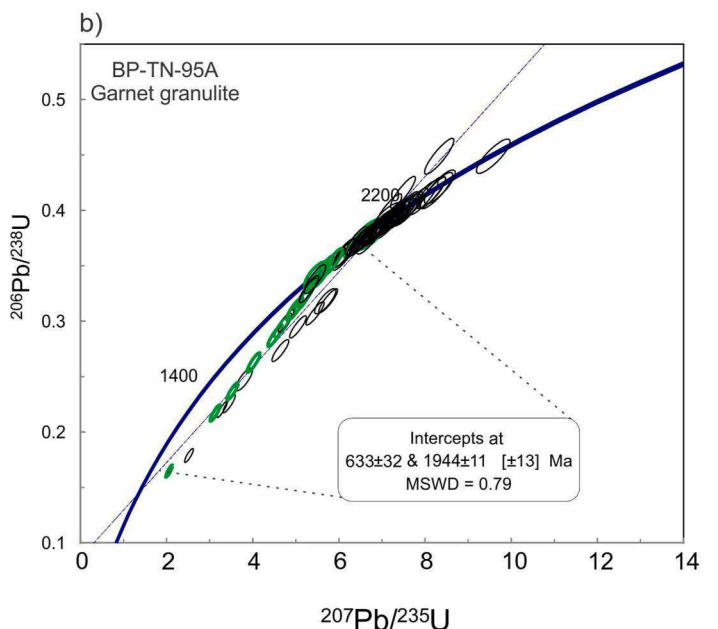
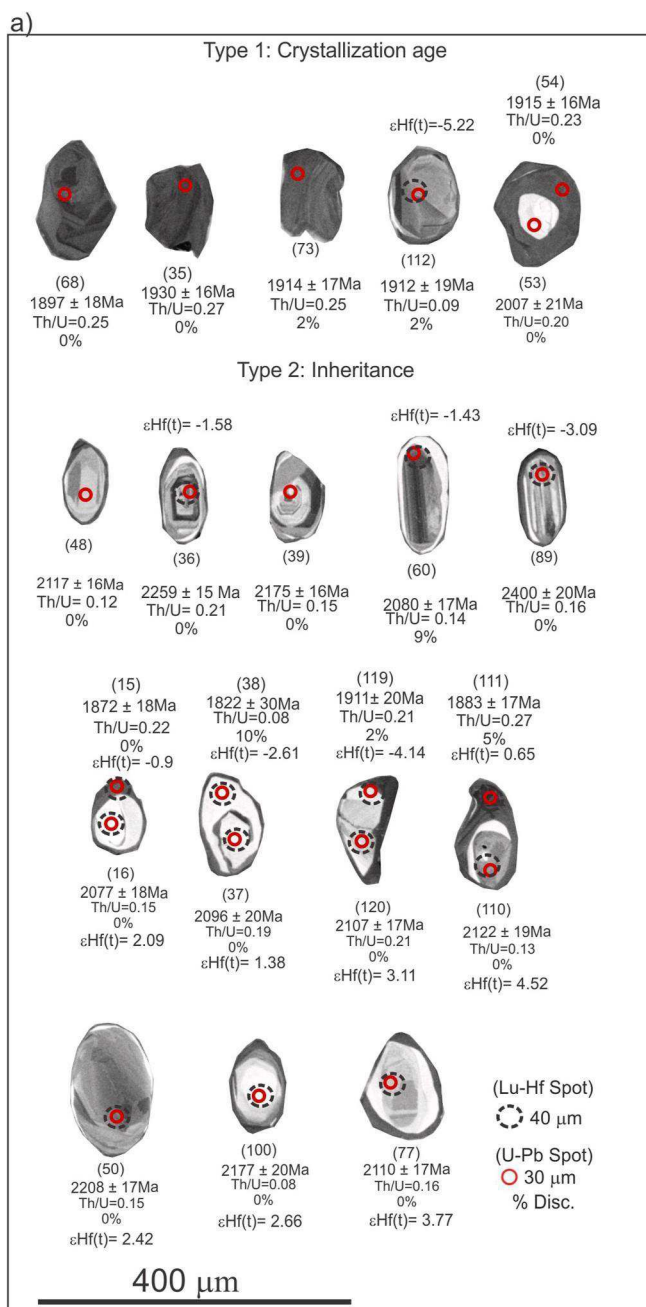


Fig. 7. a) Cathodoluminescence (CL) images of analyzed zircon crystals of the BP-TN-95 A sample with identification of the crystallization age and inheritance. The dashed black circles represent the Lu-Hf spot while the empty red circles represent the U-Pb spots. b) Concordia diagram for the BP-TN-95 A with the upper intercept given the crystallization age of 1944 ± 11 Ma with Brasilianno lead-loss resulting in a lower intercept of ca. 633 Ma. c) <sup>176</sup>Hf/<sup>177</sup>Hf ratios showing the overspread values according to the age.

field in the Nb–Zr–Y triangular diagram (after Meschede, 1986) (Fig. 6c) and in the E-MORB field in the tectonic diagram of Pearce (2008) (Fig. 6d).

The involvement of continental input in these samples can be recognized by using N-MORB normalized by Sun and McDonough (1989) spidergrams (Fig. 6b), exhibiting slightly negative anomalies of P and Ti for compressional settings. This pattern can be also recognized in the previously cited works within the Juiz de Fora Complex (Fig. 6c and d). The tectonic discrimination diagrams, combined with mafic granulite data from previous studies, corroborate with the signature presented by the trace elements, as the Juiz de Fora mafic granulites plotted mostly in the island-arc affinity fields and also within the extensional field (Fig. 6). It is noticed that JFC mafic granulites can also present within plate signatures, however in this study just the E-MORB and IAT signatures were recognized.

#### 4.3. U–Pb geochronology and Lu–Hf isotope results

In order to determine the age and isotopic signatures of the two different geochemical groups, samples BP-TN-95 A, with a MORB signature, and MRT-MI-04 A, with an IAT signature, were selected for geochronological investigation. Both samples have some degree of crustal contamination revealed by geochemical and isotopic studies (tables S3, S6 and S7).

##### Sample BP-TN-95a.

Eighty-four zircon analyses were obtained from sample BP-TN-95 A mafic rock hosted in the Juiz de Fora Complex. The zircon crystals have short prismatic shapes with rounded, equidimensional, and sub-rounded borders (Fig. 7a). In the CL images, the majority of the crystals have both CL bright and dark rims, which characterize completely homogeneous domains (Fig. 7a). Resorption texture is present, as well as concentric and planar zoning to a lesser extent (Corfu et al., 2003). Sample BP-TN-95 A (Table S4) shows data spreading over the concordia, from ca. 2.4 to 1.97 Ga, besides a trend of Pb loss defined by a discordia line, revealing a complexity of this sample (Fig. 7). Given the texture complexity and a wide age range found for these zircon grains, the Lu–Hf isotope data helped the data evaluation. Twenty analyses (see Supplementary Table S6) of Lu–Hf isotopes for zircons from sample BP-TN-95 A show a large variation in  $^{176}\text{Hf}/^{177}\text{Hf}$ (i) ratios of 0.28119–0.28160.

The zircon textures together with the obtained Hf analyses, the younger Paleoproterozoic zircon grains, encompassing grains with igneous oscillatory zoning and grains with total or partially homogeneous dark domains, together with a trend of discordant grains, with complex tips and reabsorption textures yielded a discordia line with a MSWD of 0.79. The upper intercept of  $1944 \pm 11$  Ma (Fig. 7c, zircons i. e., 35, 68, 76, 79, and 112) is considered the crystallization age of the mafic rock, supported by the  $^{176}\text{Hf}/^{176}\text{Hf}$  initial ratios varying from 0.2813 to 0.2816, indicating addition of a fresh magmatic batch, with  $\epsilon\text{Hf(t)}$  between +2.05 and –8.56. On the other hand, the lower intercept of  $653 \pm 32$  Ma indicates a Neoproterozoic high-grade metamorphic overprint.

All the older Paleoproterozoic ages were interpreted as inheritance from the country rocks Th/U ratios between 0.05 and 0.35 (see Supplementary Table S4). These oldest spots yielded  $^{207}\text{Pb}/^{206}\text{Pb}$  ages between  $2400 \pm 20$  Ma (disc 0%) and  $2077 \pm 20$  Ma (disc 0%), with a large variation in the  $\epsilon\text{Hf(t)}$  values and in the  $^{176}\text{Hf}/^{176}\text{Hf}$  initial ratios. Most of the older inherited grains show textural evidence of partial Pb loss during the metamorphic overprint.

##### 4.3.1. Sample MRT-MI-04a, Juiz de Fora complex

Fifty-two zircon spots from the mafic granulite with arc-like affinities (MRT-MI-04 A) of the Juiz de Fora Complex were analyzed. The zircon crystals have short prismatic shapes with elongated, equidimensional, and sub-rounded borders (Fig. 14a, i.e., 16, 87, 117). CL images reveal that most cores present a fine magmatic oscillatory zoning. The MRT-MI-04 A (see Supplementary Table S5) that most of the crystals are

discordant due to Pb loss. The upper intercept age (Fig. 8b) is interpreted as the timing of magmatic crystallization at  $2201 \pm 6$  Ma. The lower intercept marked the Neoproterozoic metamorphic overprint at  $592 \pm 6.1$  Ma (Fig. 8c), controlled by analysis of the grey rims (i.e., 60, 75, 76, 107).

In sample MRT-MI-04 A (see Supplementary Table S5) most of the crystals show a predominance of Paleoproterozoic  $^{207}\text{Pb}/^{206}\text{Pb}$  ages (Fig. 8); these oldest spots yield Th/U ratios between 0.05 and 0.35. Ages around 2.2 Ga, to a lesser extent, possess crystals with high CL- bright combined with concentric and planar zoning.

#### 4.4. Sm-Nd-Sr isotopes

The location of the samples is shown in Figs. 1b and 2, and the analytical results are presented in Table 1 (see Table S7 of Supplementary Material for more details). The Juiz de Fora Complex yields late Paleoproterozoic TDM model ages, between 2.39 and 2.32 Ga and  $\epsilon\text{Nd}(0)$  shows values between –24.8 and –6.82 (Fig. 9). Sample BP-TN-95 A and 95 B have  $\epsilon\text{Nd(t)}$  values between +0.5 and –1.5 for the calculated age  $^{207}\text{Pb}/^{206}\text{Pb}$  of  $1944 \pm 11$  Ma. Sample MRT-MI-04 A shows  $\epsilon\text{Nd(t)}$  value of –0.42 for the calculated  $^{207}\text{Pb}/^{206}\text{Pb}$  of  $2201 \pm 6$  Ma. The initial  $^{87}\text{Sr}/^{86}\text{Sr}$  ratios for the three samples of the Juiz de Fora Complex range between 0.7037 and 0.7026.

#### 4.5. P-T modeling results

To provide a better constraint for the metamorphic evolutionary path of the Juiz de Fora Complex, the BP-TN-95 A and MRT-MI-04 A samples were chosen and correspond to garnet-granulite rocks with two different garnet textures: coarse poikiloblastic and a symplectite, respectively. The rock foliation and such complex garnet textures reflect the presence of strong metamorphic events in these samples, which will be further discussed in the following topics.

##### 4.5.1. Sample BP-TN-95 A

In this sample, garnet is texturally early, forming coarse (up to 5 mm diameter) grains and the matrix foliation is defined by bands of clinopyroxene, plagioclase and orthopyroxene. Amphibole occurs between clinopyroxene grains and also occurs as coarse grains in discrete layers (one of which occurs in the middle of the thin section). Quartz occurs only locally, generally between coarse amphibole grains. Due to the pervasive foliation and generally large grain size of this sample (2–5 mm grains), we interpret most minerals to have grown in response to metamorphism and suggest a peak metamorphic assemblage consisting of garnet + plagioclase + clinopyroxene + orthopyroxene + ilmenite + melt ± amphibole. This sample has small felsic layers and late quartz, which crystallizes with large amphibole grains. We interpret this to be a result of the presence of melt, indicating that melt was likely part of the peak P-T assemblage.

The P-MFe<sub>2</sub>O<sub>3</sub> and T-MH<sub>2</sub>O diagrams were used to determine appropriate values for Fe<sub>3+</sub> and H<sub>2</sub>O for this sample. The peak assemblage does not appear to be strongly dependent of Fe<sub>3+</sub> with magnetite occurring in the sample only for much higher values. A moderate value of 5% Fe<sub>3+</sub> was selected. For H<sub>2</sub>O, a significant increase in H<sub>2</sub>O content results in the loss of orthopyroxene stability, while a decrease results in more stable quartz. To balance between these two factors, H<sub>2</sub>O at 20% was used for the P-T pseudosection (Fig. 10).

The P-T pseudosection has the interpreted peak assemblage occurring at 6–8 kbar and 800–900 °C. To further constrain the P-T evolution of the sample and the peak conditions, isopleths of XGrs in garnet, XAb in plagioclase, garnet mode, plagioclase mode and XMg of clinopyroxene, orthopyroxene and amphibole were also calculated. The prograde evolution is defined by an increase in garnet mode (see the dashed part of P-T path in Fig. 10d). Peak conditions are defined by XGrs, XAb and XMg of orthopyroxene and clinopyroxene. The XMg of clinopyroxene, the XGrs composition of garnet and the lowest values of XAb in plagioclase all

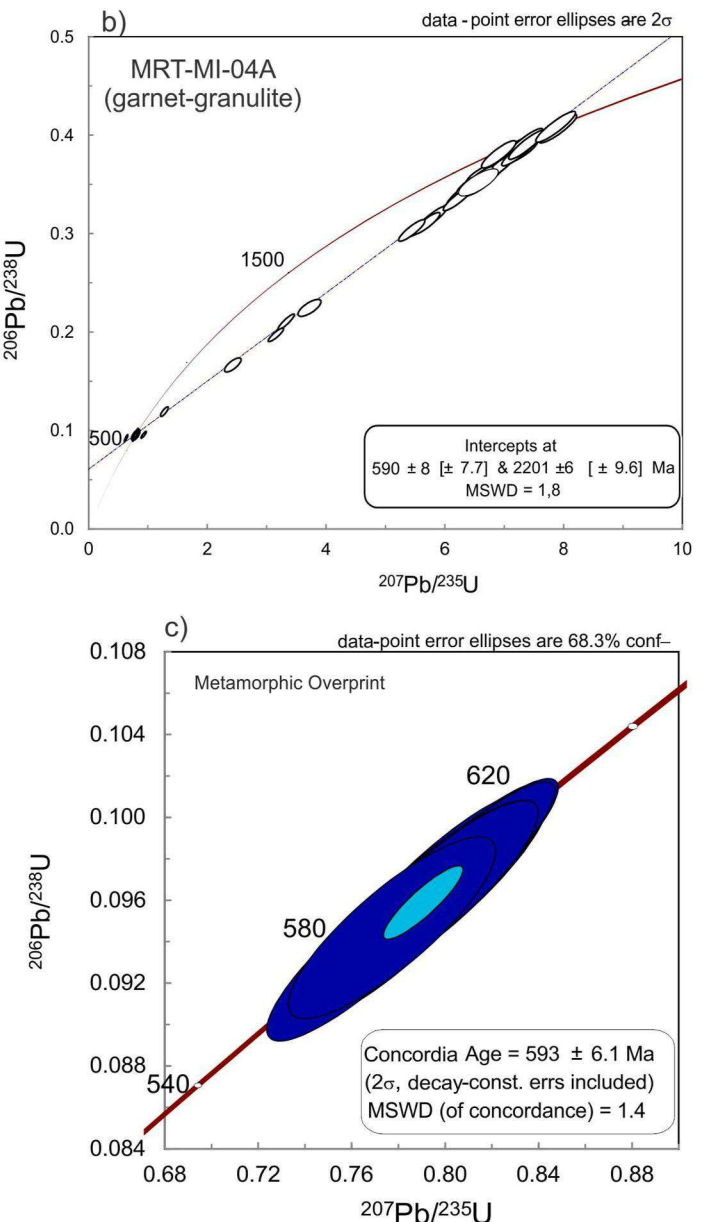
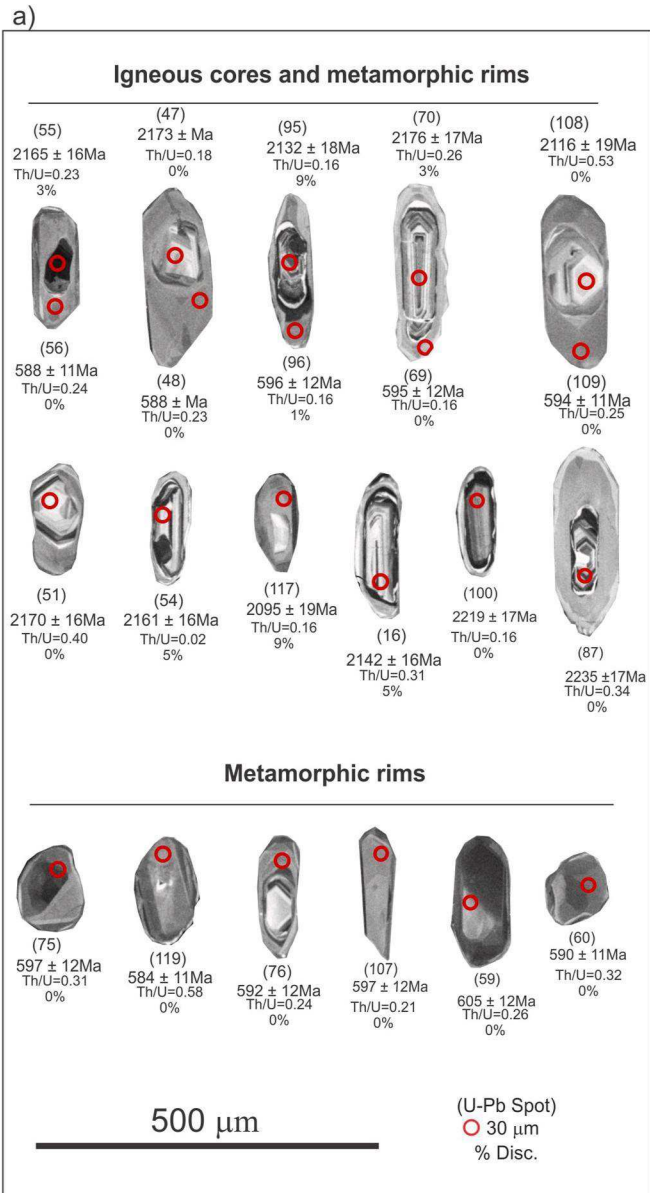


**Fig. 8.** a) Cathodoluminescence (CL) images of analyzed zircon crystals of the MRT-MI-04 A sample with identification of the igneous cores and metamorphic rims. b) Concordia diagram for the MRT-MI-04 A with the upper intercept given the crystallization age of 2201 ± 6 Ma. c) Calculated metamorphic overprint at 593 ± 6 Ma.

**Table 1**

Synthesis of Sm–Nd and Sr isotopic data of the metabasic rocks.

SAMPLE	Geochemical	Group	Sm	Nd	143Nd/	147Sm/	87Sr/	$\epsilon$	f	143Nd/	143Nd/	$\epsilon$	T (DM)	87Sr/	
	Group		ppm	ppm	144Nd	144Nd	86Sr(m)	0 Ma		(Sm/ Nd)	144Nd	144Nd	(t)	Ga	86Sr(i)
BP-TN-95 B	E-MORB	JFC	4,06	14,65	0,16,741	0,16,741	0.71775	-6,82	-0,1489	0,51,015	0,51,015	0,5 <sup>1</sup>	2,32	0,70,307	
BP-TN-95 A	E-MORB	JFC	8,90	40,60	0,13,190	0,13,190	0.71105	-17,50	-0,3294	0,51,004	0,51,005	-1,5 <sup>1</sup>	2,34	0,70,373	
MRT-MI-04A	IAT	JFC	9,80	53,70	0,10,980	0,10,980	0.71091	-24,83	-0,4418	0,50,977	0,50,977	-0,4 <sup>2</sup>	2,39	0,70,239	

References  $\epsilon(t)$ <sup>1</sup> calculated for 1.94 Ga (crystallization age for the BP-TN-95 A) and  $\epsilon(t)$ <sup>2</sup> calculated for 2.2 Ga (crystallization age for the MRT-MI-04 A).

overlap in a restricted part of P-T space at 8–9 kbar and 825–900 °C (see the dashed area on Fig. 10d). This region of overlap occurs outside of the orthopyroxene stability field and within the quartz stability field. Given

that quartz is present in the sample as an inclusion in garnet, it is plausible that it was part of the peak assemblage. Orthopyroxene occurs only as small grains in the matrix, suggesting that it grew during the

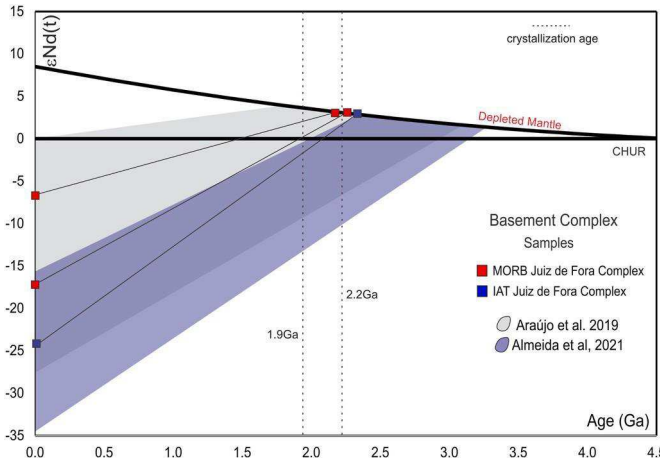


**Fig. 9.** Nd evolution diagram ( $\epsilon_{\text{Nd}}(t)$  x Time) for the basic rocks of the JJC. Data compilation with previous studies from Araújo et al. (2019) and Almeida et al. (2021). Depleted Mantle data extracted from DePaolo (1988).

retrograde evolution of the sample rather than belonging to the peak assemblage.

The retrograde path is well defined by the absence of quartz in the matrix, the  $X_{\text{Mg}}$  of orthopyroxene, then the presence and  $X_{\text{Mg}}$  of amphibole, as well as the decrease in garnet mode and increase in plagioclase mode. The retrograde path characterizes a nearly isothermal decrease in pressure.

**4.5.1.1. Sample MRT-MI-04 A.** This sample has a well-defined fabric made up of elongated grains of plagioclase, orthopyroxene and clino- pyroxene. Garnet is symplectitic and grows over the foliation-defining minerals. K-feldspar occurs as small blobs on the edge of foliation- defining minerals, and also surrounds garnet grains. Quartz occurs within the garnet symplectite and as small blobs between matrix grains, similar to K-feldspar. Biotite and amphibole are texturally late, amphi- bole is generally oriented parallel to the foliation and can surround orthopyroxene and clinopyroxene. Due to the strong foliation of this sample, we interpret that this sample experiences significant meta- morphic recrystallization with potentially only the cores of plagioclase grains retaining their igneous compositions.

We interpret the peak mineral assemblage of this sample to be garnet + orthopyroxene + clinopyroxene + plagioclase + melt + ilmenite  $\pm$  amphibole. The matrix quartz, K-feldspar and biotite are interpreted to be crystallized melt.

This sample was first modelled using P-MFe<sub>2</sub>O<sub>3</sub> and T-MH<sub>2</sub>O dia- grams in order to select appropriate values for Fe<sup>3+</sup> and H<sub>2</sub>O. Due to the absence of quartz and magnetite, and the presence of ilmenite, the Fe<sup>3+</sup> was set as 2% (Fig. 11a). The T-MH<sub>2</sub>O diagram indicates a variation in the hydrous minerals (i.e., amphibole and biotite). If a large amount of H<sub>2</sub>O is present, then orthopyroxene stability decreases. For this reason, a medium value was chosen (Fig. 11b).

The interpreted peak assemblage field (garnet + orthopyroxene + clinopyroxene + plagioclase + melt + ilmenite  $\pm$  amphibole) does not occur on the P-T diagram. However, it may occur at higher T, outside of the temperature window. However, the presence of biotite on the P-T diagram is over- stabilized by the inclusion of K<sub>2</sub>O in the system. This means that the assemblage field of garnet + orthopyroxene + clino- pyroxene + plagioclase + melt + ilmenite + biotite  $\pm$  amphibole, which occurs at 800–900 °C and 7–11 kbar (Fig. 11c) likely corresponds to the peak P-T conditions of this sample. Garnet XGrs and plagioclase XAb isopleths were used to constrain the peak conditions to 800–850 °C and 8–9 kbar (Fig. 11d).

Using the mode of garnet, we can interpret the prograde evolution of this sample as passing through the orthopyroxene + clinopyroxene +

melt fields and then entering the garnet-bearing field (Fig. 11d).

## 5. Discussion

Combining the new and available isotopic/geochronological data with the geochemical and P-T-t constraints (Duarte et al., 1997, 2000; Heilbron et al., 2010; Kuribara et al., 2019; Araújo et al., 2019; 2021; Almeida et al., 2021) lead to a better understanding of the polycyclic evolution of the JJC, considering the perspective of the studied high-grade metabasic rocks. In addition, the new data corroborates with two collisional stages in the studied area: the oldest one occurred during the Rhyacian event at ca. 2.2 Ga (MRT-MI-04 A sample), followed by post-collisional period (BP-TN-95 A sample), and the youngest one is represented by the Brasiliano collage at 590 Ma (recorded in both MRT-MI-04 A and BP-TN-95 A). The P-T-t investigation path for the analyzed rocks ties up the high-grade metamorphic peak conditions at 800–850 °C under pressures of 8–9 kbar, related to the Brasiliano event.

### 5.1. Age of the mafic granulite of the Juiz de Fora complex

Sample BP-TN-95 A presents a range of concordant Paleoproterozoic ages between 2.4 and 1.9 Ga. It also displays a lead loss trend with in- tercepts at ca. 1.9 Ga and 630 Ma. Along with a common lead trend and reverse discordance (these data points are removed from the calculations). The oldest ages spanning from 2.4 to 2.0 Ga are obtained from oscillatory or sector-zoned cores (i.e., analyses 89, 48, 36, 39 and 60) and in zircon grains that display unzoned CL bright cores and dark rims or vice-versa (i.e. analyses 15, 16, 37, 38, 119, 120, 110, 111, 50, 77 and 100). These ages are interpreted to be inherited. There are also numerous CL dark grains without rims that have either no clear zonation or are sector zoned (i.e., analyses 68, 35, 73 and 112). These together with dark rims occurring in the previous group (CL bright and dark grains with cores and rims) contribute to the upper intercept age at ca. 1950 Ma, we suggest that this likely corresponds to the crystallization age for these samples. Some of these grains have low Th/U ratios suggesting that this group may be related to metamorphism, however, given the overspread <sup>176</sup>Hf/<sup>177</sup>Hf ratios (Fig. 7c), indicates incorporation from different magmatic reservoirs (Slama et al., 2008). Previous workers have suggested Paleoproterozoic metamorphism for the Juiz de Fora Complex (2013 Ma-Duarte et al., 2000; Araújo et al., 2021), but at least for the sample BP-TN-95 A sample the usage of <sup>176</sup>Hf/<sup>177</sup>Hf ratios showed that this Paleoproterozoic age (ca. 1950 Ma) is indeed the crystallization age for this sample.

Sample MRT-MI-04 in contrast has numerous clear oscillatory zoned grain cores that give an age range of 2.1–2.23 Ga. Only one clear Paleoproterozoic rim is obtained (117) with an age of 2095 Ma, whereas there are numerous Brasiliano age rims that produce a concordia age of 593 Ma. Thus, this sample is interpreted to have a crystallization age of ca. 2.2 Ga and a metamorphic overprint during the Brasiliano at 593 Ma.

### 5.2. Geochemical significance for the JJC mafic granulites

The investigated samples combined with the geochemical compilation data from other rocks of the JJC (see section 4.2) reinforce the new geochemical data found for this unit. The JJC rocks typically encompass primitive IAT and medium-K calc-alkaline series as well as high-K series granitoids and MORB-like metabasic rocks; minor occurrences of alkaline and within-plate magmatism can also be recognized (Duarte et al., 2000; Heilbron et al., 2010; Degler et al., 2018; Araújo et al., 2019, 2021; Kuribara et al., 2019) as seen in Fig. 6c and d.

This geochemical variety suggests the involvement of various basic rocks with different tectonic settings. In order to illustrate this scenario, a schematic model was built exploring the geochemical signature of these rocks and also the geochronological constraints (Fig. 12).

Initially, the first subduction event took place at 2.4 Ga, represented by arc-related low-K tholeiites, indicative of a primitive intra-oceanic

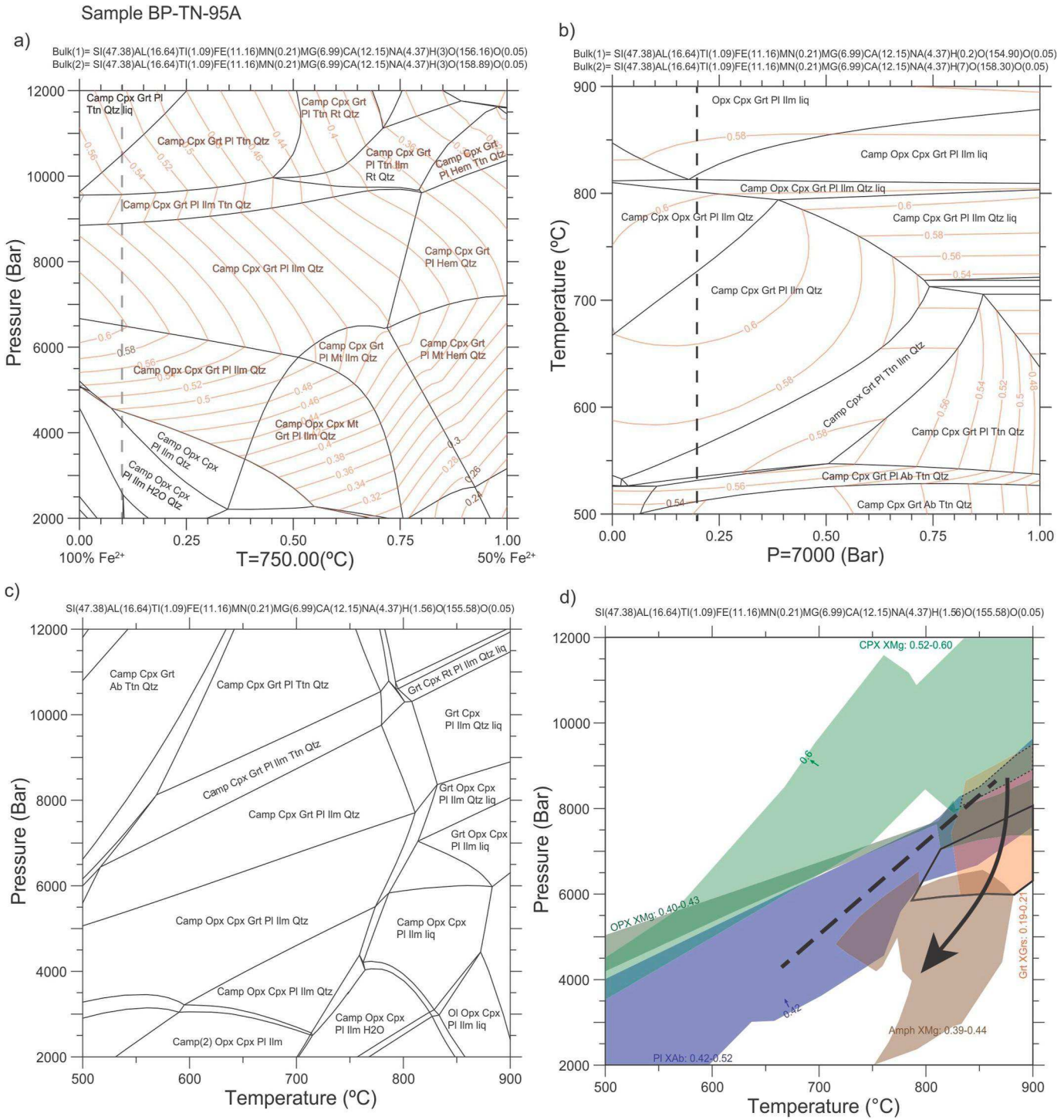


**Fig. 10.** a)  $P\text{-MFe}_2\text{O}_3$  diagram for sample BP-TN-95 A, with  $X_{\text{Alm}}$  isopleths of garnet given in red. The dashed line indicates the  $\text{Fe}^{3+}$  value used for further calculations. b)  $T\text{-MH}_2\text{O}$  diagram for sample BP-TN-95 A, with  $X_{\text{Alm}}$  isopleths of garnet given in red. The dashed line indicates the amount of  $\text{H}_2\text{O}$  used to calculate the  $P\text{-T}$  pseudosection. c)  $P\text{-T}$  pseudosection for sample BP-TN-95 A, the interpreted peak field is outlined in bold. d) Simplified  $P\text{-T}$  pseudosection for sample BP-TN-95 A with just the interpreted peak field indicated together with compositional information for clinopyroxene ( $X_{\text{Mg}}$ , pale green), orthopyroxene ( $X_{\text{Mg}}$ , dark green), plagioclase ( $X_{\text{Ab}}$ , blue), garnet ( $X_{\text{Grs}}$ , orange) and amphibole ( $X_{\text{Mg}}$ , brown). The small black dashed field indicates the overlap region for the compositions of garnet, plagioclase and clinopyroxene which are all interpreted to belong to the peak assemblage of the sample. The thick black arrow indicates the retrograde evolution defined by the mineral compositions, an increase in plagioclase mode and a decrease in garnet mode. The dashed part of the path (the prograde evolution) is only defined by an increase in garnet mode.

arc, and E-MORB magmatism probably illustrating the relics of the ancient ocean floor or plateau basalts record (Heilbron et al., 2010; Araújo et al., 2019, 2021).

A typically evolved arc-stage (2.2–2.18 Ga) expanded calc-alkaline

series is a common feature of the JFC, which is corroborated by trace element arc-like patterns with typical LILE enrichment and troughs in Ti, Nb, P, and Ta. Coeval TTG and sanukitoid magmatism is also reported for this pre-accretionary stage (Araújo et al., 2021; Almeida et al., 2021),

## Sample MRT-MI-04A

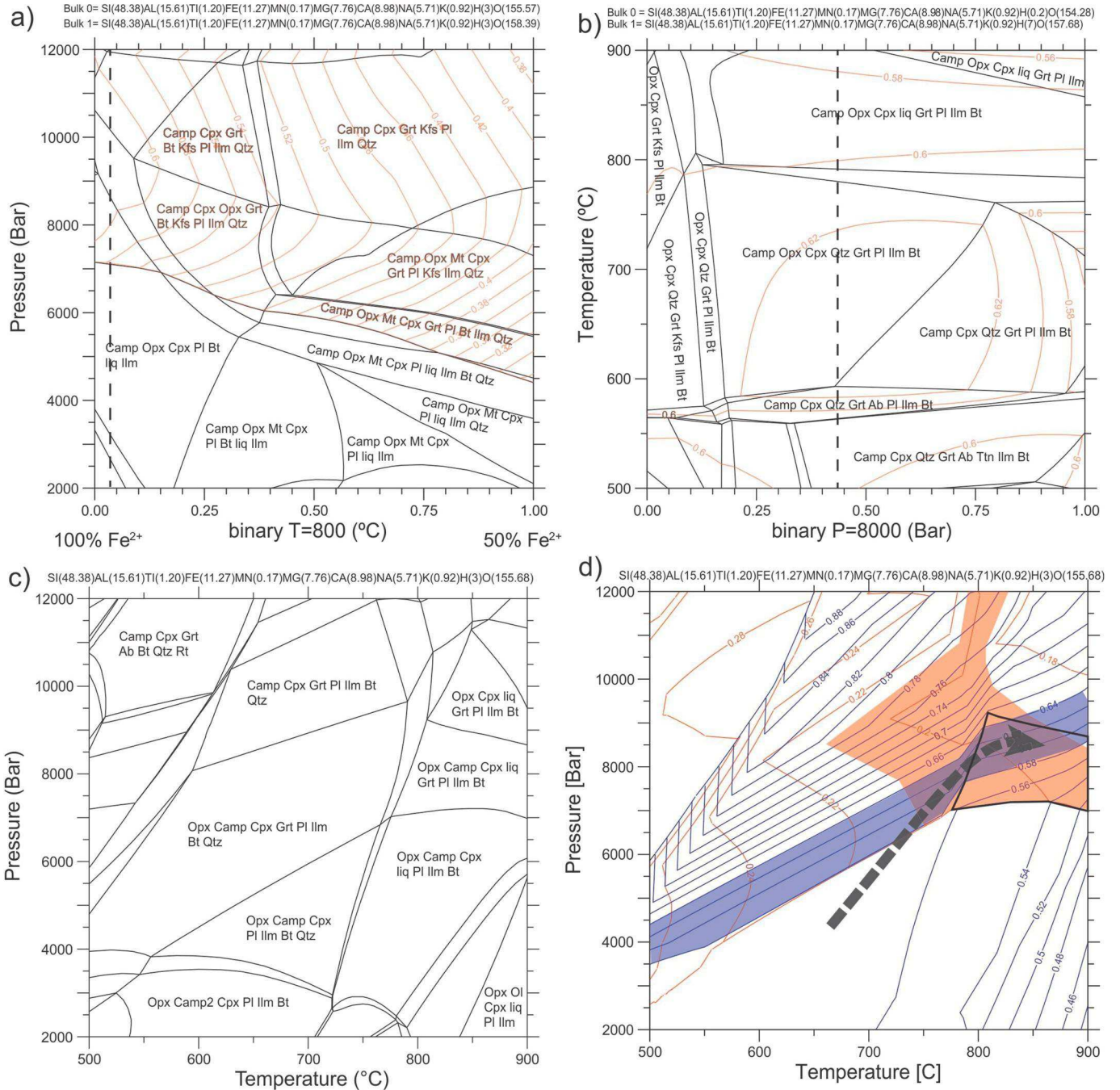


**Fig. 11.** Calculated P-T diagrams for sample MRT-MI-04 A. a)  $P\text{-MFe}_2\text{O}_3$  diagram calculated at  $800\text{ }^{\circ}\text{C}$ . Pale red lines are isopleths of  $X_{\text{Alm}}$  in garnet. b)  $T\text{-MH}_2\text{O}$  diagram calculated at 8 kbar. Pale red lines are isopleths of  $X_{\text{Alm}}$  in garnet. c) P-T pseudosection for the whole rock composition of sample MRT-MI-04 A using the previously determine  $\text{Fe}^{2+}$  and  $\text{H}_2\text{O}$  contents. d) simplified P-T diagram for MRT-MI-04 A with the interpreted peak field indicated in bold. The orange field rep- presents the  $X_{\text{Grs}}$  composition of garnet observed in the sample. The blue field represents the composition of plagioclase rims in the sample. The dashed arrow indicates the interpreted prograde evolution for this sample.

together with hybrid collisional granitoids (2.15 Ga, Heilbron et al., 2010). In this stage, the Rhyacian rocks found in the Juiz de Fora Complex possess a negative  $\epsilon\text{Nd(t)}$  as also negative  $\epsilon\text{Hf(t)}$  plus the record of Archean ages (e.g., Araújo et al., 2019; 2021). Having this in mind, two main hypotheses can be advocated: the contribution from Piedade Block rocks (Bruno et al., 2020) or the single Archean sample dated within JFC by Silva et al. (2002), suggesting assimilation or crustal recycling.

The collisional event at ca. 2.07 and 2.05 Ga between the Mantiqueira and Juiz de Fora Complexes were assigned indirectly based on the metamorphic zircon rims and metamorphic monazite dated for the Mantiqueira orthogneisses (Heilbron et al., 2010; Cutts et al., 2018, 2020). This accretionary event represents the collage of the Juiz de Fora arc onto the active continental margin of the southern São Francisco Craton (Heilbron et al., 2010; Cutts et al., 2018, 2020). The late-to post-collisional stage ca. 2.04 Ga–1.93 Ga is marked by the association of the metabasic rock with E-MORB type signature and hybrid granitoids of Araújo et al., 2021 and Almeida et al. (2021),

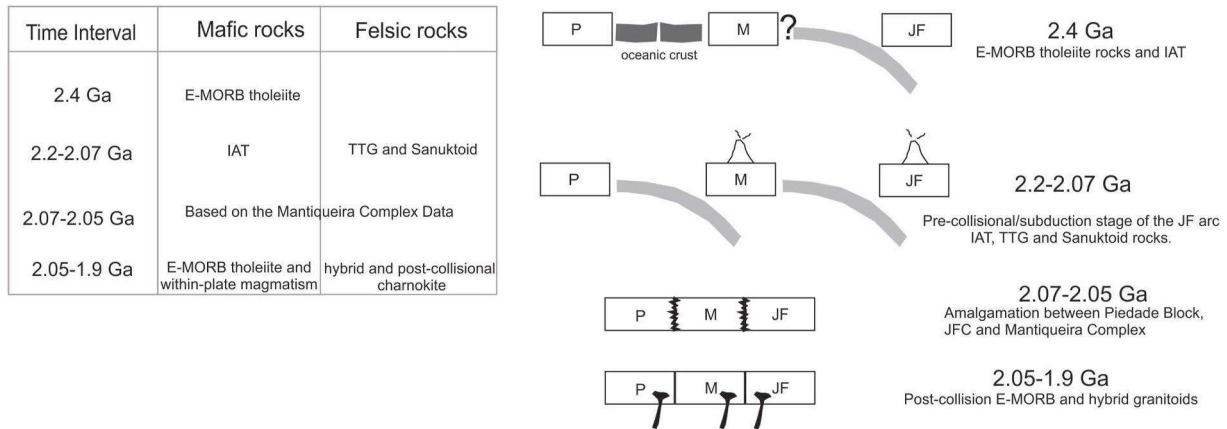


**Fig. 12.** A schematic tectonic model illustrating geological history of the Juiz de Fora Complex. At 2.4 Ga, early intra-oceanic juvenile stage with E-MORB tholeiites and island arc tholeiites. Mature arc stage at ca. 2.2–2.07 Ga with island arc tholeiites, TTG and sanuktoid rocks; Orogenic collision at ca. 2.07–2.05 Ga between the Piedade Block, Mantiqueira and Juiz de Fora Complexes; 2.05–1.9 Ga Post-collision with E-MORB magmatism and hybrid granitoids associations.

respectively. The combination of such features reveals the heterogeneous source mix with contributions from asthenospheric mantle upwelling within an extensional post-collisional setting (Iwamori and Nakamura, 2015; Santosh et al., 2015; Yang et al., 2020).

The IAT signature sample (MRT-MI-04 A) yields the oldest TDM age of 2.39 Ga and a negative  $\epsilon\text{Nd}$  (2.2) of  $-0.5$ , suggesting a crustal component involvement, supporting the tectonic classification for this rock. The zircon U-Pb data yielded a Paleoproterozoic Rhyacian age record of 2203 Ma, which is interpreted to be the magmatic age of the protolith (crystallization age, see red analyses in Fig. 8), with the metamorphic Brasiliano age of ca. 592 Ma. This age is compatible with the widespread occurrence of arc-related rocks found, exhibiting the typical arc-like patterns with typical LILE enrichment and depletion in Ti, Nb, P, and Ta (Fig. 6b, blue square symbol).

Sample BP-TN-95 A displays an E-MORB signature, negative  $\epsilon\text{Nd(t)}$  of  $-1.51$ , and a crystallization age of ca. 1.9 Ga. The granulite facies metamorphism was so overpowering that even the absence of metamorphic zircon shows a clear trend of lead loss during the Brasiliano event (Fig. 7b). In this sample, the evidence for this Archean contribution is highlighted by the Rhyacian inherited zircon grains displaying the mixing juvenile and crustal source contribution with  $\epsilon\text{Hf(t)}$  values of  $+5.68$  to  $-6.98$  and Hf model ages between 2.29 and 2.64 Ga (TDM) (Fig. 13). The oldest zircon of 2.4 Ga can be representative of the initial subduction stage for the JFC, supported by the  $\epsilon\text{Hf(t)}$  of  $-3.09$  and a Hf model age of 2.82 Ga.

### 5.3. P-T-t modeling of the Juiz de Fora complex mafic granulites

Superficially both samples present quite similar peak P-T conditions with sample BP-TN-95 A reaching ca. 8–9 kbar and 825–900 °C and sample MRT-MI-04 A reaching 8–9 kbar and 800–900 °C with a clockwise prograde evolution. Sample BP-TN-95 A also has near isothermal decompression retrograde path and it is unclear if this is also the case for sample MRT-MI-04 A. Given the similarity between these peak conditions and the clear late garnet with melt relationship in sample MRT-MI-04 A, the simplest interpretation is that these conditions reflect the conditions of the Brasiliano overprint.

Sample BP-TN-95 A has a texturally early garnet, which is wrapped by the matrix foliation. It is plausible that this garnet grew during an earlier metamorphic event and has been thermally re-equilibrated during the Brasiliano metamorphic event. Sample MRT-MI-04 A in contrast has texturally late garnet which is clearly related to melt (K-feldspar films on grain boundaries). This sample also has significant growth of zircon rims during the later metamorphic event (in contrast to lead-loss resetting producing a lower intercept in BP-TN-95 A).

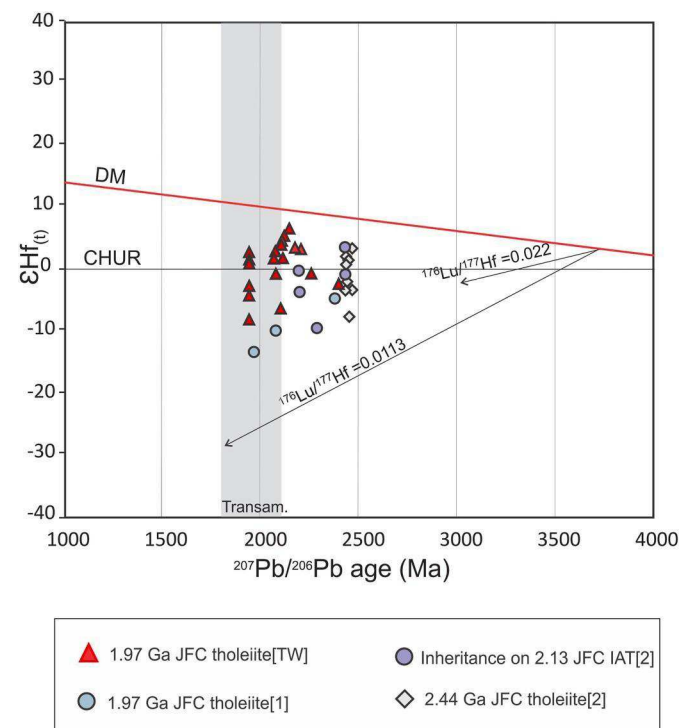


**Fig. 13.** Hf Isotopic characteristics of the mafic rocks of the Juiz de Fora Complex References: 1-Kuribara et al. (2019); 2- Araújo et al. (2021). DM- Depleted mantle. TW- This work. The vertical grey band corresponds to the 2.1–1.8 Ga Transamazonian orogeny (Alkmim and Marshak, 1998). The arrows indicate the Hf crustal evolution trends for average continental crust ( $^{176}\text{Lu}/^{177}\text{Hf}$  of 0.0113) and average mafic crust ( $^{176}\text{Lu}/^{177}\text{Hf}$  of 0.022).

The Paleoproterozoic metamorphic event, also proposed by Duarte et al. (2000) and Araújo et al. (2021) for the Juiz de Fora Complex is challenging to constrain given the extreme deformational conditions of the Brasiliano Event but is supposed to hold high temperatures and intermediate pressures. This would be consistent with a lack of early garnet in MRT-MI-04 A which sees garnet only at higher pressures (over 7 kbar). In the adjacent Mantiqueira Complex, Cutts et al., 2018 obtained 750–800 °C and 6 kbar for metamorphism at 2015 Ma.

During the Brasiliano Event, the collisional process generated shear and thrust zones that placed supracrustal rocks and the granulitic basement (Juiz de Fora Complex) at the same crustal level (Choudhuri

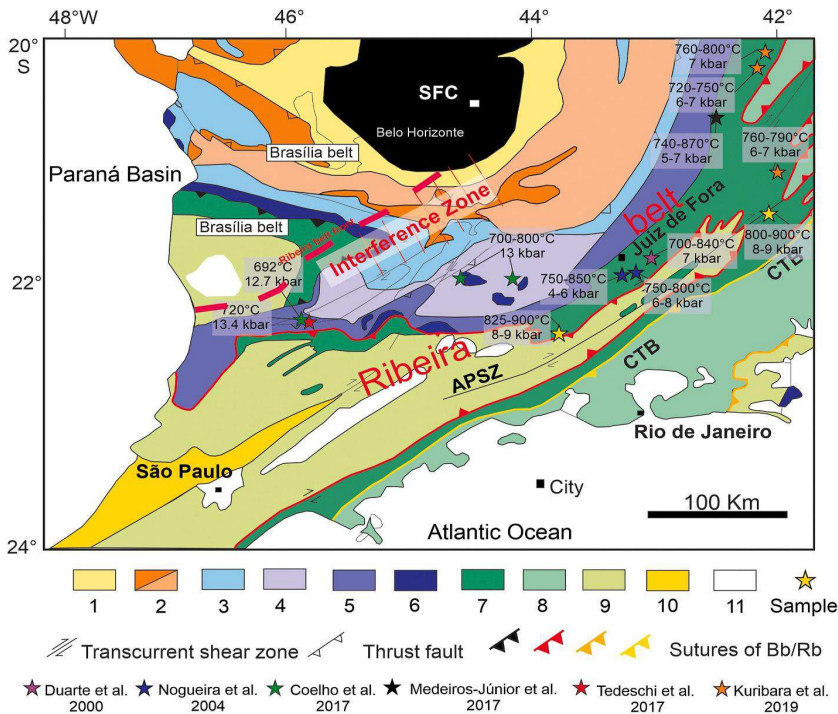


**Fig. 14.** Metamorphic map of the Southern Brasília belt and the Ribeira Belt (modified from Trouw et al., 2013), including the Superposition Zone between the belts. The red dashed line shows the extent of the superposition of the Ribeira belt metamorphism over the Southern Brasília Belt. In both belts, the inverted distribution of moderate to high pressure paragenesis are preserved in the Lower plate that includes the passive margin sequence and basement rocks. In the figure we add all the information regarding metamorphic data reported for basic rocks cropping out at the Upper Thrust and Lower Thrust Systems of the Ribeira belt side. Legend: 1 Greenschist facies without biotite; 2 Greenschist facies with biotite and garnet (dark color); 3 Amphibolite facies with garnet, staurolite and kyanite; 4 Amphibolite facies with kyanite and sillimanite; 5 Amphibolite/granulite facies with sillimanite and K-feldspar, ± orthopyroxene (without kyanite); 6 High pressure granulite facies kyanite and K-feldspar, ± sillimanite; 7 Granulite facies with garnet, sillimanite, K-feldspar and orthopyroxene; 8 Granulite facies with garnet, sillimanite and locally cordierite; 9 Amphibolite facies with garnet and sillimanite; 10 Low to medium pressure greenschist facies; 11 Unmetamorphosed younger rocks. The main Suture zones are identified by colors: black ca. 640–630 Ma (Brasília belt thrusts), red ca. 620–65 Ma, yellow ca. 605–565 Ma and orange ca. 535–510 Ma. CTB Central tectonic boundary, APSZ Alem Paráiba shear zone.

and Silva, 2000). Duarte et al. (2000), observed textures where the development of garnet coronas took place around orthopyroxene and together with hornblende was interpreted as the last stage of Brasiliano metamorphism. The paragneisses belonging to the Raposos Group, Upper Thrust System, also present granulite facies assemblages and the authors above suggest that the Brasiliano metamorphism caused H<sub>2</sub>O mobilization from the metasedimentary rocks to the orthogranulites of the Juiz de Fora Complex promoting the retrograde assemblages.

The metamorphic conditions of supracrustal rocks of the Andrelândia Group (Fig. 14) in the Upper Thrust System of the Occidental Terrane were estimated using fluid inclusions by Nogueira et al. (2004), producing pressures of 6–8 kbar and temperatures of around 750–800 °C.

Degler et al. (2018) reported a Tmax of 733 °C and Pmax of 6.43 kbar, for paragneisses of the Andrelândia Group located in the northern Juiz de Fora Complex using the garnet-biotite Fe-Mg exchange geo-thermometer and the garnet-plagioclase Ca-net-transfer geobarometer. However, it is important to mention that the paragneisses studied by Degler et al. (2018) do not contain the typical granulite mineral assemblage of the Juiz de Fora Complex, recording just the retrograde metamorphic path. High-pressure garnet-clinopyroxene amphibolites found in the Lower Thrust System were formed under metamorphic conditions of 12–16 kbar and 700–800 °C (e.g., Coelho et al., 2017; Tedeschi et al., 2017), with a time constraint of 630 Ma. The decompression associated with the continent-continent collisional event was estimated at ~603 Ma under metamorphic conditions of ~600 °C at 5 kbar, based on compositional maps and P-T conditions of garnet coronas and symplectites (e.g., Tedeschi et al., 2017). Such high-pressure conditions calculated for these rocks can be assigned to deeper subduction and colder gradients, attributed by Brown and Johnson (2018) for the Neoproterozoic period. Taking the results from previous studies, the Brasiliano metamorphic overprint conditions recorded in the orthogranulites of the Juiz de Fora Complex (Fig. 14) have been estimated to be 700–850 °C with pressures of 4–7 kbar, associated with a clockwise P-T-t path. This estimate was

based on mineral assemblages and fluid inclusions (Duarte, 1998; Nogueira et al., 2004; Medeiros-Junior et al., 2017; Kuribara et al., 2019). In this study, the garnet granulite samples have shown slightly higher pressures and temperatures of ca. 8–9 kbar and 800–900 °C. This can be due to a better and more detailed characterization due to the use of quantitative composition maps improving the investigation of the chemical composition of the phases, including internal chemical zoning.

## 6. Conclusion

The studied mafic rocks of the Juiz de Fora reveal two continental cycles: the oldest occurred during the Rhyacian, represented by the IAT signature MRT-MT-04 A sample of 2.2 Ga, followed by an extensional period recorded by the E-MORB like sample BP-TN-95 A of 1.9 Ga and the youngest one at ca. 590 Ma resulted in the Gondwana amalgamation. Obtained P-T data indicates that the Brasiliano metamorphic event resulted in temperatures of 800–900 °C and pressures of 8–9 kbar, which is slightly higher than previous studies regarding basic rocks within the Juiz de Fora Complex.

## CRediT authorship contribution statement

**Talitta Nunes:** Manoel, Writing – review & editing, Writing – original draft, Visualization, Investigation, Conceptualization. **Kathryn Cutts:** Writing – review & editing, Validation, Supervision, Methodology, Investigation, Conceptualization. **Monica Heilbron:** Writing – review & editing, Supervision, Resources, Methodology, Data curation, Conceptualization. **George Luvizotto:** Software, Methodology, Data curation. **Henrique Bruno:** Methodology, Investigation. **Cristiano Lana:** Software, Methodology, Data curation. **Ivo Dussin:** Supervision, Software, Methodology, Data curation. **Claudio de Morrison Valeriano:** Software, Methodology, Investigation, Data curation.

## Declaration of competing interest

The authors declare that they have no known competing financial interests or personal relationships that could have appeared to influence the work reported in this paper.

## Data availability

data will be shared as supplementary material

## Appendix A. Supplementary data

Supplementary data to this article can be found online at <https://doi.org/10.1016/j.james.2023.104238>.

## References

- Alkmim, F.F., Marshak, S., 1998. Transamazonian orogeny in the southern São Francisco craton region, Minas Gerais, Brazil: evidence for paleoproterozoic collision and collapse in the quadrilátero ferrífero. *Precambrian Res.* 90, 29–58.
- Alkmim, F.F., Teixeira, W., 2017. The paleoproterozoic mineiro belt and the quadrilátero ferrífero. In: Heilbron, M., Cordani, U., Alkmim, F.F. (Eds.), São Francisco Craton, Eastern Brazil: Tectonic Genealogy of a Miniature Continent. Regional Geology Reviews. Springer, pp. 71–94.
- Almeida, F.F.M.D., 1977. O cratão do São Francisco. *Rev. Bras. Geociências* 7 (4), 349–364.
- Almeida, F.F.M., Hasui, Y., de Brito Neves, B.B., Fuck, R.A., 1981. Brazilian structural provinces: an introduction. *Earth Sci. Rev.* 17 (1–2), 1–29.
- Almeida, R., Elizeu, V., Bruno, H., Bersan, S.M., Araujo, L.E.D.A.B., Dussin, I., et al., 2021. Rhyacian–Orosirian tectonic history of the Juiz de Fora Complex: evidence for an Archean crustal reservoir within an island-arc system. *Geosci. Front.* 12, 101292.
- Andre', J.L.F., Valladares, C.S., Duarte, B.P., 2009. O Complexo Juiz de Fora na região do Triângulo Mineiro (RJ): litogeocronologia U-Pb (LA-ICPMS) e geoquímica isotópica de Nd e Sr. *Rev. Bras. Geociências* 39 (4), 773–793.
- Araujo, L.E.A.B., Heilbron, M., Teixeira, W., Dussin, I.A., de Morisson Valeriano, C., Bruno, H., Sato, K., Paravindini, G., Castro, M., 2021. Siderian to Rhyacian evolution of the Juiz de Fora Complex: Arc fingerprints and correlations within the Minas-Bahia Orogen and the Western Central Africa Belt. *Precambrian Research* 359, 106118.
- Araujo, L.E.A.B., Heilbron, M., Valeriano, C.M., Teixeira, W., Neto, C.C.A., 2019. Lithogeochemical and Nd-Sr isotope data of the orthogranulites of the Juiz de Fora complex, SE-Brazil: insights from a hidden Rhyacian Orogen within the Ribeira belt. *Braz. J. Geol.* 49 (3), e20190007.
- Brito Neves, B.B., 1995. A tafrogênese estateriana nos blocos paleoproterozóicos da América do Sul e processos subsequentes. *Geonomos* 3, 1–21.
- Brown, M., Johnson, T., 2018. Secular change in metamorphism and the onset of global plate tectonics. *Am Mineral* 103, 181–196.
- Bruno, H., Elizeu, V., Heilbron, M., Valeriano, C.M., Strachan, R., Fowler, M., Bersan, S., Moreira, H., Dussin, I., Silva, L.G.E., Tupinambá, M., Almeida, J.C.H., Neto, C., Storey, C., 2020. Neoarchean and Rhyacian TTG-Samukitoid suites in the southern São Francisco Paleοcontinent, Brazil: evidence for diachronous changes towards modern tectonics. *Geosci. Front.* 11 (5), 1763–1787.
- Bruno, H., Heilbron, M., Strachan, R., Fowler, M., de Morisson Valeriano, C., Bersan, S., et al., 2021. Earth's new tectonic regime at the dawn of the Paleoproterozoic: Hf isotope evidence for efficient crustal growth and reworking in the São Francisco craton, Brazil. *Geology* 49 (10), 1214–1219.
- Bouvier, A., Vervoort, J.D., Patchett, P.J., 2008. The Lu-Hf and Sm-Nd isotopic composition of CHUR: constraints from unequilibrated chondrites and implications for the bulk composition of terrestrial planets. *Earth Planet Sci. Lett.* 273, 48–57.
- Boynton, W.V., 1984. Cosmochemistry of the rare earth elements: meteorite studies. In: Henderson, P. (Ed.), Rare Earth Element Geochemistry. Elsevier Sci. Publ. Co., Amsterdam, pp. 63–114.
- Bucher, K., Grapes, R., 2011. Metamorphism of ultramafic rocks. *Petrogenesis of Metamorphic Rocks*. Springer, Berlin, Heidelberg, pp. 191–224.
- Cabanis, B., Thieblemont, D., 1988. Discrimination of continental tholeiites and back-arc basin basalts using a Th-Tb-Ta diagram. *Chem. Geol.* 70 (1–2), 5.
- Cardoso, C.D., A'Vila, C.A., Neumann, R., Oliveira, E.P., Valeriano, C.M., Dussin, I., 2019. A rhyacian continental arc during the evolution of the mineiro belt, Brazil: constraints from the Rio grande and brumado metadiorites. *Lithos* 326–327, 246–264.
- Choudhuri, A., Silva, D., 2000. A clinopyroxene-orthopyroxene-plagioclase symplectite formed by garnet breakdown in granulite facies, Guaxupe, Minas Gerais, Brazil. *Gondwana Research* 3 (4), 445–452.
- Coelho, M.B., Trouw, R.A.J., Ganade de Araújo, C.E., Vinagre, R., Mendes, J.C., Sato, K., 2017. Constraining timing and P-T conditions of continental collision and late overprinting in the Southern Brasília Orogen (SE-Brazil): U-Pb zircon ages and geothermobarometry of the Andrelândia Nappe System. *Precambrian Res.* 292, 194–215. <https://doi.org/10.1016/j.precamres.2017.02.001>.
- Corfu, F., Hanchar, J.M., Hoskin, P.W., Kinny, P., 2003. Atlas of zircon textures. *Rev. Mineral. Geochem.* 53 (1), 469–500.
- Cox, K.G., Bell, J.D., Pankhurst, 1979. The Interpretation of Igneous Rocks. Allen Unwin, London.
- Cutts, K., Lana, C., Alkmim, F., Peres, G.G., 2018. Metamorphic imprints on units of the southern Araçai belt, SE Brazil. The history of superimposed Transamazonian and Brasiliano orogenesis 58, 211–234.
- Cutts, K., Lana, C., Moreira, H., Alkmim, F., Peres, G.G., 2020. Zircon U-Pb and Lu-Hf record from high-grade complexes within the Mantiqueira Complex: first evidence of juvenile crustal input at 2.4–2.2 Ga and implications for the Palaeoproterozoic evolution of the São Francisco Craton. *Precambrian Res.* 338, 105567.
- de Capitani, C., Petrakakis, K., 2010. The computation of equilibrium assemblage diagrams with Theriax/Domino software. *Am. Mineral.* 95 (7), 1006–1016.
- Degler, R., Pedrosa-Soares, A.C., Novo, T., Tedeschi, M., Silva, L.C., Dussin, I., Lana, C., 2018. Rhyacian–Orosirian isotopic records from the basement of the Araçai-Ribeira orogenic system (SE Brazil): links in the Congo–São Francisco paleocontinent. *Precambrian Res.* 317, 179–195.
- DePaolo, D.J., 1988. Neodymium Isotope Geochemistry: an Introduction. New York, 187pp.
- Droop, G.T.R., 1987. A general equation for estimating Fe<sup>3+</sup> concentrations in ferromagnesian silicates and oxides from microprobe analyses, using stoichiometric criteria. *Mineral. Mag.* 51 (361), 431–435.
- Duarte, B.P., Figueiredo, M.C.H., Campos Neto, M., Heilbron, M., 1997. Geochemistry of the granulite facies orthogneisses of Juiz de Fora complex, central segment of the Ribeira belt, southeastern Brazil. *Rev. Bras. Geociências* 27 (1), 67–82.
- Duarte, B.P., Heilbron, M., Campos Neto, M.D.C., 2000. Granulite/charnockite from the Juiz de Fora domain, central segment of the Brasiliano Ribeira belt. *Rev. Bras. Geociências* 30 (3), 358–362.
- Duarte, B.P., Heilbron, M., Gonçalo-Pascutti, A.H., Silva, T.M.D., Valladares, C.S., Almeida, J.C.H., et al., 2012. Geologia e recursos minerais da folha Itaperuna SF. VCI, p. 24.
- Foley, S., Tiepolo, M., Vanucci, R., 2002. Growth of early continental crust controlled by melting of amphibolite in subduction zones. *Nature* 417 (6891), 837–840.
- Gerdes, A., Zeh, A., 2006. Combined U-Pb and Hf isotope LA-(MC)-ICP-MS analyses of detrital zircons: comparison with SHRIMP and new constraints for the provenance and age of an Armorican metasediment in central Germany. *Earth Planet Sci. Lett.* 249, 47–61.
- Gerdes, A., Zeh, A., 2009. Zircon formation versus zircon alteration – new insights from combined U-Pb and Lu-Hf in-situ LA-ICP-MS analyses, and consequences for the interpretation of Archean zircon from the Central Zone of the Limpopo Belt. *Chem. Geol.* 261, 230–243.
- Green, E.C.R., White, R.W., Diener, J.F.A., Powell, R., Holland, T.J.B., Palin, R.M., 2016. Activity-composition relations for the calculation of partial melting equilibria in metabasic rocks. *J. Metamorph. Geol.* 34 (9), 845–869.
- Gutiérrez-Aguilar, F., Schaaf, P., Solís-Pachardo, G., Arrieta-García, G.F., Hernández-Treviño, T., Linares-Lopez, C., 2021. Phase equilibrium modelling of the amphibolite facies metamorphism in the Yelapa-Chimalapas Metamorphic Complex, Mexico. *Geosci. Front.* 12 (1), 293–312.
- Hammarstrom, J.M., Zen, E.A., 1986. Aluminum in hornblende: an empirical igneous geobarometer. *Am. Mineral.* 71, 1297–1313.
- Harley, S.L., 1989. The origins of granulites: a metamorphic perspective. *Geol. Mag.* 126 (3), 215–247.
- Hawkesworth, C.J., Gallagher, K., Hergt, J.M., McDermott, F., 1994. Destructive plate margin magmatism: geochemistry and melt generation. *Lithos* 33 (1–3), 169–188.
- Hawkesworth, C.J., Dhuime, B., Pietranik, A.B., Cawood, P.A., Kemp, A.I., Storey, C.D., 2010. The generation and evolution of the continental crust. *J. Geol. Soc.* 167 (2), 229–248.
- Heilbron, M., Duarte, B.P., Nogueira, J.R., 1998. The Juiz de Fora complex of the Central Ribeira belt, SE Brazil: a segment of Palaeoproterozoic granulitic crust thrust during the Pan-African Orogen. *Gondwana Research* 1 (3–4), 373–382.
- Heilbron, M., Mohriak, W., Valeriano, C.M., Milani, E., Almeida, J.C.H., Tupinambá, M., 2000. From collision to extension: the roots of the South-eastern continental margin of Brazil. In: Talwani, Mohriak (Ed.), *Atlantic Riffs and Continental Margin*, vol. 115. AGU Geophysical Monograph Series, p. 354.
- Heilbron, M., Pedrosa-Soares, A.C., Campos Neto, M.D.C., Silva, L.D., Trouw, R.A.J., Janasi, V.D.A., 2004. Província mantiqueira. *Geologia do continente sul-americano: evolução da obra de Fernando Flávio Marques de Almeida*, pp. 203–235.
- Heilbron, M., Valeriano, C.M., Tassinari, C.C.G., Almeida, J.C.H., Tupinambá, M., Siga, O., Trouw, R., 2008. Correlation of Neoproterozoic Terranes between the Ribeira Belt, SE Brazil and its African Counterpart: Comparative Tectonic Evolution and Open Questions, vol. 294. Geological Society of London, Special Publication.
- Heilbron, M., Duarte, B.P., Valeriano, C.M., Simonetti, A., Machado, N., Nogueira, J.R., 2010. Evolution of reworked Paleoproterozoic basement rocks within the Ribeira belt (Neoproterozoic), SE-Brazil, based on U/Pb geochronology: implications for paleogeographic reconstructions of the São Francisco-Congo paleocontinent. *Precambrian Res.* 178, 136–148.
- Heilbron, M., Euzebio, R., Peixoto, C., Tupinambá, M., Clayton, G.U.I.A., Peteruel, R., et al., 2013. O complexo Juiz de Fora na folha Santo Antônio de Paúba 1: 100.000: geologia e geoquímica. *Geociências= Geociências* 32 (1), 1–22.
- Heilbron, M., Ribeiro, A., Valeriano, C.M., Paciullo, F.V.P., Almeida, J.C.H., Trouw, R.A.J., Tupinambá, M., Silva, L.G.E., 2017. The Ribeira belt. In: Heilbron, M., Cordani, U., Alkmim, F.F. (Eds.), São Francisco Craton, Eastern Brazil: Tectonic Genealogy of a Miniature Continent. Regional Geology Reviews. Springer International Publishing Co., Switzerland, pp. 277–304. <https://doi.org/10.1007/978-3-319-01715-0>.
- Holland, T., Blundy, J., 1994. Non-ideal interactions in calcic amphiboles and their bearing on amphibole-plagioclase thermometry. *Contrib. Mineral. Petrol.* 116, 433–447.

- Holland, T., Powell, R., 2003. Activity–composition relations for phases in petrological calculations: an asymmetric multicomponent formulation. *Contrib. Mineral. Petrol.* 145 (4), 492–501.
- Holland, T.J.B., Powell, R., 2011. An improved and extended internally consistent thermodynamic dataset for phases of petrological interest, involving a new equation of state for solids. *J. Metamorph. Geol.* 29, 333–383.
- Irvine, T.M., Baragar, W.R., 1971. A guide to the chemical classification of common volcanic rocks. *Can. J. Earth Sci.* 8 (5), 523–548. <https://doi.org/10.1139/c71-055>.
- Iwamori, H., Nakamura, H., 2015. Isotopic heterogeneity of oceanic, arc and continental basalts and its implications for mantle dynamics. *Gondwana Res.* 27, 1131–1151.
- Jackson, S.E., Pearson, N.J., Griffin, W.L., Belousova, E.A., 2004. The application of laser ablation-inductively coupled plasma-mass spectrometry to in situ U-Pb zircon geochronology. *Chem. Geol.* 211, 47–69.
- Janoušek, V., Farrow, C.M., Erban, V., 2006. Interpretation of whole-rock geochemical data in igneous geochemistry: introducing Geochemical Data Toolkit (GCDkit). *J. Petrol.* 47 (6), 1255–1259.
- Jørgensen, T.R., Tinkham, D.K., Lesser, C.M., 2019. Low-P and high-T metamorphism of basalts: insights from the Sudbury impact melt sheet aureole and thermodynamic modelling. *J. Metamorph. Geol.* 37 (2), 271–313.
- Kelsey, D.E., Clark, C., Hand, M., 2008. Thermobarometric modelling of zircon and monazite growth in melt-bearing systems: examples using model metapelitic and metapsammitic granulites. *J. Metamorph. Geol.* 26 (2), 199–212.
- Kunz, B.E., White, R.W., 2019. Phase equilibrium modelling of the amphibolite to granulite facies transition in metabasic rocks (Ivrea Zone, NW Italy). *J. Metamorph. Geol.* 37 (7), 935–950.
- Kuribara, Y., Tsunogae, T., Takamura, Y., Santosh, M., Costa, A., Rosi'ere, C., 2019. Eoarchean to Neoproterozoic crustal evolution of the Mantiqueira and the Juiz de Fora Complexes, SE Brazil: petrology, geochemistry, zircon U-Pb geochronology and Lu-Hf isotopes. *Precambrian Res.* 323, 82–101.
- Lanari, P., Riel, N., Guillot, S., Vidal, O., Schwartz, S., Pecher, A., Hattori, K.H., 2013. Deciphering high-pressure metamorphism in collisional context using microprobe mapping methods: application to the Stak eclogitic massif (northwest Himalaya). *Geology* 41 (2), 111–114. <https://doi.org/10.1130/g33523.1>.
- Lanari, P., Vidal, O., De Andrade, V., et al., 2014. XMapTools: a MATLAB®-based program for electron microprobe X-ray image processing and geothermobarometry. *Comput. Geosci.* 62, 227–240. <https://doi.org/10.1016/j.cageo.2013.08.010>.
- Kuster, K., Ribeiro, A., Trouw, R.J., Dussin, I., Marimon, R., 2020. The Neoproterozoic Andrelândia group: Evolution from an intraplate continental margin to an early collisional basin south of the São Francisco craton, Brazil. *Journal of South American Earth Sciences* 102666.
- Lanari, P., Duesterhoeft, E., 2019. Modeling metamorphic rocks using equilibrium thermodynamics and internally consistent databases: past achievements, problems and perspectives. *J. Petrol.* 60, 19–56.
- Ludwig, K.R., 2008. User's Manual for Isoplot 3.70: A Geochronological Toolkit for Microsoft Excel, vol. 4. Berkeley Geochronology Center Special Publication, p. 76.
- Martins-Neto, M.A., 2000. Tectonics and sedimentation in a Proterozoic rift-sag basin (Espinhaço basin, southeastern Brazil). *Precambrian Research* 103, 147–173.
- Medeiros-Júnior, E.B.M., Evangelista, H.J., de Abreu Marques, R., Velasco, T.C., Soares, C.C.V., 2017. Geothermobarometry of granulites of the Juiz de Fora complex and the Andrelândia group in the region of abre campo and manhuaçu, minas gerais, Brazil. *Geosciences+Geociências* 36 (3), 437–446.
- Meschede, M., 1986. A method of discriminating between different types of mid-ocean ridge basalts and continental tholeiites with the Nb-Zr-Y diagram. *Chem. Geol.* 56 (3–4), 207–218. [https://doi.org/10.1016/0099-2541\(86\)90004-5](https://doi.org/10.1016/0099-2541(86)90004-5).
- Moreira, H., Seixas, L., Storey, C., Fowler, M., Lasalle, S., Stevenson, R., Lana, C., 2018. Evolution of siderian juvenile crust to rhyacian high Ba-Sr magmatism in the mineiro belt, southern São Francisco craton. *Geosci. Front.* 9 (4), 977–995.
- Noce, C.M., Romano, A.W., Pinheiro, C., Mol, V., Pedrosa-Soares, A.C., 2003. Geologia das folhas ub'a E muria'e 1:100.000. In: Pedrosa-Soares, A.C., Noce, C.M., Trouw, R.A.J., Heilbron, M. (Eds.), Projeto Sul De Minas. Codemig, Belo Horizonte, pp. 623–659. Brazil.
- Noce, C., Pedrosa-Soares, A.C., Silva, L.C., Armstrong, R., Piuza, D., 2007. Evolution of polycyclic basement complexes in the Araçuaí Orogen, based on U-Pb SHRIMP data: implications for Brazil Africa links in Paleoproterozoic time. *Precambrian Res.* 159, 60–78.
- Nogueira, J.R., Choudhuri, A., Bello, R.M.D.S., 2004. Incluso es fluidas em granulitos e caminhos PT retrometamórficos para o complexo Juiz de Fora. *Rev. Bras. Geociencias* 34 (4), 509–520.
- Paciullo, F.V.P., Ribeiro, A., Andreis, R.R., Trouw, R.A.J., 2000. The Andrelândia basin, a neoproterozoic intra-plate continental margin, southern Brasília belt. *Rev. Bras. Geociencias* 30 (1), 200–202.
- Pearce, J.A., Cann, J.R., 1973. Tectonic setting of basic volcanic rocks determined using trace element analyses. *Earth Planet. Sci. Lett.* 19 (2), 290–300.
- Pearce, T.H., Gorman, B.E., Birkett, T.C., 1975. The TiO<sub>2</sub>-K<sub>2</sub>O-P<sub>2</sub>O<sub>5</sub> diagram: a method of discriminating between oceanic and non-oceanic basalts. *Earth Planet. Sci. Lett.* 24 (3), 419–426.
- Patchett, P.J., Tatsumoto, M., 1980. Hafnium isotope variations in oceanic basalts. *Geophysical Research Letters* 7 (12), 1077–1080.
- Pearce, J.A., 1983. Role of the Sub-continental Lithosphere in Magma Genesis at Active Continental Margins.
- Pearce, J.A., Parkinson, I.J., 1993. Trace element models for mantle melting: application to volcanic arc petrogenesis. Geological Society, London, Special Publications 76 (1), 373–403.
- Pearce, J.A., 2008. Geochemical fingerprinting of oceanic basalts with applications to ophiolite classification, the search for Archean oceanic crust. *Lithos* 100 (1), 14–48.
- Pearce, J.A., 2014. Immobile element fingerprinting of ophiolites. *Elements* 10, 101–108 (Links).
- Pedrosa-Soares, A.C., Alkmim, F.F., Tack, L., Noce, C.M., Babinski, M., Silva, L.C., Martins-Neto, M.A., 2008. Similarities and differences between the Brazilian and African counterparts of the neoproterozoic aracuaí-west Congo orogen. In: Pankhurst, R.J., Trouw, R.A.J., Brito Neves, B.B., De Wit, M.J. (Eds.), West Gondwana: Pre-cenozoic Correlations across the South Atlantic Region. Geological Society, Special Publications, London, pp. 153–172.
- Pedrosa-Soares, A.C., Alkmim, F.F., 2011. How many rifting events preceded the development of the Araçuaí-West Congo orogen? *Geonomos* 19, 244–251.
- Ross, P.S., Be'ard, J.H., 2009. Magmatic affinity of modern and ancient subalkaline volcanic rocks determined from trace-element discriminant diagrams. *Can. J. Earth Sci.* 46 (11), 823–839.
- Saccani, E., 2015. A new method of discriminating different types of post-Archean ophiolitic basalts and their tectonic significance using Th-Nb and Ce-Dy-Yb systematics. *Geoscience Frontiers* 6 (4), 481–501.
- Santosh, M., Yang, Q.Y., Shaji, E., Tsunogae, T., Ram Mohan, M., Satyanarayanan, M., 2015. An exotic Mesoarchean microcontinent: the Coog Block, southern India. *Gondwana Res.* 27, 165–195.
- Seixas, L.A.R., David, J., Stevenson, R., 2012. Geochemistry, Nd isotopes and U-Pb geochronology of a 2350 Ma TTG suite, Minas Gerais, Brazil: implications for the crustal evolution of the southern São Francisco craton. *Precambrian Res.* 196, 61–80.
- Sla'ma, J., Ko'sler, J., Condon, D.J., Crowley, J.L., Gerdes, A., Hanchar, J.M., Horstwood, M.S., Morris, G.A., Nasdala, L., Norberg, N., Schaltegger, U., 2008. Ple'sovice zircon—a new natural reference material for U-Pb and Hf isotopic microanalysis. *Chem. Geol.* 249, 1–35.
- So'derlund, U., Patchett, P.J., Vervoort, J.D., Isachsen, C.E., 2004. The 176 Lu decay constant determined by Lu-Hf and U-Pb isotope systematics of Precambrian mafic intrusions. *Earth Planet. Sci. Lett.* 219, 311–324.
- Sun, S.-S., McDonough, W.F., 1989. Chemical and isotopic systematics of oceanic basalts: implications for mantle composition and processes. In: Saunders and Norry, A.D. M.J. (Ed.), *Magmatism in the Ocean Basins*, vol. 42. Geol. Soc. Spec. Publ., pp. 313–345.
- Tedeschi, M., Lanari, P., Rubatto, D., Pedrosa-Soares, A., Hermann, J., Dussin, I., Pinheiro, M.A.P., Bouvier, A.S., Baumgartner, L., 2017. Reconstruction of multiple P-T-t stages from retrogressed mafic rocks: subduction versus collision in the Southern Brasília orogen (SE Brazil). *Lithos* 294–295, 283–303.
- Teixeira, W., Oliveira, E.P., Peng, P., Dantas, E.L., Holland, M.H., 2017. U-Pb geochronology of the 2.0 Ga Itapecerica graphite-rich supracrustal succession in the São Francisco Craton: tectonic matches with the North China Craton and paleogeographic inferences. *Precambrian Res.* 293, 91–111.
- Tindle, A.G., Webb, P.C., 1994. PROBE-AMPH—a spreadsheet program to classify microprobe-derived amphibole analyses. *Comput. Geosci.* 20 (7–8), 1201–1228.
- Trouw, R.A.J., Heilbron, M., Ribeiro, A., Valeriano, C., Paciullo, F., Almeida, J.C.H., Tupinamba', M., 2000. The central segment of the Ribeira belt. In: Cordani, U., Milani, E., Thomas-Filho, A., Campos, D. (Eds.), *Geotectonics of South America*, vol. 1. Rio de Janeiro, CPRM, pp. 287–310.
- Trouw, R.A.J., Petermel, R., Ribeiro, A., Heilbron, M., Vinagre, R., Duffles, P., Trouw, C.C., Fontainha, M., Kussama, H.H., 2013. A new interpretation for the interference zone between the southern Brasília belt and the central Ribeira belt, SE Brazil. *J. S. Am. Earth Sci.* 48, 43–57.
- Van Achterbergh, E., Ryan, C.G., Jackson, S.E., Griffin, W., 2001. Data reduction software for La-ICP-MS. In: Sylvester, P. (Ed.), *Laser Ablation-ICPMS in the Earth Science*, vol. 29. Mineralogical Association Of Canada, pp. 239–243.
- Vermeschi, P., 2006. Tectonic discrimination of basalts with classification trees. *Geochim. Cosmochim. Acta* 70 (7), 1839–1848.
- White, R.W., Powell, R., Holland, T.J.B., Worley, B.A., 2000. The effect of TiO<sub>2</sub> and Fe<sub>2</sub>O<sub>3</sub> on metapelitic assemblages at greenschist and amphibolite facies conditions: mineral equilibria calculations in the system K<sub>2</sub>O–FeO–MgO–Al<sub>2</sub>O<sub>3</sub>–SiO<sub>2</sub>–H<sub>2</sub>O–TiO<sub>2</sub>–Fe<sub>2</sub>O<sub>3</sub>. *J. Metamorph. Geol.* 2001.
- White, R.W., Powell, R., Clarke, G.L., 2002. The interpretation of reaction textures in Fe-rich metapelitic granulites of the Musgrave Block, central Australia: constraints from mineral equilibria calculations in the system K<sub>2</sub>O–FeO–MgO–Al<sub>2</sub>O<sub>3</sub>–SiO<sub>2</sub>–H<sub>2</sub>O–TiO<sub>2</sub>–Fe<sub>2</sub>O<sub>3</sub>. *J. Metamorph. Geol.* 20 (1), 41–55.
- White, R.W., Powell, R., Johnson, T.E., 2014. The effect of Mn on mineral stability in metapelites revisited: new a-x relations for manganese-bearing minerals. *J. Metamorph. Geol.* 32 (8), 809–828.
- Wilson, M. (Ed.), 1989. *Igneous Petrogenesis*. Springer Netherlands, Dordrecht.
- Xia, L., Li, X., 2019. Basalt geochemistry as a diagnostic indicator of tectonic setting. *Gondwana Res.* 65, 43–67.
- Yang, H., Zhang, H., Xiao, W., Luo, B., Gao, Z., Tao, L., Guo, L., 2020. Petrogenesis of Early Paleozoic high Sr/Y intrusive rocks from the North Qilian orogen: implication for diachronous continental collision. *Lithosphere* 12, 53–73.

## 4 DISCUSSÃO

O Grupo Andrelândia corresponde a uma variedade de rochas que ocorrem em vários ambientes diferentes, e a nomenclatura (Paciullo *et al.*, 2000; Campos Neto *et al.*, 1999; Trouw *et al.*, 2000; 2013) foi usada para todas as sequências de margem passiva em torno da margem sudeste e sul do SFC (Figura 3). Isso inclui rochas que ocorrem em: a) as nappes da porção leste externas da Faixa Brasília na zona de interferência entre os orógenos Brasília e Ribeira (Trouw *et al.*, 2000; 2013; Westin *et al.*, 2016; 2019; 2021; Kuster *et al.*, 2020); b) o Sistema de Nappes inferiores do Terreno Ocidental da Faixa Ribeira (Domínio Estrutural Andrelândia do Terreno Ocidental); e c) o Sistema de Empurrão Superior (Domínio Juiz de Fora) do Terreno Ocidental da Faixa Ribeira, que apresenta a porção distal da bacia representada pelo Grupo Raposos.

Na borda sul do Cráton São Francisco, inserido no Orógeno da Ribeira Central, rochas metassedimentares deformadas em fácies anfibolito a granulito do Grupo Andrelândia e rochas metabásicas associadas testemunharam todo o estágio evolutivo da bacia de Andrelândia. Unidades siliciclásticas de margem passiva de calibração de tempo costumam ser uma tarefa delicada porque geralmente há um grande intervalo de tempo entre o zircão detritico mais jovem e a idade de sedimentação. A tarefa é delicada quando se trata de rochas metamórficas de alto grau com intenso retrabalhamento tectônico. Apesar de mapas geológicos detalhados e estudos de proveniência, ainda existe uma lacuna de conhecimento e debate sobre a pilha estratigráfica e a idade de sedimentação dessas unidades. Novo mapeamento geológico detalhado, litogeocímica, isótopos Sm-Nd e Rb-Sr e geocronologia LA-ICPMS U-Pb zircão das rochas metabásicas intercaladas em ambas as sequências é apresentado. As rochas metabásicas aparecem em lentes centimétricas a métricas, com contatos nítidos com as rochas metassedimentares secundárias, exibindo o mesmo ca. 620-580 Ma metamorfismo e deformação. Os resultados geoquímicos indicam assinaturas de alto TiO<sub>2</sub> intraplaca e baixo TiO<sub>2</sub> com assinaturas N-MORB a E-MORB para as unidades inferior e superior do grupo Distal Raposos, respectivamente. Por outro lado, apenas metabasitos de baixo teor de titânio tipo MORB foram encontrados na unidade mais proximal (Grupo Andrelândia). Uma única amostra inserida no Grupo Raposos distal apresentou idade de cristalização em ca. 653 Ma, metamorfismo em ca. 579 Ma e herança Paleo a Mesoproterozóica. Para as rochas metabásicas intercaladas no grupo Andrelândia, no Sistema de Empurrão Inferior, as idades do modelo Nd TDM estão entre 1,1 e 1,9 Ga, com  $\epsilon_{Nd}$  (653) variando entre -8 a +2,12 e  $87_{Sr/Sr(i)}$  valores

de 0,7144 a 0,7033 Nd TDM as idades do modelo estão entre 1,8 e 2,0 Ga, com  $\varepsilon$  Nd (653) negativo - 14 a -0,27 e  $^{87}\text{Sr}/^{86}\text{Sr}$  (i) entre 0,7157 a 0,7043. Os resultados isotópicos obtidos indicam uma similaridade isotópica com os metassedimentos da Unidade Biotita Xisto Santo Antônio, anteriormente considerados como derivados de rochas relacionadas ao arco em ambiente de margem ativa (Frugis et al., 2019). Juntamente com dados isotópicos e geocronológicos publicados anteriormente, juntamente com a distribuição estrutural das unidades e fatias tectônicas de embasamento intercaladas no grupo Raposos distal, vislumbramos um modelo tectônico abrangente com magmatismo básico metabásico sin-até tardí entre ca. 760 a 653 Ma. O modelo proposto compara a evolução da bacia de Andrelândia- Raposos com margens hiper-estendidas modernas pobres em magma como um cenário tectônico plausível.

Para as rochas do Complexo Juiz de Fora, combinando os dados isotópicos/geocronológicos novos e disponíveis com os dados geoquímicos e P-T-t (Duarte et al., 1997; 2000; Heilbron et al., 2010; Kuribara et al., 2019; Araújo et al., 2019; 2021; Almeida et al., 2021) levaram a uma melhor compreensão da evolução policíclica do JFC, considerando a perspectiva das rochas metabásicas de alto grau estudadas. Além disso, os novos dados corroboram com dois estágios colisionais na área estudada: o mais antigo ocorreu durante o evento Riaciano em ca. 2,2 Ga (amostra MRT-MI-04A), seguido pelo período pós-colisional (amostra BP-TN-95A), e o mais novo representado pela colagem Brasiliano em 590 Ma (presente tanto na MRT-MI-04A quanto em BP-TN-95A). O caminho de investigação P-T-t para as rochas analisadas amarra as condições de pico metamórfico de alto grau em 800-850 °C sob pressões de 8-9 kbar, relacionadas ao evento Brasiliano.

## CONSIDERAÇÕES FINAIS

As rochas metabásicas analisadas são interpretadas como exemplos de magmatismo máfico extensional contemporâneo a distintos estágios evolutivos da evolução da bacia Andrelândia-Raposos, correlacionados com idades e químicas similares de rochas magmáticas máficas descritas para o Orógeno Araçuaí, a norte. Atualmente, três eventos entre o Toniano e o Criogeniano foram detectados para todo o segmento AROS em ca. 900, 766 e 660-650 Ma.

A idade obtida de ca. 653 Ma de um metabasito com assinaturas intraplacas restringe a evolução final da bacia ao final do período Criogeniano. Esta avaliação é guiada por texturas internas de zircônio, altos valores de TiO<sub>2</sub> (2,1%) e Zr (161ppm) e idades semelhantes (~645 Ma) registradas por lascas ofiolíticas intercaladas por plagiogranitos na Faixa Araçuaí. Como esperado para a sobreimpressão metamórfica de alta temperatura, a morfologia e as texturas internas são essenciais para reconhecer a herança, as idades de cristalização e a sobreimpressão metamórfica. Além disso, este corpo máfico mais jovem também pode ser uma fonte potencial para as unidades superiores da bacia.

A química e as assinaturas isotópicas evoluem de típico magmatismo intraplaca de alto TiO<sub>2</sub> para rochas máficas do tipo MORB nas partes distais da bacia, mas sempre com alguns zircões herdados mais antigos e idades de modelo TDM Mesoproterozóicas principalmente mistas. Uma conclusão importante da contribuição é que o biotita xisto rico em plagioclásio (unidade A5) da bacia Andrelândia-Raposos, recém detectado no grupo Andrelândia, apresenta assinaturas isotópicas semelhantes ao magmatismo máfico estudado, sugerindo que uma origem vulcanoclástica intrabasinal.

Os dados sugerem que, juntas, as amostras de alto TiO<sub>2</sub> podem ser associadas ao estágio de rifteamento continental, enquanto as rochas do tipo MORB são indicativas de um estágio mais evoluído de afinamento da litosfera e exumação do SCLM. A prevalência de assinaturas intraplaca nas unidades inferiores reforça a ideia de que o evento extensional continental iniciado durante o Toniano desencadeou a fragmentação do paleocontinente SF, e que episódios extensionais com magmatismo coevos podem ter durado até o período Criogeniano. Por outro lado, como o cenário marinho profundo prevaleceu nas unidades superiores, o magmatismo tipo MORB ilustra a fase extensional severa, com exumação de SCLM que desencadeia algum derretimento parcial por descompressão, gerando os metabasitos tipo MORB até a fase de fragmentação com início de oceânica crosta para leste.

Por fim, o modelo tectônico previsto aponta para uma espécie de margem Neoproterozóica hiper-extendida, com altos do embasamento na parte distal da bacia, magmatismo relativamente pobre e ocorrência de lascas ultramáficas no interior das unidades metassedimentares.

Na investigação que contempla as rochas máficas estudadas de Juiz de Fora revelam dois ciclos continentais: o mais antigo ocorreu durante o Riaciano, representado pela assinatura IAT MRT-MT-04A amostra de 2,2 Ga, seguido por um período extensional registrado pelo E-MORB como amostra BP -TN-95A de 1,9 Ga e o mais novo em ca. 590 Ma resultou na composição Gondwana.

Os dados P-T obtidos indicam que esse evento metamórfico foi tão intenso que registrou nessas rochas temperaturas de 800-900 °C e pressões de 8-9 kbar, o que configura condições ligeiramente superiores a estudos anteriores sobre rochas básicas no Complexo de Juiz de Fora. A exumação final dessas rochas é evidenciada nos cristais de granada com textura simplectita retrógrada.

## REFERÊNCIAS

- ALKMIN, F. F.; TEIXEIRA, W. The Paleoproterozoic Mineiro Belt and the Quadrilátero Ferrífero. In: HEILBRON, M.; CORDANI, U.; ALKMIM, F. F. (eds.). *São Francisco Craton, Eastern Brazil: tectonic genealogy of a miniature continent*. Springer: Nova York, 2017, p. 71-94.
- ALMEIDA, R. *et al.* Rhyacian-Orosirian tectonic history of the Juiz de Fora Complex: Evidence for an Archean crustal reservoir within an island-arc system. *Geoscience Frontiers*, v. 12, 2021. Disponível em: <https://doi.org/10.1016/j.gsf.2021.101292>. Acesso em 21 fev. 2025.
- BARBOSA, N. S. *et al.* U-Pb geochronology and coupled Hf-Nd-Sr isotopic-chemical constraints of the Cassiterita Orthogneiss (2.47-2.41-Ga) in the Mineiro belt, São Francisco craton: geodynamic fingerprints beyond the Archean-Paleoproterozoic Transition. *Precambrian Research*, v. 326, p. 399-416, 2019. Disponível em: <https://doi.org/10.1016/j.precamres.2018.01.017>.
- BELÉM, J. *et al.* Bacia precursora versus bacias orogênicas: exemplos do Grupo Andrelândia com base em datações U-Pb (LA-ICP-MS) em zircão e análises litoquímicas. *Geonomos*, v. 19, n. 2, p. 224-243, 2011. Disponível em: <https://doi.org/10.18285/geonomos.v19i2.55>.
- BRITO NEVES, B. B. A tafrogênese estateriana nos blocos paleoproterozóicos da América do Sul e processos subseqüentes. *Geonomos*, v. 3, p. 1–21, 1995. Disponível em: <https://doi.org/10.18285/geonomos.v3i2.205>.
- BRUNO, H. *et al.* Neoarchean and Rhyacian TTG-Sanukitoid suites in the southern São Francisco Paleocontinent, Brazil: evidence for diachronous change towards modern tectonics. *Geoscience Frontiers*, v. 11, n. 5, p. 1763-1787, 2020. Disponível em: <https://doi.org/10.1016/j.gsf.2020.01.015>.
- BRUNO, H. *et al.* Earth's new tectonic regime at the dawn of the Paleoproterozoic: Hf isotope evidence for efficient crustal growth and reworking in the São Francisco craton, Brazil. *Geology*, v. 49, n. 10, p. 1214-1219, 2021. Disponível em: <https://doi.org/10.1130/G49024.1>.
- CAMPOS NETO, M. C.; CABY, R. Lower crust extrusion and terrane accretion in the Neoproterozoic nappes of southeast Brazil. *Tectonics*, v. 19, p. 669–687, 2000. Disponível em: <https://doi.org/10.1029/1999tc900065>.
- CIOFFI, C. R. *et al.* Paleoproterozoic continental crust generation events at 2.15 and 2.08 Ga in the basement of the southern Brasília Orogen, SE Brazil. *Precambrian Research*, v. 275, p. 176-196, 2016. Disponível em: <https://doi.org/10.1016/j.precamres.2016.01.007>.
- COELHO, M. B. *et al.* Constraining timing and P-T conditions of continental collision and late overprinting in the Southern Brasília Orogen (SE-Brazil): U-Pb zircon ages and geothermobarometry of the Andrelândia Nappe System. *Precambrian Research*, v. 292, p.

194-215, 2017. Disponível em: <https://doi.org/10.1016/j.precamres.2017.02.001>.

CUTTS, K. *et al.* Zircon U-Pb and Lu-Hf record from high-grade complexes within the Mantiqueira Complex: first evidence of juvenile crustal input at 2.4–2.2 Ga and implications for the Palaeoproterozoic evolution of the São Francisco Craton. *Precambrian Research*, v. 338, p. 105567, 2020. Disponível em: <https://doi.org/10.1016/j.precamres.2019.105567>.

DEGLER, R. *et al.* Rhyacian-Orosirian isotopic records from the basement of the Araçuaí-Ribeira orogenic system (SE Brazil): Links in the Congo-São Francisco paleocontinent. *Precambrian Research*, v. 317, p. 179-195, 2018. Disponível em: <https://doi.org/10.1016/j.precamres.2018.08.018>.

DORÉ, T.; LUNDIN, E. Research focus: Hyperextended continental margins—knowns and unknowns. *Geology*, v. 43, n. 1, p. 95-96, 2015. Disponível em: <https://doi.org/10.1130/focus012015.1>.

DUARTE, B. P. *et al.* Geochemistry of the granulite fácies orthogneisses of Juiz de Fora Complex, Central Segment of the Ribeira Belt, Southeastern Brazil. *Revista Brasileira de Geociências*, v. 27, n. 1, p. 67-82, 1997. Disponível em: <https://bjg.siteoficial.ws/1997/n.1/8.pdf>.

DUARTE, B. P.; HEILBRON, M.; NETO, M. D. C. C. Granulite/charnockite from the Juiz de Fora Domain, central segment of the Brasiliano Ribeira Belt. *Brazilian Journal of Geology*, v. 30, n. 3, p. 358-362, 2000. Disponível em: <https://repositorio.usp.br/directbitstream/c2a6cd04-9010-4f4a-9719-7ee2a73d3605/1133424.pdf>.

FRUGIS, G. L. *et al.* Eastern Paranapanema and Southern São Francisco orogenic margins: records of enduring Neoproterozoic oceanic convergence and collision in the Southern Brasília Orogen. *Precambrian Research*, 2018. Disponível em: <https://doi.org/10.1016/j.precamres.2018.02.005>.

GANADE DE ARAUJO, C. E. *Evolução Tectônica da Margem ativa Neoproterozóica do Orógeno Gondwana Oeste na Província Borborema (NE-Brasil)*. 2014. 243 f. Tese (Doutorado) – Universidade de São Paulo, São Paulo, 2014.

GONÇALVES, M. L.; FIGUEIREDO, M. C. H. Geoquímica dos Anfibolitos de Santana do Garambêu (MG): Implicações Tectônicas sobre a Evolução do Grupo Andrelândia. *Geochimica Brasiliensis*, v. 6, n. 2, p. 127-140, 1992. Disponível em: <https://doi.org/10.21715/gb.v6i2.52>.

GUTIÉRREZ-AGUILAR, F. *et al.* Phase equilibrium modelling of the amphibolite facies metamorphism in the Yelapa-Chimo Metamorphic Complex, Mexico. *Geoscience Frontiers*, v. 12, n. 1, p. 293-312, 2021. Disponível em: <https://doi.org/10.1016/j.gsf.2020.05.001>.

HAMMARSTROM, J. M.; ZEN, E. A. Aluminum in hornblende: an empirical igneous geobarometer. *American Mineralogist*, v. 71, p. 1297–1313, 1986.

HARLEY, S. L. The origins of granulites: a metamorphic perspective. *Geological Magazine*, v. 126, n. 3, p. 215-247, 1989.

HEILBRON, M. et al. Província Mantiqueira. In: MANTESSO-NETO, V. et al. (Org.). *Geologia do Continente Sul-Americano: Evolução da Obra de Fernando Flávio Marques de Almeida*. São Paulo: Beca Produções Culturais, 2004. v. 1, p. 203-234.

HEILBRON, M. et al. Correlation of Neoproterozoic terranes between the Ribeira Belt, SE Brazil and its African counterpart: comparative tectonic evolution and open questions. *Geological Society of London, Special Publication*, v. 294, 2008. Disponível em: <https://repositorio.usp.br/directbitstream/5c21a6ec-b7db-4ca7-83de-5a3f131b1920/1808218.pdf>.

HEILBRON, M. et al. Evolution of reworked Paleoproterozoic basement rocks within the Ribeira belt (Neoproterozoic), SE-Brazil, based on U-Pb geochronology: Implications for paleogeographic reconstructions of the São Francisco-Congo paleocontinent. *Precambrian Research*, v. 178, p. 136–148, 2010. Disponível em: <https://doi.org/10.1016/j.precamres.2010.02.002>.

HEILBRON, M. et al. The Ribeira belt. In: HEILBRON, M.; CORDANI, U. G.; ALKMIM, F. F. (Eds.). *São Francisco Craton, Eastern Brazil: Tectonic Genealogy of a Miniature Continent*. Regional Geology Reviews. Springer, 2017. p. 277-304. Disponível em: <https://doi.org/10.1007/978-3-319-01715-0>.

HEILBRON, M. et al. The Barreira suite in the central Ribeira Belt (SE Brazil): a late Tonian tholeiitic intraplate magmatic event in the distal passive margin of the São Francisco Paleocontinent. *Brazilian Journal of Geology*, v. 49, n. 2, p. 1–19, 2019. Disponível em: <https://doi.org/10.1590/2317-4889201920180129>.

HEILBRON, M. et al. Proterozoic to Ordovician geology and tectonic evolution of Rio de Janeiro State, SE-Brazil: insights on the central Ribeira Orogen from the new 1:400,000 scale geologic map. *Brazilian Journal of Geology*, v. 50, 2020. Disponível em: <https://doi.org/10.1590/2317-4889202020190099>.

HOLLAND, T.; BLUNDY, J. Non-ideal interactions in calcic amphiboles and their bearing on amphibole-plagioclase thermometry. *Contributions to Mineralogy and Petrology*, v. 116, p. 433–447, 1994. Disponível em: <https://link.springer.com/article/10.1007/BF00310910>.

KUNZ, B. E.; WHITE, R. W. Phase equilibrium modelling of the amphibolite to granulite facies transition in metabasic rocks (Ivrea Zone, NW Italy). *Journal of Metamorphic Geology*, v. 37, n. 7, p. 935-950, 2019. Disponível em: <https://doi.org/10.1111/jmg.12478>. Acesso em: 21 fev. 2025.

KUSTER, K. et al. The Neoproterozoic Andrelândia group: Evolution from an intraplate continental margin to an early collisional basin south of the São Francisco craton, Brazil. *Journal of South American Earth Sciences*, v. 102666, 2020. Disponível em: <https://doi.org/10.1016/j.jsames.2020.102666>.

KURIBARA, Y. *et al.* Eoarchean to Neoproterozoic crustal evolution of the Mantiqueira and the Juiz de Fora Complexes, SE Brazil: Petrology, geochemistry, zircon U-Pb geochronology and Lu-Hf isotopes. *Precambrian Research*, v. 323, p. 82-101, 2019. Disponível em: <https://doi.org/10.1016/j.precamres.2019.01.008>.

LANARI, P. *et al.* Deciphering high-pressure metamorphism in collisional context using microprobe mapping methods: application to the Stak eclogitic massif (northwest Himalaya). *Geology*, v. 41, n. 2, p. 111–114, 2013. Disponível em: <https://doi.org/10.1130/g33523.1>.

LANARI, P. *et al.* XMapTools: A MATLAB®-based program for electron microprobe X-ray image processing and geothermobarometry. *Computers & Geosciences*, v. 62, p. 227–240, 2014. Disponível em: <https://doi.org/10.1016/j.cageo.2013.08.010>.

LANARI, P.; DUESTERHOEFT, E. Modeling Metamorphic Rocks Using Equilibrium Thermodynamics and Internally Consistent Databases: Past Achievements, Problems and Perspectives. *Journal of Petrology*, v. 60, p. 19–56, 2019. Disponível em: <https://doi.org/10.1093/petrology/egy105>.

LOBATO, M. C. *Proveniência das rochas metassedimentares dos diferentes terrenos tectono-estratigráficos da Faixa Ribeira Central, com base em dados U-Pb e Lu-Hf obtidos em grãos de zircão detriticos*. 2018. Tese (Doutorado) – Universidade do Estado do Rio de Janeiro, Rio de Janeiro, 2018. Disponível em: <http://www.bdtd.uerj.br/handle/1/23208>.

MARIMON, R. S. *et al.* U-Pb and Lu-Hf isotope systematics on detrital zircon from the southern São Francisco Craton's Neoproterozoic passive margin: tectonic implications. *Journal of South American Earth Sciences*, v. 100, p. 1–20, 2020. Disponível em: <https://doi.org/10.1016/j.jsames.2020.102539>.

MARINS, G. *Petrologia dos Anfibolitos do Domínio Juiz de Fora e da Klippe Paraíba do Sul, no Setor Central da Faixa Ribeira*. 2000. Dissertação (Mestrado) – Universidade do Estado do Rio de Janeiro, Rio de Janeiro, 2000.

MARTINS-NETO, M. A. Tectonics and sedimentation in a Proterozoic rift-sag basin (Espinhaço basin, southeastern Brazil). *Precambrian Research*, v. 103, p. 147–173, 2000. Disponível em: [https://doi.org/10.1016/S0301-9268\(00\)00080-2](https://doi.org/10.1016/S0301-9268(00)00080-2).

NOCE, C. M. *et al.* Geologia das Folhas Ubá e Muriaé 1:100.000. In: PEDROSA-SOARES, A. C. et al. (Eds.). *Projeto Sul de Minas*. Belo Horizonte: Codemig, 2003. p. 623–659.

NOCE, C. *et al.* Evolution of polycyclic basement complexes in the Araçuaí Orogen, based on U-Pb SHRIMP data: Implications for Brazil-Africa links in Paleoproterozoic time. *Precambrian Research*, v. 159, p. 60–78, 2007. Disponível em: <https://doi.org/10.1016/j.precamres.2007.06.001>.

PACÍULLO, F. V. P. *A Sequência Deposicional Andrelândia*. 1997. Tese (Doutorado) – Universidade Federal do Rio de Janeiro, Rio de Janeiro, 1997.

PACÍULLO, F. V. P. *et al.* The Andrelândia Basin, a Neoproterozoic intra-plate continental margin, southern Brasília Belt. *Revista Brasileira de Geociências*, v. 30, n. 1, p. 200-202, 2000.

PEARCE, J. A.; CANN, J. R. Tectonic setting of basic volcanic rocks determined using trace element analyses. *Earth and Planetary Science Letters*, v. 19, n. 2, p. 290-300, 1973. Disponível em: [https://doi.org/10.1016/0012-821X\(73\)90129-5](https://doi.org/10.1016/0012-821X(73)90129-5).

PEARCE, T. H. *et al.* The TiO<sub>2</sub>-K<sub>2</sub>O-P<sub>2</sub>O<sub>5</sub> diagram: a method of discriminating between oceanic and non-oceanic basalts. *Earth and Planetary Science Letters*, v. 24, n. 3, p. 419-426, 1975. Disponível em: [https://doi.org/10.1016/0012-821X\(75\)90149-1](https://doi.org/10.1016/0012-821X(75)90149-1). Acesso em: 21 fev. 2025.

PEARCE, J. A. Role of the sub-continental lithosphere in magma genesis at active continental margins. In: THORPE, R. S. (ed.). *Andesites: orogenic andesites and related rocks*. Chichester: Wiley, 1982. p. 525-548.

PEDROSA-SOARES, A. C. *et al.* Similarities and differences between the Brazilian and African counterparts of the Neoproterozoic Araçuaí-West Congo orogen. In: PANKHURST, R. J. *et al.* (Eds.). *West Gondwana: Pre-Cenozoic Correlations Across the South Atlantic Region*. Londres: Geological Society, Special Publications, 2008. p. 153–172.

PEDROSA-SOARES, A. C.; ALKMIM, F. F. How many rifting events preceded the development of the Araçuaí-West Congo orogen? *Geonomos*, v. 19, p. 244–251, 2011.

PERON-PINVIDIC, G.; MANATSCHAL, G. Rifted margins: State of the art and future challenges. *Frontiers in Earth Science*, v. 7, p. 218, 2019. Disponível em: <https://doi.org/10.3389/feart.2019.00218>. Acesso em: 22 fev. 2025.

PINHEIRO, M. A. P. *et al.* Timing and petrogenesis of metamafic-metaultramafic rocks in the Southern Brasília orogen: insights for a Rhyacian multi-system suprasubduction zone in the São Francisco paleocontinent (SE-Brazil). *Precambrian Research*, v. 321, p. 328–348, 2019. Disponível em: <https://doi.org/10.1016/j.precamres.2018.12.006>. Acesso em: 22 fev. 2025.

QUEIROGA, G. N. *Caracterização de restos de litosfera oceânica do Orógeno Araçuaí entre os paralelos 17° e 21°S*. 2010. Tese (Doutorado) – Universidade Federal de Minas Gerais, Belo Horizonte, 2010.

RENO, B. L. *et al.* Eclogite-high-pressure granulite metamorphism records early collision in West Gondwana: new data from the southern Brasília belt, Brazil. *Journal of the Geological Society*, v. 166, n. 6, p. 1013–1032, 2009. Disponível em: <https://doi.org/10.1144/0016-76492008-140>. Acesso em: 22 fev. 2025.

RIBEIRO, A. *et al.* Evolução das bacias proterozóicas e o termo-tectonismo brasiliano na margem sul do cráton do São Francisco. *Revista Brasileira de Geociências*, v. 25, p. 235-248, 1995. Disponível em: <https://bjg.siteoficial.ws/1995/n.4/2.pdf>. Acesso em: 22 fev. 2025.

SACCANI, E. A new method of discriminating different types of post-Archean ophiolitic basalts and their tectonic significance using Th-Nb and Ce-Dy-Yb systematics. *Geoscience*

*Frontiers*, v. 6, n. 4, p. 481-501, 2015. Disponível em: <https://doi.org/10.1016/j.gsf.2014.03.006>. Acesso em: 22 fev. 2025.

SANTOS, P. S. *Geocronologia, Área Fonte e Ambiente Tectônico da Unidade Santo Antônio – Megassequência Andrelândia*. 2011. Dissertação (Mestrado) – Universidade Federal do Rio de Janeiro, Rio de Janeiro, 2011.

SUTRA, E.; MANATSCHAL, G. How does the continental crust thin in a hyperextended rifted margin? Insights from the Iberia margin. *Geology*, v. 40, n. 2, p. 139-142, 2012. Disponível em: <https://doi.org/10.1130/G32786.1>. Acesso em: 22 fev. 2025.

TEDESCHI, M. et al. Reconstruction of multiple P-T-t stages from retrogressed mafic rocks: subduction versus collision in the Southern Brasília orogen (SE Brazil). *Lithos*, v. 294-295, p. 283-303, 2017. Disponível em: <https://doi.org/10.1016/j.lithos.2017.09.025>. Acesso em: 22 fev. 2025.

TROUW, R. A. J. et al. The Central Segment of the Ribeira belt. In: CORDANI, U. et al. (eds.). *Geotectonics of South America*. Rio de Janeiro: CPRM, 2000. v. 1, p. 287-310.

TROUW, R. A. J. et al. A new interpretation for the interference zone between the southern Brasília belt and the central Ribeira belt, SE Brazil. *Journal of South American Earth Sciences*, v. 48, p. 43-57, 2013. Disponível em: <https://doi.org/10.1016/j.jsames.2013.07.012>. Acesso em: 22 fev. 2025.

VALERIANO, C. M. et al. A evolução tectônica da Faixa Brasília. In: MANTESSENETO, V. (org.). *Geologia do Continente Sul-Americano: evolução e obra de Fernando Flávio Marques de Almeida*. São Paulo: Beca, 2004. p. 575-593.

VALLADARES, C. S. et al. Ages of detrital zircon from siliciclastic successions south of the São Francisco Craton, Brazil: implications for the evolution of Proterozoic basin. *Gondwana Research*, v. 7, n. 4, p. 913-921, 2004. Disponível em: [https://doi.org/10.1016/S1342-937X\(05\)71074-1](https://doi.org/10.1016/S1342-937X(05)71074-1). Acesso em: 22 fev. 2025.

ZALÁN, P. V. et al. An entirely new 3D-view of the crustal and mantle structure of a South Atlantic passive margin–Santos, Campos and Espírito Santo basins, Brazil. In: AAPG ANNUAL CONFERENCE AND EXHIBITION, 2011. v. 10, p. 13.